
KTH Engineering Sciences

# A method to apply ISO 3745 for the sound power measurement of I.C. Engines in a limited space

**Mehdi Mehrgou**

Master's Degree Project

TRITA-AVE 2012:42

ISSN 1651-7660


Postal address
Royal Institute of Technology, MWL/AVE
SE-100 44 Stockholm Sweden

Visiting address
Teknikringen 8 Stockholm

Contact
Email: mmehrgou@yahoo.com

## Abstract

The Reduction of engine noise, one of the primary noise sources in trucks and busses, is essential in order to fulfill various noise emission regulations such as ISO 362 [**1**]. At the same time, it is equally important to meet market demands in order to attract new customers while competing with other brands to lower overall noise levels.

Sound power is a convenient descriptor of noise emissions when compared to sound pressure it is not dependent on the distance from the source and the surrounding environment. A number of standards for sound power measurement exist, requiring different methods, tools and environments. In engine development at Scania the sound power level is measured for different engine types for noise level determination and comparison purposes. Additionally, attempts to reduce noise through modifications of engine parts require many iterations in which sound pressures recorded at specific microphone positions are of primary interest. The necessity of running each engine at different speeds and load conditions with various modifications during development (combined with time restrictions) narrows down the choices to ISO 3745 which involves measuring sound power with stationary microphones.

Despite ISO3745 apparent ease of use, prerequisites such as the number of microphones, the distance limitation of the microphones and free field conditions often pose a practical challenge. In Scania's anechoic chamber it is impossible to meet these requirements due to limitations inherent to the room design such as size, poor absorption and limited space on the underside of the engine. This thesis comprises engine acoustic simulations in Nastran together with various measurements. Based on these, guidelines for power calculation have been developed taking into account the level of uncertainty and correction factors.

## Acknowledgments

I would like to thank everyone at Scania that helped me with this thesis and for providing the hardware and software necessary for calculation and measurement. I would also like to thank my supervisor at Scania, Ola Jönsson, for his comments and guides at different stages of the project, as well as the group manager at NMBD, Peter Daelander, for providing the facilities, and granting permission to publish this work. In addition, special thanks to Tony Algarp for his help in measurements, and last but not least my supervisor at KTH, Leping Feng.

# Table of Contents

# 1 Introduction

Legislators around the globe have steadily been tightening noise limits for almost every type of motorized vehicle. An end to this trend is not likely. Mandatory limits on noise emissions from combustion engines do not exist, however, legislators do limit the noise emitted by an entire vehicle, such as in ISO 362 [**1**] which involves measurement of Pass-By-Noise. Manufacturers are individually left to decide whether or not to enclose their engines or develop fundamentally quiet engines. Since encapsulation methods normally incur heat problems and limit the possible number of vehicle variants, inherently quieter engines are a better solution.

Achieving the above is an ongoing task. The “acoustic efficiency”, i.e. the ratio of engine sound power to rated engine power, has been dropping continually [**2**] . Sound power is a convenient descriptor for noise emissions such as engine noise, and standard ISO 3745 is one of the typical methods for this purpose. Its implementation in Scania’s anechoic chamber is discussed below.

## *1.1 Engine noise*

There are many different noise sources in engines. These are categorized into three major groups [**2**]:

- Engine surface (surface noise) vibrations
- Pulsation (aerodynamic noise) generated by intake, exhaust and cooling systems
- Transmission of the vibrations by the engine mounts to the chassis foundation (structure-borne sound)

In the case of Pass-By-Noise, the engine surface plays the biggest role, and this is the subject of this study. Sound power is a measure to compare different engines and various modifications to reduce noise emissions.

## *1.2 Scope*

The existing anechoic room at Scania Södertalje is used for sound power measurement of I.C. engines specifically based on ISO 3745. The requirements of the standard are described in detail in chapter two. The difficulties in meeting these requirements for the mentioned room are explained in section 2.3.6. The schematic view of the room is shown in Figure 1-1.

The dimensions of the room are 8 × 7 × 5.35 meters; the frequency range of interest is from 80 Hz to 16 kHz. Measurement here has been done using stationary microphones which makes it easier to characterize the sound. This work, studies the engine sound field with simulation and measurements, suggest different ways to conquer limitations of the room and finally present recommendations and identify uncertainties in the measurements.

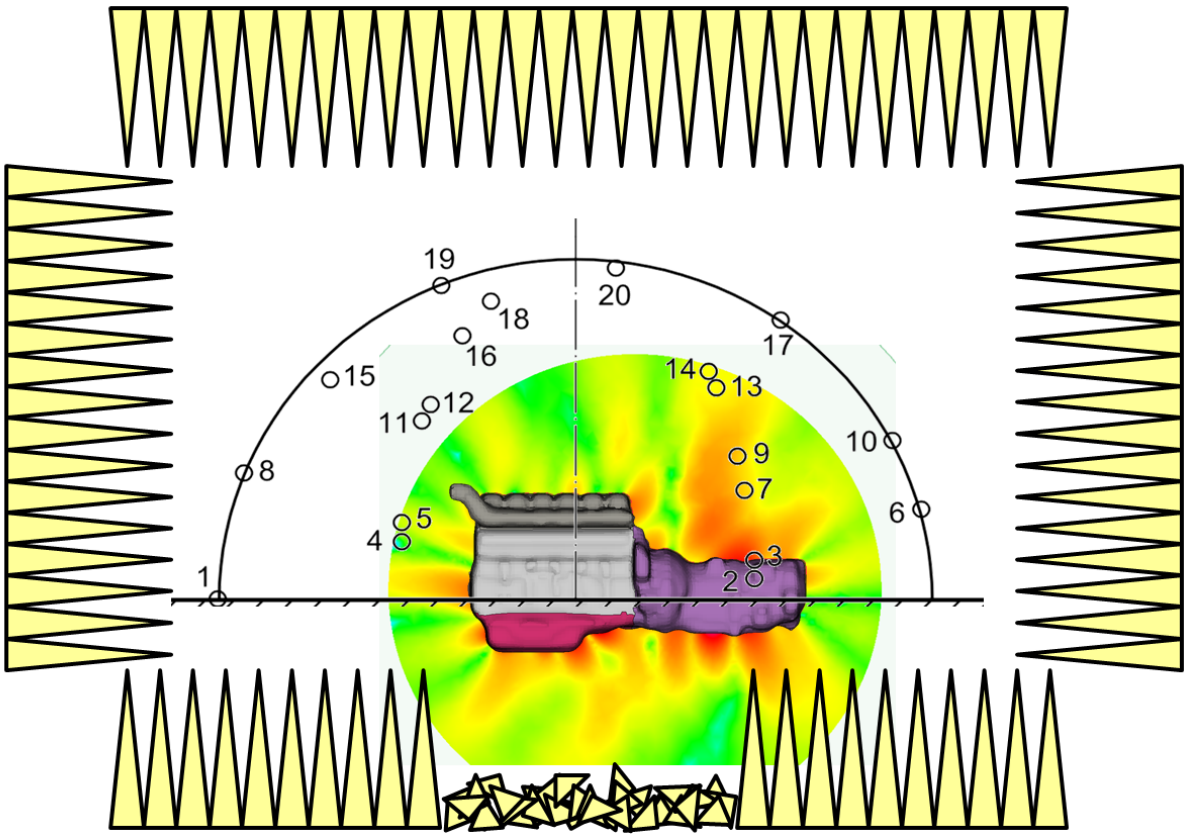


**Figure 1-1 The schematic model of the engine and anechoic chamber (the scale of the engine and room are not realistic)**

# 2 Sound Field and Sound Power

## *2.1 Sound power calculations and methods*

Sound power is a convenient descriptor for a noise source and describes how much noise is produced. However, in highly directional sources, information about the directivity index is also required. [**3**]

The sound field generated by a source is also dependent on the environment surrounding the source. A Sound field in an environment generates a radiation load, which in turn affects the source. It is in other words a coupled system. [**3**] An example

of this effect is illustrated by Fahy [**4**] through sound generation by a loudspeaker in different rooms. However in the free field, which is the case in this study, this effect is small beside the high stiffness of the engine structure which makes it less sensitive to acoustic loads from the surrounding environment.

In many cases, it is necessary to determine the sound source for the following reasons [**4**]:

1. For comparisons of sound power between different systems and devices and also other brands
2. For predicting the sound field in different environments after installation of a device/system
3. To check regularity or legal requirements
4. To provide information to source diagnostic
5. For product labeling purposes
6. For identifying the most powerful noise source in the system

### 2.1.1 Standards for sound power measurements

As mentioned before, sound powers are internationally standardized [**5**]. There are four different forms by Fahy [4]:

1. Measurements are made of the mean square sound pressure distributed over an enclosed measurement surface in free field conditions. Assuming that $|I| = \tilde{p}^2 / \rho_0 c_0$ (will be discussed later) the pressures are equivalent to normal intensities ($L_I = L_P$) and the intensities are integrated by spatial averaging the pressure over the surface. This measurement method is used in Standards ISO 3745-3746 as well as in this thesis.
2. Measurement of the normal intensity distribution over an enclosed surface and integrated over the surface. This method is only used by Scania on special occasions for the following reasons:
    a. extremely time consuming
    b. limitation in space, impossible to sweep a closed surface

c. more difficult to evaluate and compare relative to stationary microphone measurements
d. only steady state situations (not possible to use RPM sweep, Run up test) i.e. only discrete speed values, which increases the risk of missing resonance peaks.

3. Measurements are made of the space average mean square sound pressure, $\tilde{p}^2$, in a reverberation chamber and a balance is made between radiated and absorbed sound.

4. Measurements are made of the space average mean square sound pressure in a reverberant room when excited by a known source. The known source is then deactivated and measurements repeated in the presence of the source whose sound power is to be determined.

### 2.1.2 Formulation for sound power calculation using sound pressure only

In the direction of the sound propagation, the sound pressure and the sound intensity have a simple relation as $|\mathrm{I}| = \tilde{p}^2 / \rho_0 c_0$ . The sound intensity vector is normal to the center of the source. Assuming an imaginary measurement surface (S) and many measurement points to obtain enough spatial averages '⟨ ⟩' one could write the sound field as

$$\langle I \rangle = \langle \frac{\tilde{p}^2}{\rho_0 c_0} \rangle \qquad \text{Eq. 2-1}$$

$$W = \langle I \rangle \times S$$

$$\frac{W}{10^{-12}} = \frac{\langle \frac{\tilde{p}^2}{\rho_0 c_0} \rangle \times S}{10^{-12}}$$

Assuming $\rho_0 c_0 = 400$ and log of two sides

$$10 \times \log_{10} \frac{W}{W_{ref}} = 10 \times \log_{10} \frac{\langle \tilde{p}^2 \rangle}{p_{ref}^2} + 10 \times \log_{10} \frac{S}{S_{ref}}$$

$$L_w = 10 \times \log_{10} \frac{\langle \tilde{p}^2 \rangle}{p_{ref}^2} + 10 \times \log_{10} \frac{S}{S_{ref}}$$

$$L_w = \overline{L_{pf}} + 10 \times \log_{10} \frac{S}{S_{ref}} \qquad \text{Eq. 2-2}$$

Where $S_{ref}$ is equal to one $m^2$. This is the main formulation for calculating power from sound pressure only. A More general version of this equation is equation 2-8, considering the effect of atmospheric pressure and test cell temperature.

## *2.2 Terms & definitions*

Before starting with the requirements of standard ISO 3745 some acoustical terms and their significance have to be described. The direct sound field consists of three different regions: a) Hydrodynamic near field, b) geometric near field, and c) far field. Generally, measurement of sound power with only sound pressure requires measurement in the far field where the inverse square law is valid. In addition to the above, other terms such as directivity, and reverberant field are explained here.

### 2.2.1 Inverse square law

In an acoustic context the monotonical decay of the sound pressure in inverse proportion to the distance from source effective center is called the inverse square law. This is illustrated in Figure 2-1 where the same amount of energy passing through an area four times larger at double the distance results in a 6 dB lower pressure and intensity level.

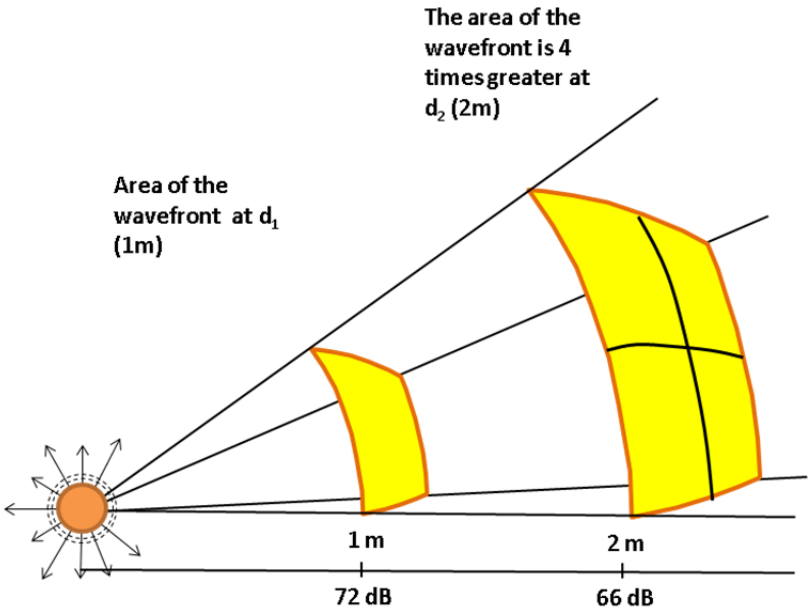


**Figure 2-1 Illustration of the inverse square law**

### 2.2.2 Hydrodynamic near field

In the immediate vicinity of the radiating surface of a source, the local particle velocity is very large and is nearly in quadrature with the sound pressure. The impedance is much greater than $\rho_0 c_0$ and the reactive intensity component (the non-propagating part, with no energy transfer) is much greater than the active component (the propagating part, with energy transfer) and so $|I| \ll \tilde{p}^2 / \rho_0 c_0$. In this region an individual intensity vector exhibits a circular pattern. [**4**]

In the far field sound pressure and velocity are in phase and the ratio between them is close to $\rho_0 c_0$ and $|I| = \tilde{p}^2 / \rho_0 c_0$ [**6**]. For a monopole source, the real and imaginary (not propagating) values of the impedance are presented in Figure 2-2. The abruptly decay in the imaginary part with increasing distance from the object is clear from the Figure 2-2.

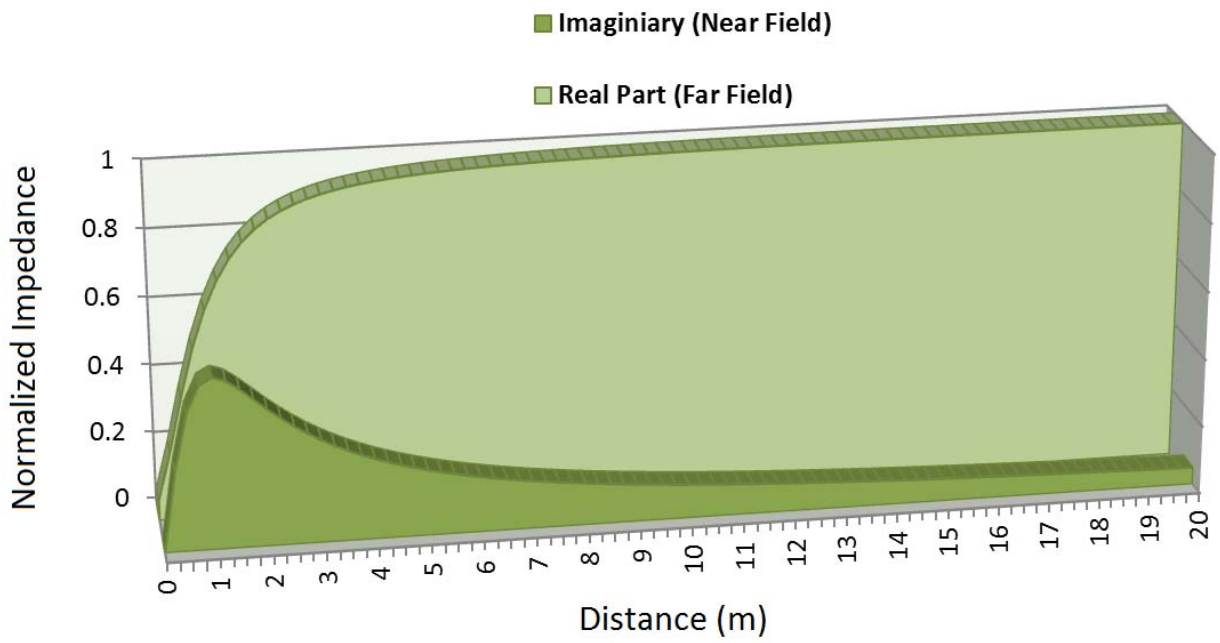


**Figure 2-2 The imaginary and real part of impedance for a monopole source (Picture recreated from [7])**

### 2.2.3 Geometric near field (Frensel region)

The sound field around a spatially distributed source is formed by interference of radiated waves from different regions of the source. The constructive and destructive interference close to the source, due to delay (Phase differences) affects the sound field considerably. For tones, this effect can be very pronounced, while for band noise such as ⅓ octave, the effects become less pronounced as the bandwidth is

increased [**8**]. Therefore, the relationship between pressure and particle velocity is an extremely complex function of position in such a field (see Figure 2-3). [**6**] However this interference requires correlated regional parts of the source to interact. As will be discussed in section 4.2.2.1 the engine is a relatively correlated source, at least in half engine orders where sound generation is dominant. However, non-uniform engine sound directivity (discussed in 4.2), is further evidence of the presence of finite–sized region of correlated source activity [**6**].

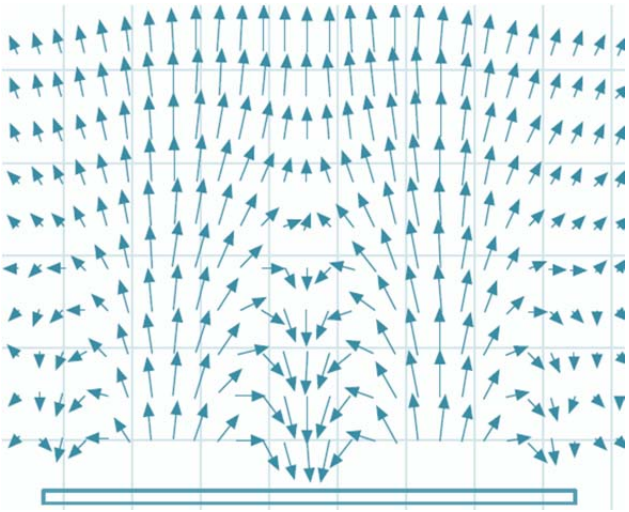

**Figure 2-3 Sound field close to the source (picture from [9])**

In the geometric near field in which the source subtends a large angle at an observation point, the pressure doesn't vary inversely by distance from the source center, and neither the particle velocity nor the intensity vector are necessarily directed from the source, although pressure and velocity phase difference may be quite small. This is illustrated by the sound field of a baffled plate in Figure 2-3. This situation is in contradiction with assumption in extracting the equation 2-2 for sound power calculation, meaning that $|\mathrm{I}| = \tilde{p}^2 / \rho_0 c_0$ is not essentially valid. [**6**]

In the geometric far field where the source subtends a solid angle of much less than a steradian[1] at any field point, the wave front is nearly spherical and pressure and particle velocity are nearly in-phase and fully radially directed, in other words, $|\mathrm{I}| = \tilde{p}^2 / \rho_0 c_0$ and there is no need for sound intensity measurement. [**6**] The subtended angle of an observer has been illustrated in Figure 2-4.

[1] The steradian (symbol: sr) is the SI unit of solid angle. It is used to quantify two-dimensional angular spans in three-dimensional space, analogously to how the radian quantifies angles in a plane.(source: Wikipedia)

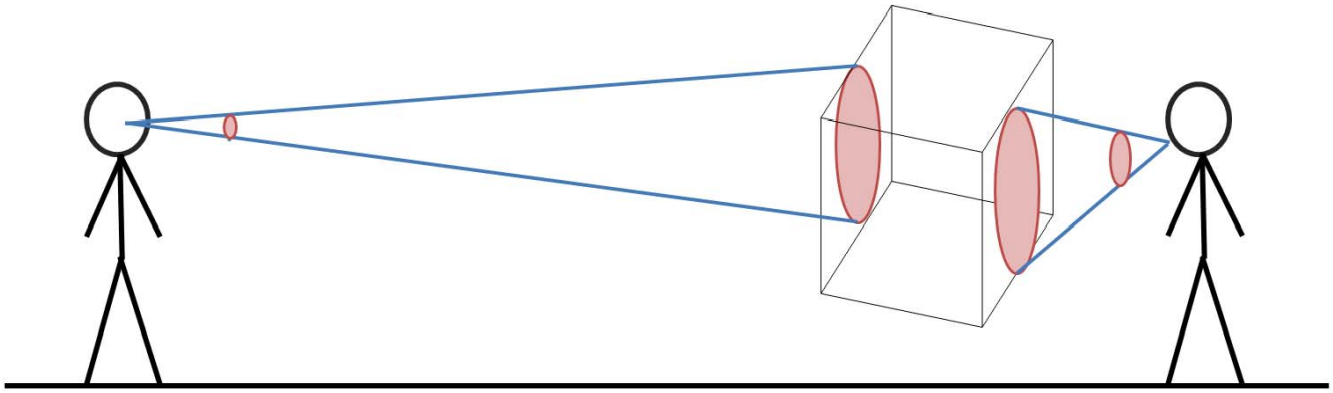

**Figure 2-4 Subtended angle; left (small angle), right (large angle)**

Bias [**8**] discussed that the sound power could be calculated in the geometric near field provided that the surface of integration can be suitably defined. Although the measurement surface in the standard may enter the geometrical near field the error in the assumption that sound power propagates in a direction normal to the measurement will probably be quite acceptable [**8**]. However any directivity measurement made in this region, must be interpreted with caution [**8**].

### 2.2.4 Acoustic center

While the term "acoustic center" is not explicitly described in ISO 3745 it is still mentioned that the measurement surface (generally a sphere or hemisphere) should be positioned in the acoustic center of the test object. [**1**] There is a definition formulated by Jonasson [**10**] which is as follows: "*The postulated position of the equivalent point source yielding the same sound pressure level in an emission measurement point as the source under study*".

Acoustic center is basically the effective source center and the reference for calculating the measurement radius such as hemispherical/spherical imaginary measurement surface. The typical acoustic centers for free field (anechoic) and hard floor (Semi-Anechoic) conditions are shown in Figure 2-5. [**11**]

More precisely, the acoustic center is a function of the microphone location, object size, wavelength and hemisphere radius, [**12**] so it is dependent on frequency.

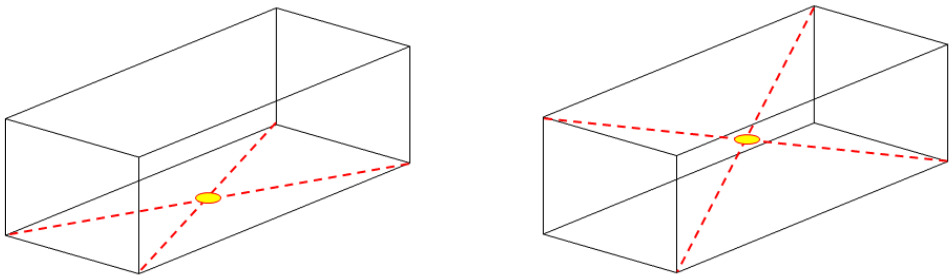

**Figure 2-5 The acoustic center for, Right: Anechoic room, Left: Semi-anechoic room**

### 2.2.5 Reverberant field

If the sound source is located in a room or enclosure which doesn't have highly absorptive walls, the reflection of the sound will be superimposed with the direct sound and the resultant sound field is called the reverberant field. In this case the absorption quality is especially poor directly beneath the engine. The measurement and the quality of absorption are described in section 4.1.1. It is clear that the monotonical decrease of pressure at the rate of 6 dB for each doubling of distance is not valid here.

Without any reflection, the sound field is not reverberant and is called the free field. One way to produce a free field for the study of the sound radiation is to construct a room that absorbs all sound waves. Such a room is known as an anechoic chamber and is similar to a boundary-free space but it has the advantage of very low background noise.

### 2.2.6 Sound directivity

Most practical sources (spatially distributed), like engines, exhibit the behavior of '*directivity*' in which the far field mean square pressure and intensity vary with angular position with regard to the source's acoustic center. This directivity can be explained in terms of the interference between the waves radiated from its various elemental regions. An example of this directivity for two point monopoles of arbitrary time dependence is presented by Fahy [**4**]. A simple point Monopole source doesn't have any directivity so the sound field can be described by only one measurement. However, the sound field for a complex source such as an engine, multiple measurement points are required (Figure 2-6 ). A two dimensional cross-section of engine sound directivity is indicated in Figure 2-7.

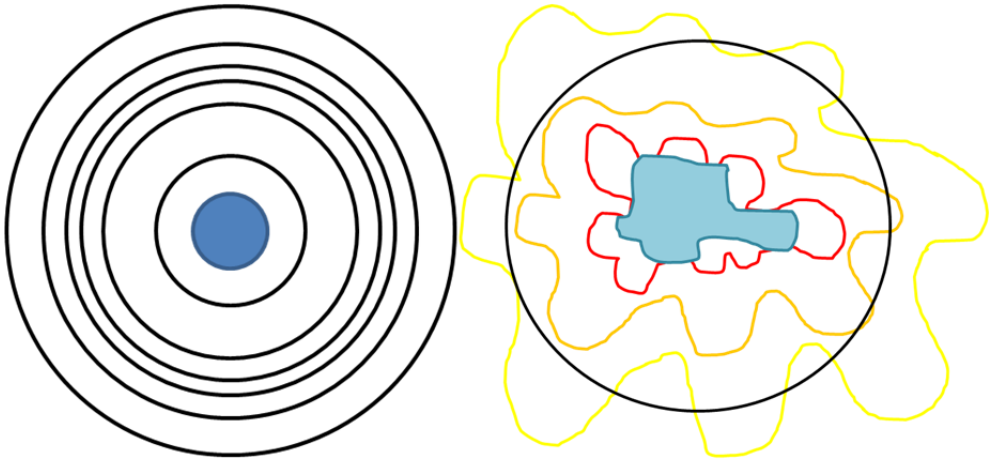

**Figure 2-6 The directivity of monopole (left) vs. engine sound field (right), shown with Iso-pressure lines[2]**

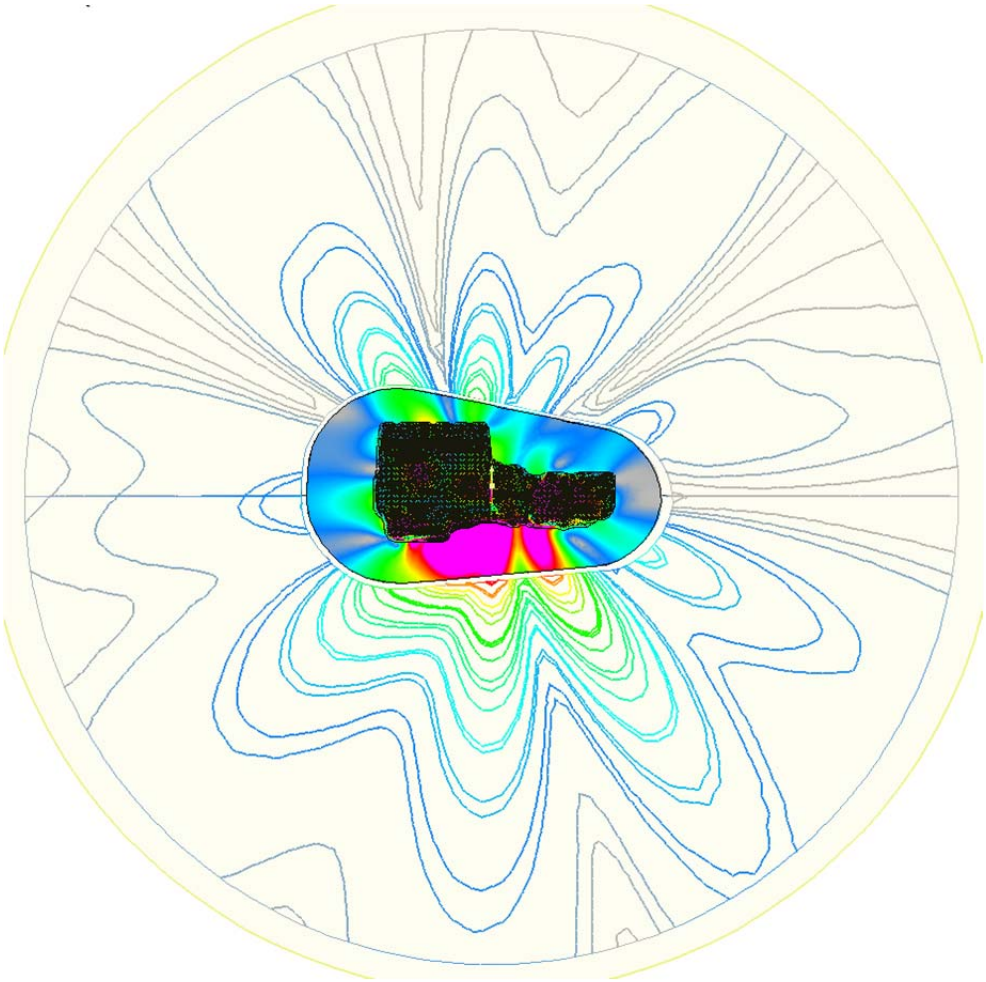

**Figure 2-7 The engine sound field directivity in 540 Hz and 1500 rpm, Iso-pressure[2] lines**

[2] Iso–pressure: The Surfaces (in 3D or lines in 2D) in the fluid mesh (air), which have same pressures value, the word is borrowed from µETA a multi-purpose post-processor.

Considering the ⟨I⟩ as average sound intensity over an encompassing spherical surface, it could be written that:

$$\langle I \rangle = \frac{W}{4\pi r^2} \qquad \textbf{Eq. 2-3}$$

Where W is the total power and r is the radius of the encompassing sphere. The directivity factor has been described by Bias [**3**] as follows:

$$D_\theta = \frac{I_\theta}{\langle I \rangle} \qquad \textbf{Eq. 2-4}$$

And the directivity index is defined as:

$$DI = 10 log_{10} D_\theta \qquad \textbf{Eq. 2-5}$$

However, it has been described differently based on the pressure by Jonsson [**10**]

$$DI_i = L_{pi} - \langle L_P \rangle \qquad \textbf{Eq. 2-6}$$

As will be discussed in section 5.3, this is one of the most important requirements of the standard to fulfill and, as will later be demonstrated by the results, this is also the most difficult requirement to deal with.

It should be noted that standard criteria limit neither of these directivity indexes, instead limiting $Max(L_P)$-$Min(L_P)$, which is basically the difference between the maximum and minimum measured sound pressure levels in the array of microphones in the hypothetical sphere. This value should be lower than half of the number of microphones [**13**].

### 2.2.7 Sound Coherence

In a signal analysis context, coherence is a measure of linear association between two signals or in the other words, how much two signals have in common. A high coherence between two microphones in different positions in the sound field means that the noise in these positions comes from the same source. If these positions are well apart we can assume that different engine surfaces radiate with a fixed phase relationship and that the basic mechanical source is the same (for instance the crank motion). As an effect of destructive/constructive interference the directivity will be larger compared to a non-coherent case.

As a measure of the degree of linear association between two signals (here two sound pressures signals), the ordinary coherence function is widely used. The ordinary coherence function (or simply the coherence function, $\gamma_{xy}$) between two signals x(t) and y(t) is defined as equation 2-7 [**14**].

$$\gamma_{xy}^2 = \frac{\left|G_{xy}(f)\right|^2}{G_{xx}(f)G_{yy}(f)} = \frac{\left|S_{xy}(f)\right|^2}{S_{xx}(f)S_{yy}(f)} \qquad \text{Eq. 2-7}$$

Where $S_{xx}, S_{yy}$ are the power spectral density function, and $S_{xy}$ is cross-spectral density function, and $G_{xx}, G_{yy}$ are the one sided power spectral density function, and $G_{xy}$ is one sided Cross-spectral Density Function [**14**].

### 2.2.8 Far field condition (Franhaufer region)

As discussed previously there are three regions of sound field around a sound source in a free field. However, the margins between these fields are not sharply defined but rather merged into one another.

Far field conditions have been explained in various literatures. Based on Bies the far field can be characterized by three criteria [**3**], [**8**]:

1- The pressure decreases monotonically relative to the inverse of the distance from the effective source center

2- The angular pressure amplitude distribution does not vary with increasing distance.

3- The specific acoustic impedance is the same as in the plane-wave case,

All three criteria may be reformulated in terms of characteristic length and wavelength:

$$\begin{cases} R \gg l^2/\lambda \\ R \gg l \\ R \gg \lambda \end{cases}$$

Where $\lambda$ is the wavelength and $l$ is the characteristic dimension of the source in meter and *R* is the distance from effective source center to the observation point, in meter.

These three criteria can be presented graphically as Figure 2-8 [**3**]. These criteria are very conservative and much tighter than the ones in standard ISO 3745 but share the same underlying physics.

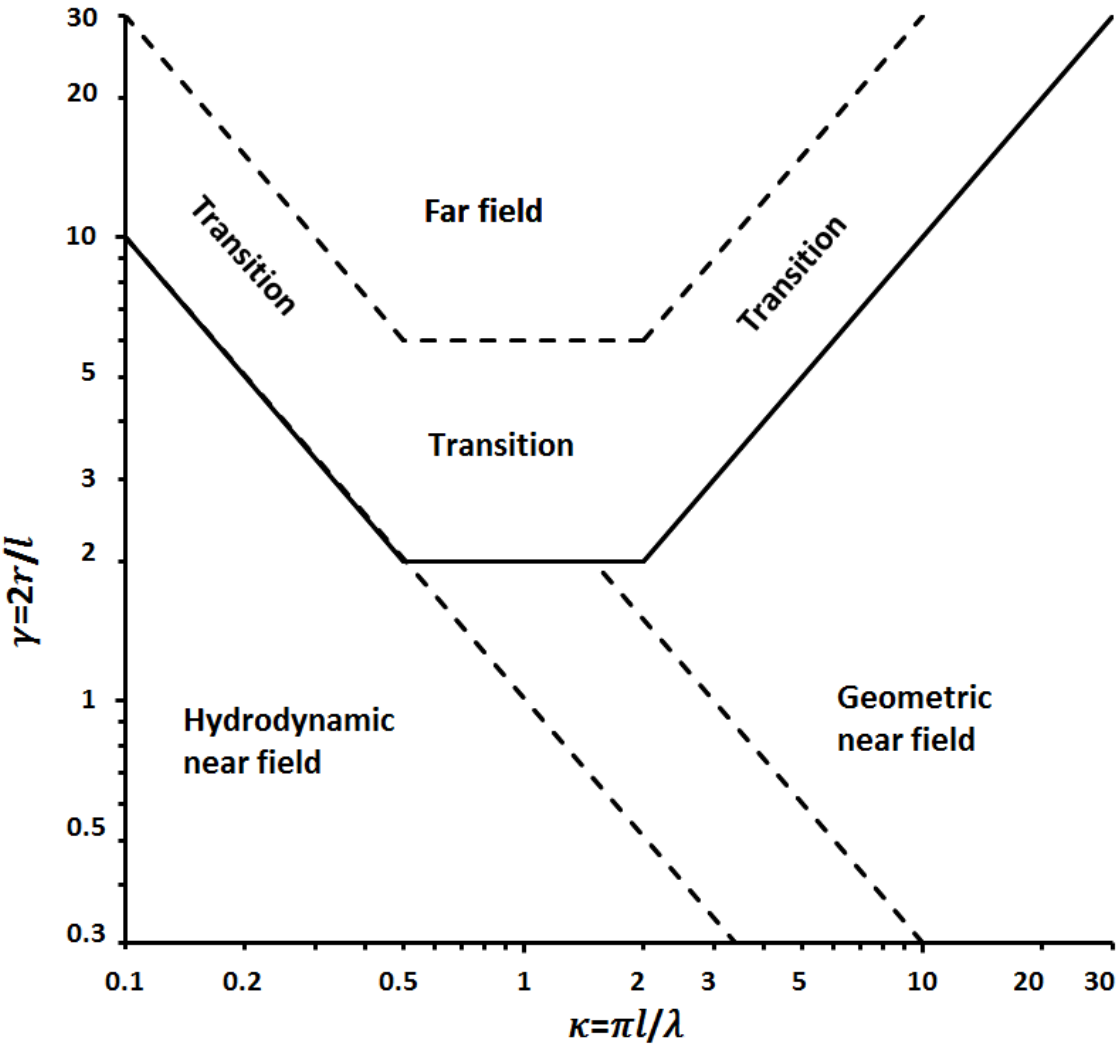


**Figure 2-8 The radiation field of a source, picture reproduce from [3].**

## *2.3 ISO 3745*

As it has been discussed before the method ISO 3745 was chosen for sound power measurement. The sound power is obtained by integrating sound intensity (or more accurately the average sound pressure) over a hypothetical spherical surface assuming plane wave conditions. The main formulation is based on the equation 2-2. This standard requires an anechoic or semi-anechoic room i.e. free field conditions. The standard also limits the minimum number of microphones and their locations. Since this is a precision method there is a low *acceptable uncertainty level* in measurement as shown in Table 2-1.

**Table 2-1 Acceptable uncertainty in Standard ISO 3745 [13]**

| One-third-octave midband frequency Hz | Upper values of standard deviation of reproducibility, $\sigma_R$ dB | |
|---|---|---|
| | Anechoic room | Hemi-anechoic room |
| 50 to 80[a] | 2,0 | 2,0 |
| 100 to 630 | 1,0 | 1,5 |
| 800 to 5 000 | 0,5 | 1,0 |
| 6 300 to 10 000 | 1,0 | 1,5 |
| 12 500 to 20 000[b] | 2,0 | 2,0 |
| A-weighted | 0,5 | 0,5 |

### 2.3.1 Requirements for Microphone location

The hypothetical surface of microphones has to encompass the object, like a hemisphere in a semi-anechoic room and a full sphere for an anechoic room. The center of the sphere should coincide with the acoustic center of the object (approximately the geometrical center of the source).

The sphere should be chosen such that its measurement surface is located in the far field or where the sound intensity is in direct relation to sound pressure. At the very least, the surface may lie within the geometric near field in which sound power levels (although perhaps not reliable directivity) can be obtained. However, it should not be inside the hydrodynamic near field [**15**] .

According to the standard the sound sphere radius should be larger than a quarter of the wavelength of the propagating wave, and should have a radius of at least twice the major machine dimensions, but not less than 1 m. Besides that the microphones should be at a distance of a quarter wavelength from all room walls as well. For an engine with a major dimension of 2 m and for a frequency of 125 Hz the geometric near field is from about 1.3 to 2.3 m and the far field will lie at distances greater than roughly 6.5 m. It can be seen that a rather large room is required for such a measurement. Excessively large anechoic rooms are strongly recommended (based on recommendation in ISO 3745:2004, two hundred times the object major dimension) however due to resource and space limitations this is not always achievable.

As a part of this thesis, the effects of microphone location have been studied for different cases with the engine model. It has been discussed how much uncertainty

the different microphone arrangements at different distances will introduce in the system.

### 2.3.2 Microphones arrangement

There are different microphone arrangements in this standard [**13**] consisting of both stationary and rotating microphones. One stationary arrangement for semi-anechoic rooms, an ISO hemisphere, is shown in Figure 2-9 below.

The reason for the high number of microphones in this standard is to have sufficient averaging points for highly directive sound sources. The number of microphones is twenty and if the directivity ($Max(L_P)$-$Min(L_P)$) is higher than 10 dB, a new set of measurements (after rotating the microphone array or source by 180 degrees) have to be performed. The total number of microphones has been increased in a recent edition of this standard to 40.

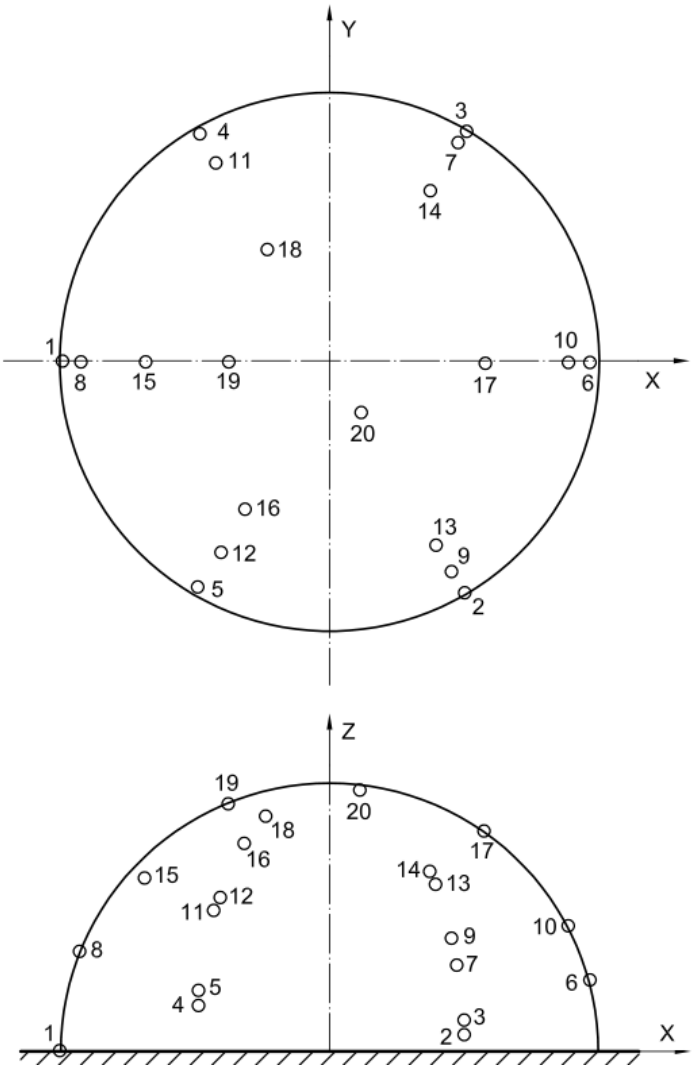


**Figure 2-9 The array of the michropones (Picture from [13])**

### 2.3.3 Room qualification

Calibration of the semi-anechoic chamber A1 at Scania in Södertälje has been performed and reported by Tyrens [**11**]. The measurements were performed according to standard ISO 3745:2004 Appendix A [**13**]. The purpose of this survey was to determine how large the deviation from a free field was in the room. This deviation is described as the deviation from the inverse-square law.

A broadband noise source was placed in the middle of the room. From the sound source, traverse microphone paths were created in nine different directions. Sound pressure levels were measured when the loudspeaker rotating at a constant rate. In order to guarantee sufficiently omni-directional characteristics throughout the entire frequency range (20 Hz - 12.5 kHz) two sound sources were been used.

In Scania-predefined positions, microphone positions 2, 3, 4 and 6 (the arrangement shown in Figure 2-9) are ideally placed for measurement in room A1 in accordance with the requirements contained in the above standard for the limited frequency range 50 Hz - 12.5 kHz. Some of the other measurement positions do not satisfy the criteria of ISO 3745:2004 for all frequencies [**11**].

The room deviation from the free field tends to become smaller as the distance from the sound source is increased (the sound source is placed on the floor plates in the middle of the room). A likely explanation for this is that close to the floor plates, engine mounts and connecting pipes have an audible effect by reflections, possible sound radiation and cavity resonance increasing deviation from the free field. Furthermore, the measurement results show that acoustic room resonances in ⅓ octave bands 40 Hz and 50 Hz result in large deviations from the free field in some positions. [**11**]

### 2.3.4 Sound Measurement

The measurements are to be done in ⅓-octave band. For frequency bands centered around or below 160 Hz, the measurement time interval shall be at least 30 seconds. For A-weighted sound pressure levels and for frequency bands centered around or above 200 Hz, the measurement time interval shall be at least 10 seconds. [**13**]

### 2.3.5 Sound power calculation in ISO 3745

The sound power is calculated based on the equation 2-8 where $C_1$ and $C_2$ are correction factors for room temperature and pressure respectively (Deviation from

$\rho_0 c_0 = 400$, in calculation of equation 2-2). The correction for background noise and humidity is also taken into account. It should be noted that all values reported are A-weighted [**13**].

$$L_w = \overline{L_{pf}} + 10 \times \log_{10} \frac{S_1}{S_0} + C_1 + C_2 \qquad \text{Eq. 2-8}$$

Where

$$C_1 = -10 \lg \left[ \frac{B}{B_0} \sqrt{\frac{313.15}{273.15 + \theta}} \right] \qquad \text{Eq. 2-9}$$

$$C_2 = -15 \lg \left[ \frac{B}{B_0} \sqrt{\frac{296.15}{273.15 + \theta}} \right] \qquad \text{Eq. 2-10}$$

$\overline{L_{pf}}$ is the surface sound pressure level over the test sphere, in decibels (ref. 20 μPa);

$S_1$ = 4 π $r^2$ is the area of the test sphere (of radius $r$);

$S_0$ = 1 $m^2$;

$B$ is the barometric pressure during the measurements, in pascals;

$B_0$ is the reference barometric pressure, 1,01325 × $10^5$ Pa;

$\theta$ is the air temperature during measurement, in degrees Celsius.

Eq. 2-8 is applicable in the temperature range 15 °C ≤ θ ≤ 30 °C

### 2.3.6 Case of Scania's anechoic room

So far, the standard requirements and the physics behind it have been discussed. As mentioned before, the hypothetical surface encompassing the noise source should be a closed surface in order to obtain the average of total radiated sound.

The limitations and difficulties involved with Scania's anechoic room can be listed as follows:

1. There is reflection from the floor underneath the engine (Figure 1-1)

2. There is no space for a full hemisphere microphone arrangement for the sound underneath (Figure 1-1)
3. The microphones underneath are too close to the engine surface compared to the standard criteria
4. There are not enough channels to add the desired number of microphones
5. The largest dimension of the top hemisphere is limited by the room size

# 3 Engine model

The model only studies the structural noise, which is radiated from the engine surface. The procedure of the acoustic model simulation is shown in Figure 3-1. Cylinder combustion pressures are applied to the dynamic model in AVL Excite. Engine surface velocities are extracted from the dynamic model and are then used as boundary conditions in the acoustic model to find the acoustic response of the object.

It has to be mentioned that not all components e.g. oil filter are represented in the dynamic model and neither are all the details. In addition, not all excitations are included, such as gear train. Therefore, the sound field is not exactly what it is in reality but the nature of the acoustic sound field in general is very similar to the engine. Beside the reason for using this model here is to calculate the sound power, which as will be discussed, has been used to estimate the power and compare different cases in the engine model. However, the near fields zones and limitations are rather similar because the dynamics of the engine structure and vibrational modes are very similar to the real engine.

The velocities along the block liner have been compared with measurements and simulations on an early Excite model by Adam Wikström with fair agreement in (Scania internal report). In an improved model, the crank motion has been verified with measurement, with very good agreement. Indirect verifications have been made in Scania during a period of several years when noise measures like ladder frame and other reinforcements were simulated and later tested with equal noise reductions.

## *3.1 Model description*

The acoustic FEM model of the engine has been built in Nastran. The model contains three different regions; the engine surface-wrapped mesh, which is the source of the

excitation in this model, the FEM mesh that is the fluid (air), and a non-reflective boundary condition for simulating free field conditions. These three regions are indicated in Figure 3-2. In the software approach, every node in the FEM mesh has one degree of freedom (pressure) and velocity vector is the derivative of the pressure, so there is more numerical error in velocity.

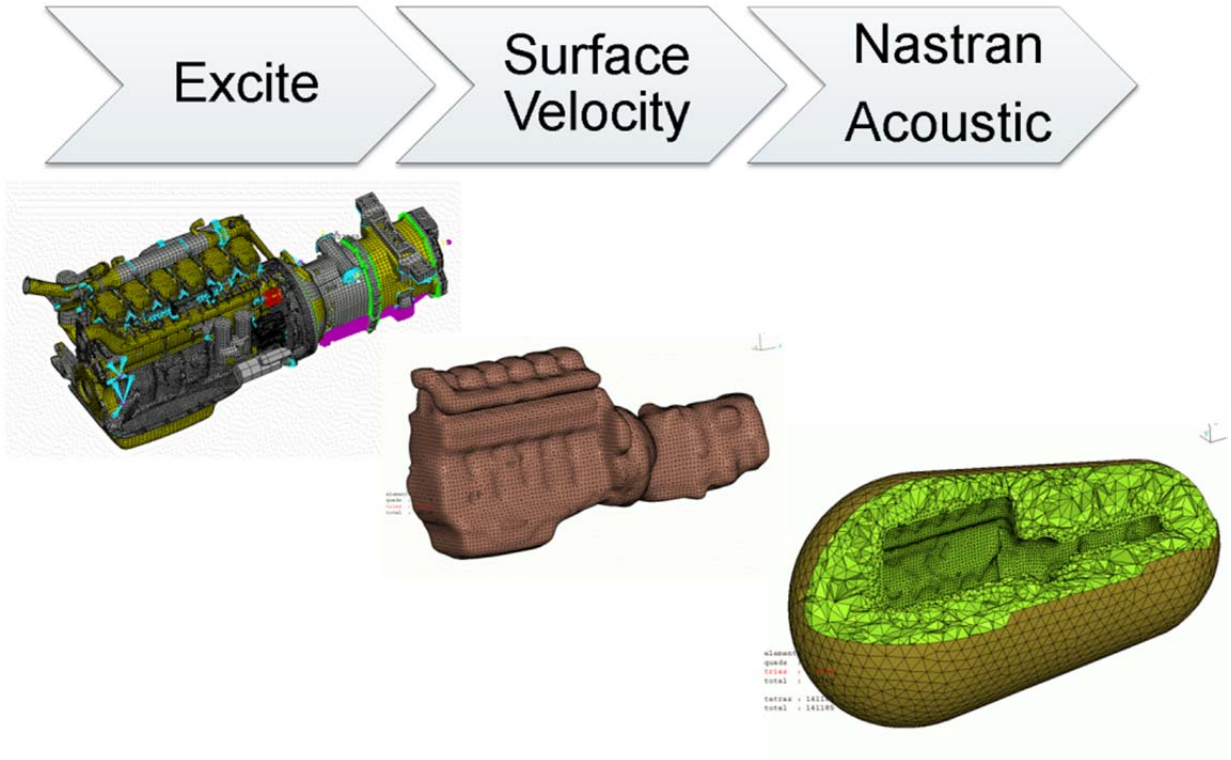


**Figure 3-1 The procedure of engine model acoustic model**

### 3.1.1 Boundary condition and Infinite elements

The reflection-free boundary condition has been provided by CACINF elements, so called infinite elements [**16**]. This element is used for exterior acoustic problem, to provide the free field condition. The acoustic center location is an input to the software to be used by this element (Figure 3-3). the interpolation order is also defined, which is basically the concept of first order for monopoles, second order for dipoles, third order for quadrupoles, and higher orders [**17**].

The numerical method used in exterior acoustics in NASTRAN considers an acoustic center for interpolation, which has to be almost at the geometrical center of the engine-wrapped surface and it has the same nature of acoustic center as discussed earlier. Adding a reflective surface creates a mirror source with a shifted acoustic center which does not fit this numerical method in NASTRAN. Therefore, it is not

possible to simulate the reflections in the room bottom in the model. This is indicated in appendix A and B for a monopole acoustic model. Therefore, dealing with absorption related problems was only possible through measurement.

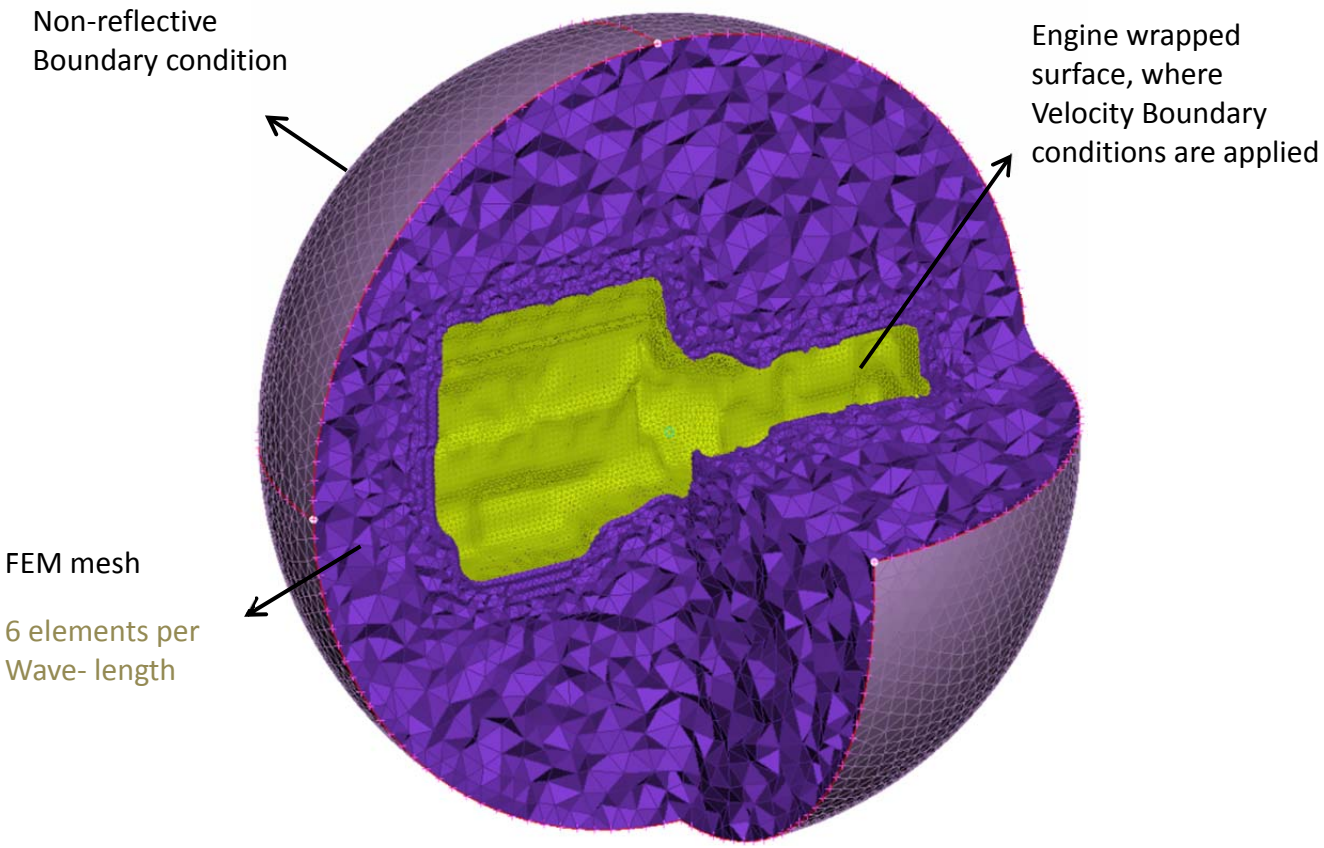


**Figure 3-2 The structure of the acoustic model in NASTRAN**

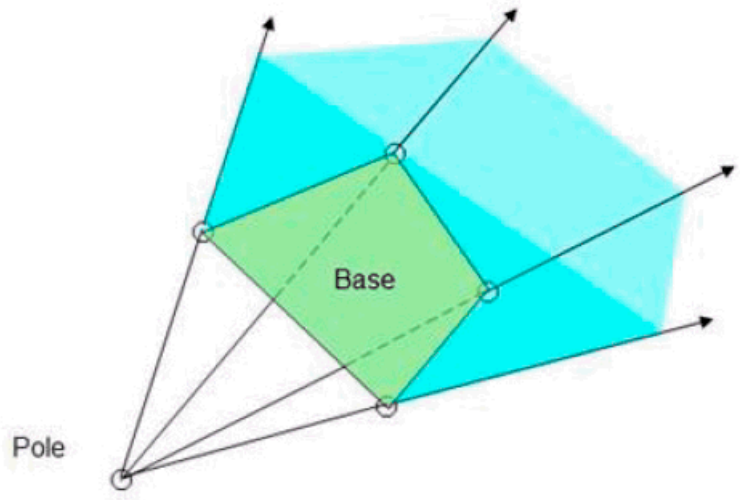


**Figure 3-3 Infinite element in NASTRAN**

The engine surface is in interaction with the fluid. The no-slip condition, that the relative velocity of fluid in contact with the solid surface is zero. This is derived from the idea that fluid molecules in the immediate vicinity of the surface are in thermodynamic equilibrium with the solid surface. This means that the normal velocity of the surface is equal the normal component of fluid velocity [**18**]. Howe has discussed this boundary condition in more details [**18**]. Velocities extracted from dynamic simulation in AVL Excite applied to shell elements. The coupling of solid shell structures with the surrounding fluid FEM mesh is generated automatically in the software. These velocities has been extracted from the engine global dynamic model in AVL\Excite for every engine speed individually, from 800 to 2300 rpm. Each one of these speeds has the fundamental frequency, (half of the engine speed in rpm divided by sixty), the engine half-order which is the engine fundamental order for a 4 stroke engine. As we will see in the measurement in section 4.2, the sound field around the engine is dominated by the engine orders .i.e. fundamental order and its multiples. The simulation has been solved for these frequencies; e.g. for engine speed 1800 rpm the fundamental order is 15 Hz, the solution would be carried out for 15, 30,45,60,75,... Hz, up to 2 kHz.

Since this is an exterior acoustic problem and we can't have infinite FEM model The engine-surrounding fluid (air) should be cut out. The smaller this enclosed surface the lower the number of elements and hence DOF, to provide the six elements per wavelength criterion in the FEM mesh. However, it has been said by MSC that this surface should only have a convex shape [**17**], the shape of this surface will affect the result by creating distortion in the pressure field which will lead to a wrong derivation i.e. velocity (Appendix B). This is another reason why absorption cannot be modeled in this exterior acoustics problem (at least for frequencies higher than 400 Hz).

The ideal cut of the fluid is a sphere but it has been shown that for this special case i.e. 25 mm on the engine surface to 50 mm in the fluid mesh it doesn't change the result very much (compared with an egg-shaped equivalent). However, sphere model is almost thirty times slower than an eggs-shaped model. The effects of an egg- or sphere-shaped model on results is discussed in Appendix C, and finally the egg shaped model, as shown in Figure 3-4, was selected due to shorter simulation time. This model contains FEM mesh with the elements size of 25 mm from engine surface to 50 mm on the outer surface, which means the model is only valid up to 1.2 kHz. Despite this fact however, results are presented and discussed up to 2 kHz. It has to

be mentioned that decreasing the size of the mesh by a factor $n$ will increase the number of elements by a factor of $n^3$ , tremendously increases the simulation time which is very impractical. Here however the frequency limit of the model is not so high; nonetheless, simulation time varies between 35 to 20 hours for each engine speed.

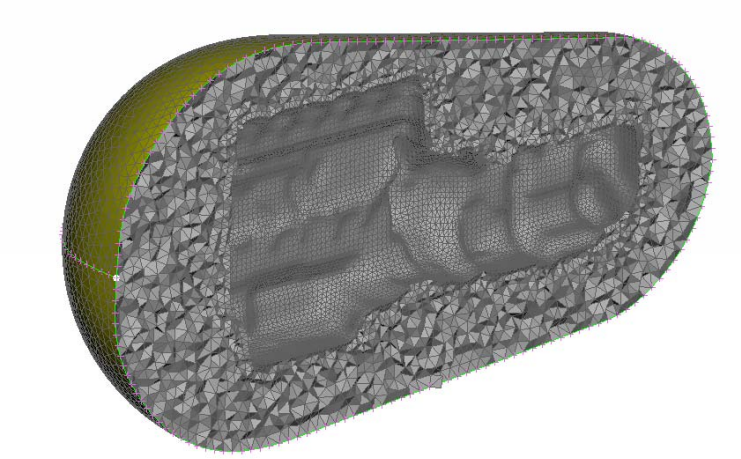

**Figure 3-4 The final Mesh which has been used in Engine acoustic model in NASTRAN**

## *3.2 Sound power calculation in NASTRAN*

In the case of fluid-structure interaction in acoustic simulations in Nastran the sound power could be evaluated on the structure surface; the "*wetted power*". Since this velocity boundary condition is applied on the structure surface, it has been observed that this power has a low error level compared to the analytical solutions of different monopole models (Appendix C). The reason lies in the fact that the velocity is known at this surface and only pressure has been calculated.

To retrieve the data outside of the reflection-free boundary condition one could ask for pressure and other results using a so-called "*field point*[3]" mesh. The sound power from the pressures in this field point mesh is calculated based on equation 2-2. An indication of the wetted surface (excitation surface) and field point mesh is shown in Figure 3-5.

[3] This name will be used extensively in the rest of thesis

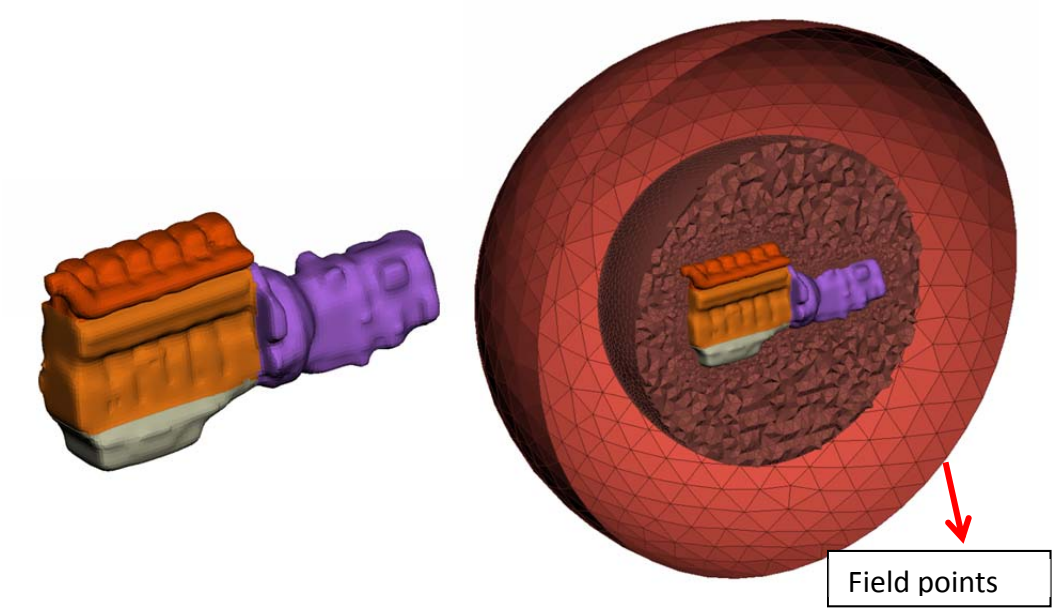


**Figure 3-5 Left: wetted surface Right: field point mesh (the larger sphere)**

## *3.3 Monopole FEM model vs. analytical solution*

To study the sensitivity of the model to mesh size, and accuracy compare to analytical solution the results are studied here. The monopole acoustic model has been built as shown in Figure 3-6.

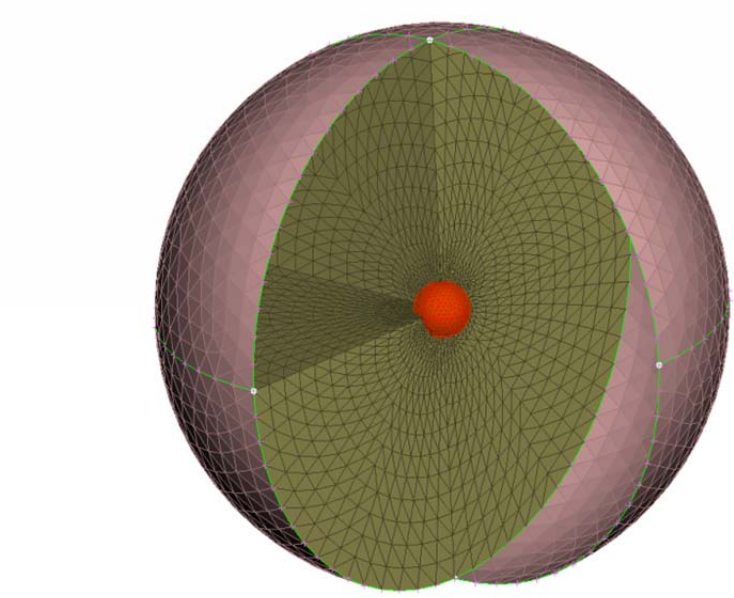

**Figure 3-6 Monopole model in NASTRAN**

The analytical solution for pressure and velocity at the distance of $r$ in the sound field of a pulsating sphere (monopole) could be presented as equation 3-1 and 3-2 [**19**]:

$$v_r = -v_a \frac{a^2}{1+jk_0a} \frac{1+jk_0r}{r^2} e^{-jk_0r} \quad \textbf{Eq. 3-1}$$

$$p_r = v_a \frac{j\omega\rho_0 a^2}{1+jk_0a} \frac{e^{-jk_0r}}{r} \quad \textbf{Eq. 3-2}$$

Where $a$ is the sphere radius, $v_a$ is the amplitude of the vibration and $k_0 = \omega/c_0$ is the wave number

The sound power calculated based on this pressure and velocity can be presented as:

$$W = \frac{1}{2} Re \left[ \int_S p_r v_r^* dS \right] = 2\pi a^2 |v_a| \rho_0 c_0 \frac{(k_0a)^2}{1+(k_0a)^2} \quad \textbf{Eq. 3-3}$$

The comparison between this result and the solution for 3.2 kHz is shown in Figure 3-7, as it is clear there are low errors in the predicted values. The element size here varies between 5 and 25 mm. In order to simulate conditions analogues to those in the engine model, two more monopole models were been studied with the same element size from 25 to 50 mm. These results are presented in Appendix C.

Deviations started almost in 1.4 kHz, however both the "*wetted power*" and "*field point*" power (from the averaging of 98 points) are rather good up to 2 kHz. It is worth repeating that the wetted power could be used as a reference since it has lower numerical error (Appendix C).

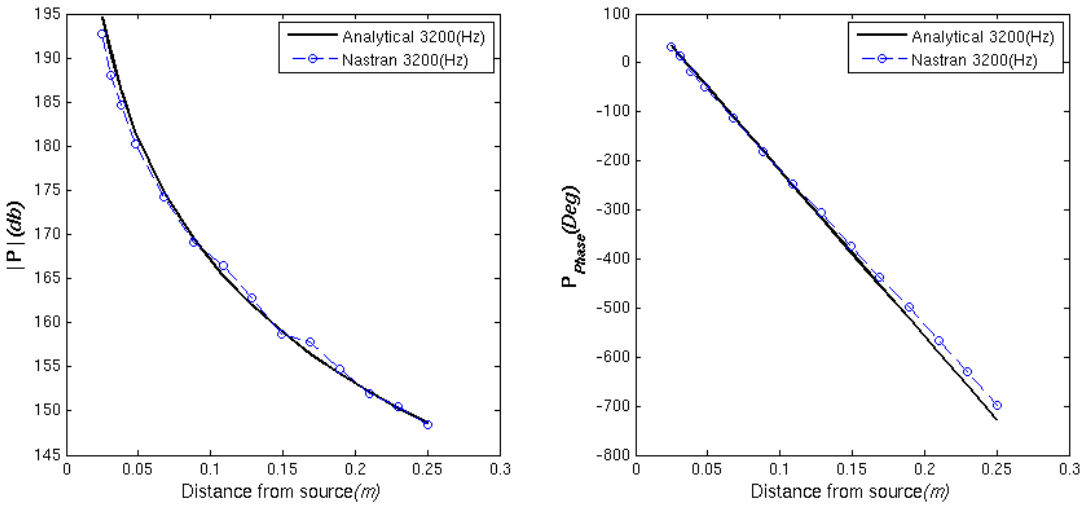


**Figure 3-7 The deviation of the pressure in the monopole problem**

# 4 Measurement

Different measurements have been performed in this thesis for different purposes, as listed in the Table 2-1.

**Table 4-1 Different measurements and their applications**

| | | Measured value | Purpose (application) |
|---|---|---|---|
| 1 | Room, Absorption Measurement | The absorption & Surface Impedance | To check the quality of absorbers, to be used in software |
| 2 | Room, Inverse Square law | The sound pressure in different distances from floor and vertical wall | To find the deviation from free field, finding correction factors |
| 3 | Engine, Inverse square law | The sound pressure in different distances from floor and vertical wall | Find the deviation in the sound field from loud speaker source in inverse square law |
| 4 | Engine, Microphone array, 4 plane measurement | Sound pressure in 4 Planes beneath the engine, with references | To check the directivity, repeatability, and coherence of the sound, |
| 5 | Engine, Top hemisphere | Sound pressure in top hemisphere | Check the directivity of the engine sound field to compare with NASTRAN model |

## *4.1 Room measurement*

### 4.1.1 Room Impedance & Absorption Coefficient

Measured surface impedance has been intended for use in the software but it has not been possible to apply it in the model due to limitations in the numerical method as discussed earlier. It is nevertheless useful to present the result to see the quality of the absorption, which tells where in the frequency domain modification or correction is required. The requirements of ISO3745:2003 on absorption coefficient of walls are for instance 99 percent absorption [**13**]. A view of the room with the source (loudspeaker) is shown in Figure 4-1.

**Figure 4-1 The loudspeaker in the anechoic room used for measurement of absorption and the inverse square law**

The measurement was carried out using an omni-directional sound source and intensity probe. Instrumentation used was as follows:

***Loudspeaker**: Omni- Power Source, B&K, S.N:95073*

***Signal generator**: Miniator MR-PRO NTI,*

***Intensity probe:** G.R.A.S Type 50GI, with 25 mm Spacer, ¼ ccp preamplifier set S.N: 121737 & 12744; Microphones: type:40GK , S.N: 118659 & 118685*

***Front end(signal acquisition):** LMS SCADAS Mobile, SCM01 , 8 channel, S.N : 47071709*

***Calibrator:** Pistonphone Type: G.R.A.S 42 AD , 114 dB, 250 Hz, S.N: 95073*

***Amplifier**: B&K Type: 2734 S.N: 014009*

There exists a great deal of literature on the measurement surface impedance and absorption in free field or in-situ, using a two-microphone technique [**20**], [**21**], [**22**]

and [**23**]**.** The intensity probe used here with a 25 mm spacer allows a frequency range between 100 Hz to 5 kHz as a result of very low phase mismatch error (less than 0.1 deg). First the microphones have been normal to the source close to a highly absorbent vertical wall, Figure 4-2. The distance was almost 5 meters from the source and with the microphones one meter away from wall. One typical FRF (Frequency Response Function) of the two microphones is presented in Figure 4-3. As it is clear there are many peaks and valleys; a deviation of this value from 'one' (Black dot-dash line) indicates different pressures in the two microphones, which reveals the presence of scattering of the sound. The intensity probe then has been checked with a calibrator (small cavity coupler) for phase mismatch error, and it has been proved that the problem is not from the probe. A good explanation for this can be the scattering of the sound by objects inside the room, such as the net floor, pipes, engine mounting arms, etc. With small displacement of the source or microphones (0.1 meter) the FRF is changed. By rotating the microphones 90 degrees, the transfer function for reflection could be calculated, but the reflection is not completely from the wall but also from other objects in room and varies from point to point.

It has to mention that this "sweeping" method does not work for real sound absorption measurement. Instead, this only gives some kind of average results in a certain frequency band. Since the room is designed for noise measurements and what we are interested is only the results in 1/3 octave band.

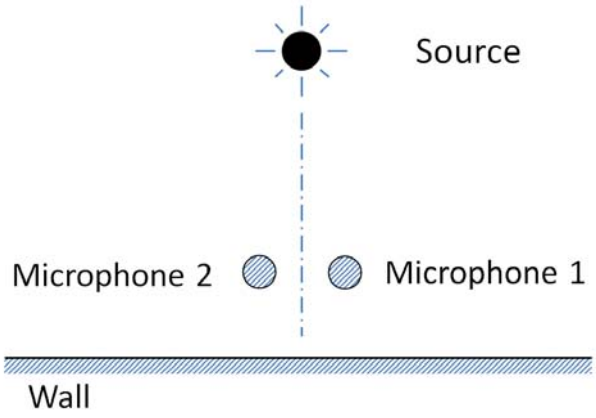


**Figure 4-2 Parallel arrangement of microphones relative to source**

As such, it has been decided to perform averaging by sweeping over the surface using an intensity probe as shown in Figure 4-4. On the other hand, absorbers underneath

the engine are randomly placed and are not uniform (Figure 4-5) which makes it more convenient to use a sweep method.

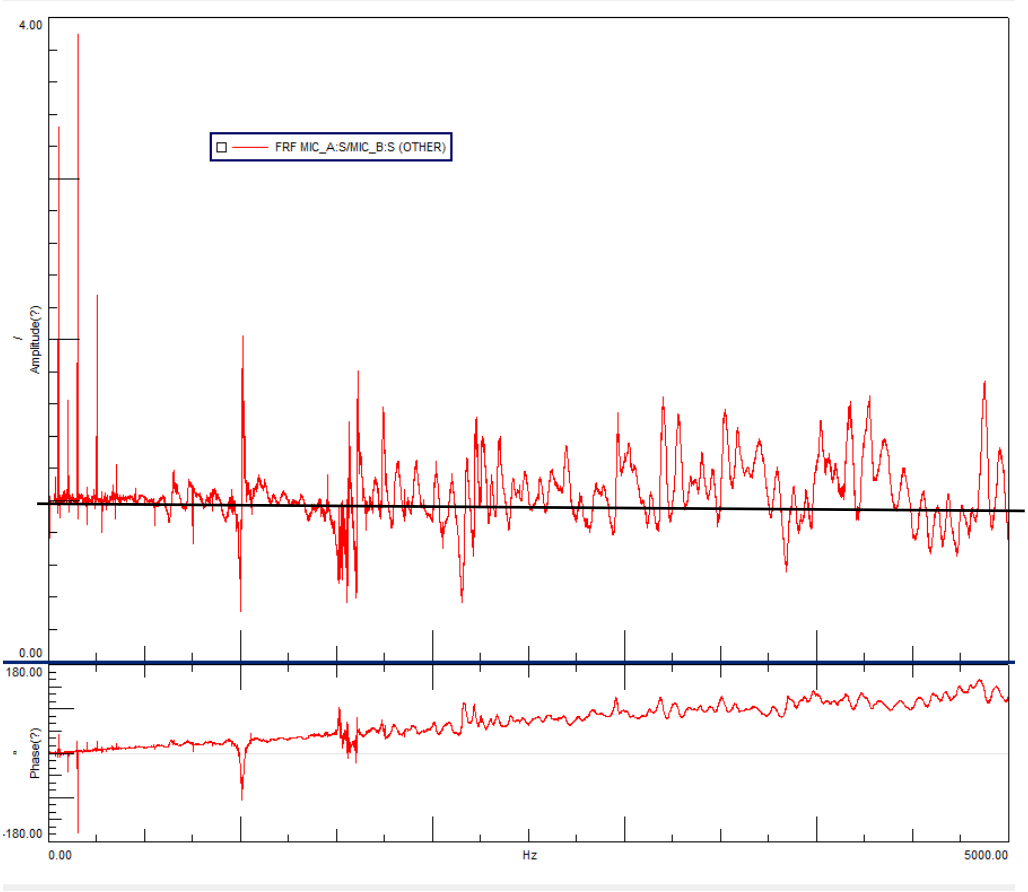


**Figure 4-3 The FRF function , Top: Amplitude, Bottom: Phase**

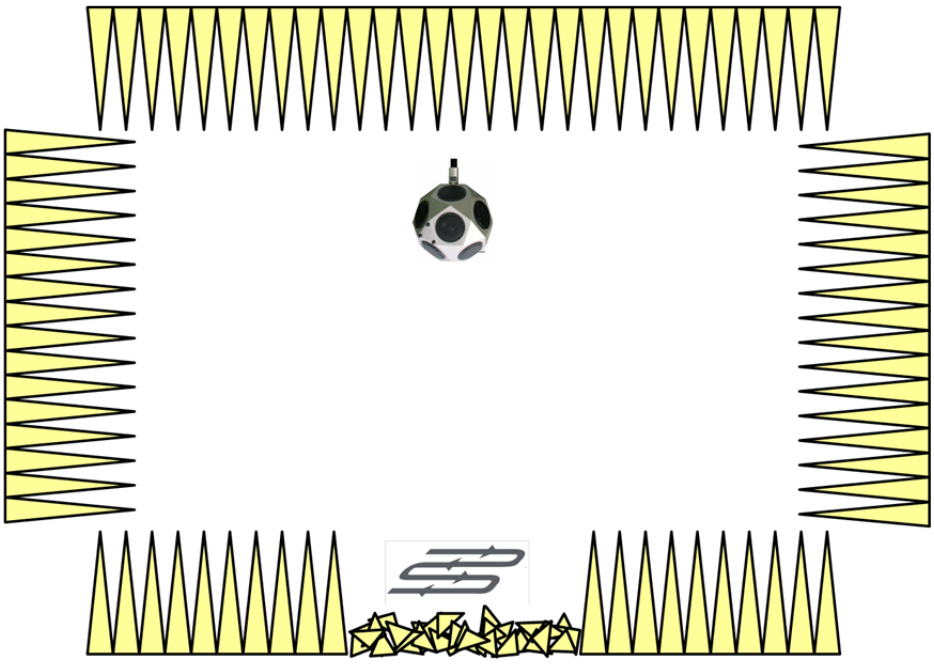

**Figure 4-4 The sweep for measuring the sound absorption**

**Figure 4-5 The surface of the absorber underneath the engine**

The loudspeaker has very low directionality [**24**], at least for low frequency, and it has been kept stationary during measurement at almost 3.2 meters away from the surface, to have a similar sound field. The measurement has been done with 25 averages and 1 Hz resolution. By measuring the FRF between two microphones as $H_{12}$ , the formulation for calculation of absorption ($\alpha$) and reflection ($R$) coefficient are as follows (for plane waves [**5**]):

$$\omega = 2\pi f, k_0 = \omega/c,$$

$$HI = e^{ik_0 s}, HR = e^{-ik_0 s},$$

*where **s** is spacer length(here 25 mm)*

$$\alpha = \frac{2 \times [real(HR \times H_{12}) - real(HI \times H_{12})]}{[1 + abs(H_{12}) \times abs(H_{12})]} - 2 \times real(HI \times H_{12})$$

$$R = \sqrt{1 - \alpha}$$

For comparison, the measurement has been carried out for a vertical wall and floor in the anechoic room. Filtration has been required as a result of the averaging method. Results have been filtered using MATLAB (Appendix D). The absorption and reflection coefficients are presented for the vertical wall and floor in Figure 4-6 and Figure 4-7. It is clear that the absorption of the floor is not good especially at low frequencies. Below 1 kHz is problematic and so requires special attention. In the next part the deviation from the inverse square law for this frequency range has been studied.

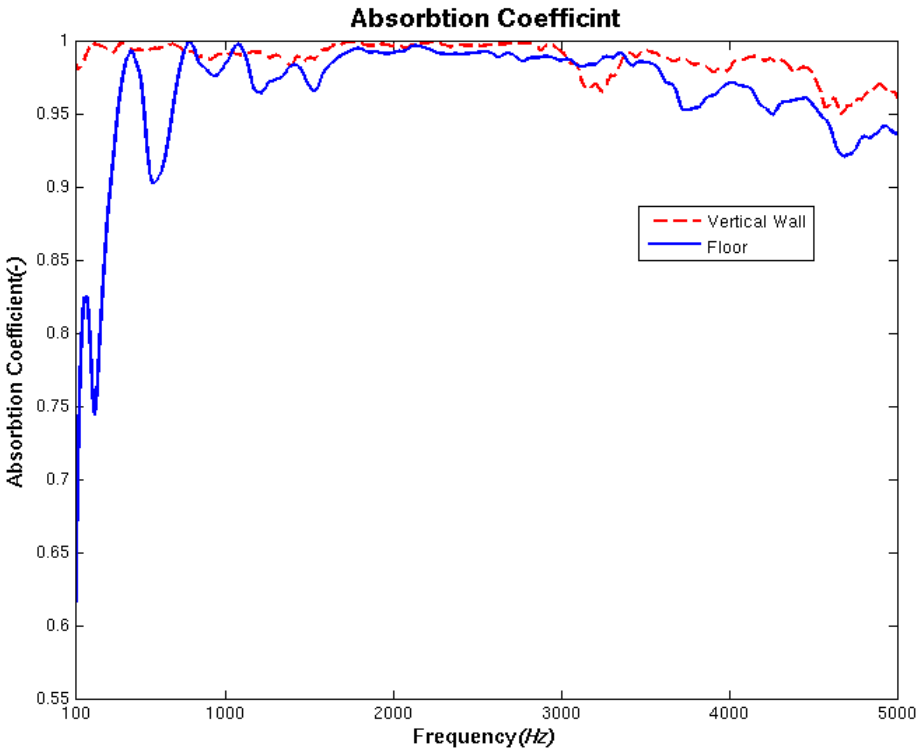


**Figure 4-6 The absorption coefficient of the floor and vertical wall**

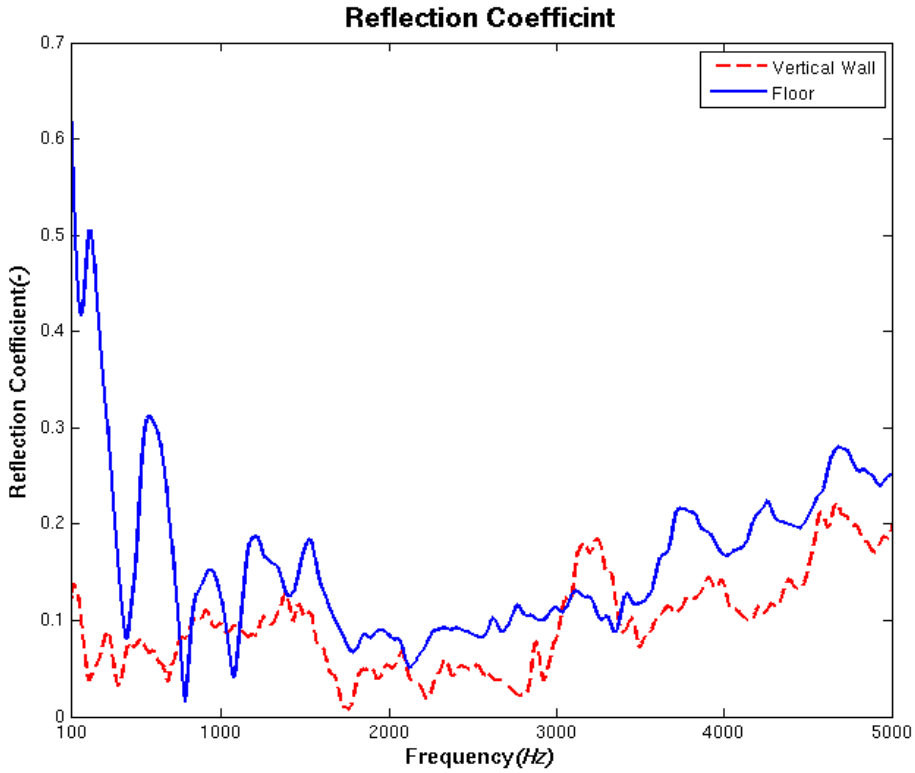


**Figure 4-7 The reflection coefficient**

### 4.1.2 Inverse square law (Measurement)

To study the effect of reflections from the walls a series of measurements have been carried out based on the inverse square law as shown in Figure 4-8; two sets on the floor (close ,1.36 m, and far, 3.2 m from the surface) to observe the effect of source distance and one on the vertical wall. The microphones were shifted every 10 cm. The results of the measurement are presented in appendix E for different ⅓ octave frequency bands between 63 and 1250 Hz .The result in 63 Hz band is presented but the room is not qualified at this frequency based on ISO 3745 (the evaluation discussed in section 2.3.3).

The results of this part it is presented in appendix E and have been used in section 5.2 to develop the correction factors for reflection.

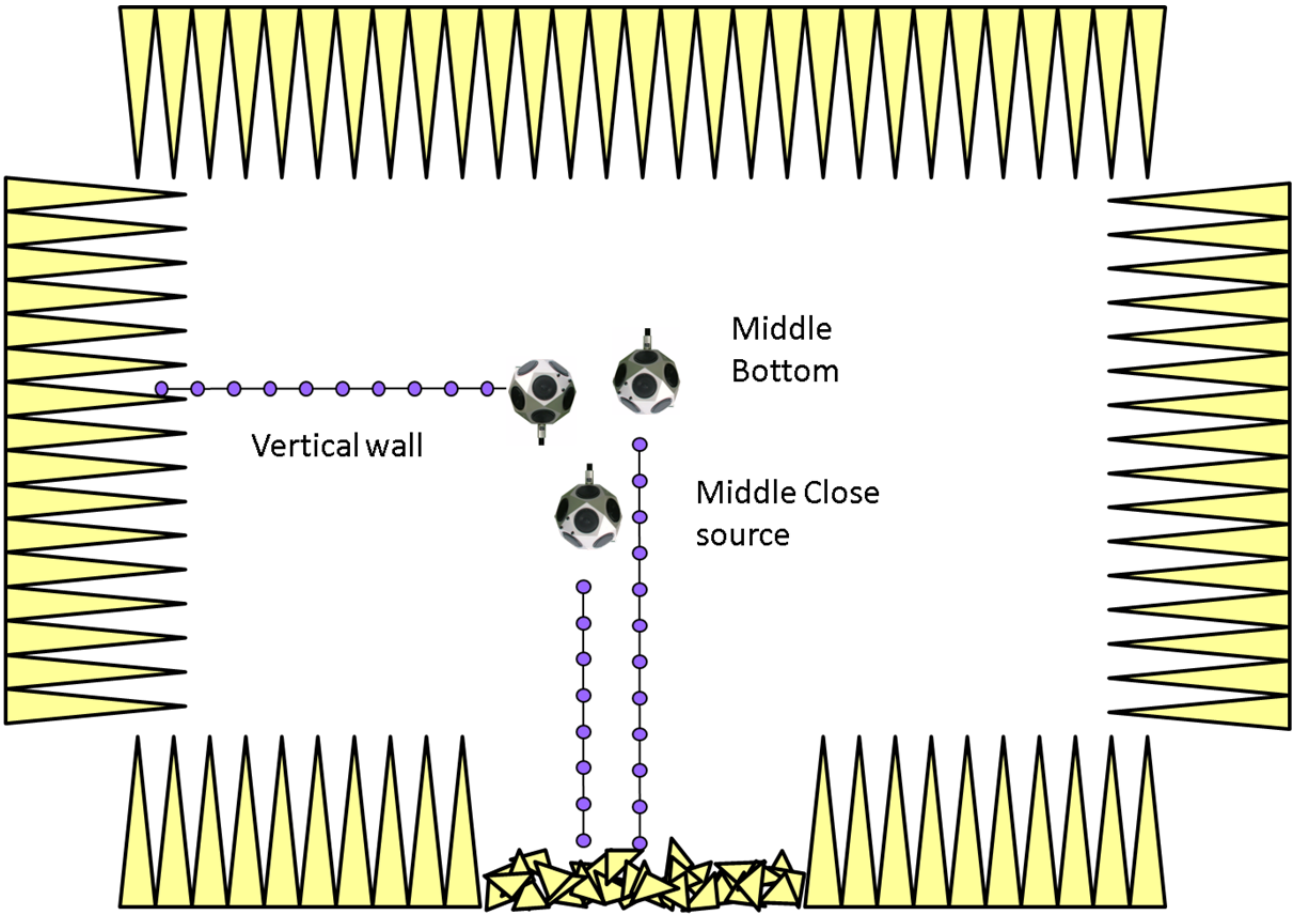


**Figure 4-8 Inverse square law measurement with a loudspeaker**

## *4.2 Engine measurement*

The engine sound field is a complex function of speed, power, torque and many other parameters. However, measurements are typically carried out for different speeds and powers in steady state situations i.e. where temperature, speed and torque do not change. In all cases, the gearbox is attached to the engine since it has a considerable effect on the modes in the engine and consequently the sound field. A typical narrow band result of the sound pressure level of the engine is presented in Figure 4-9. It clear that the sound pressure level is dominant in the engine half orders.

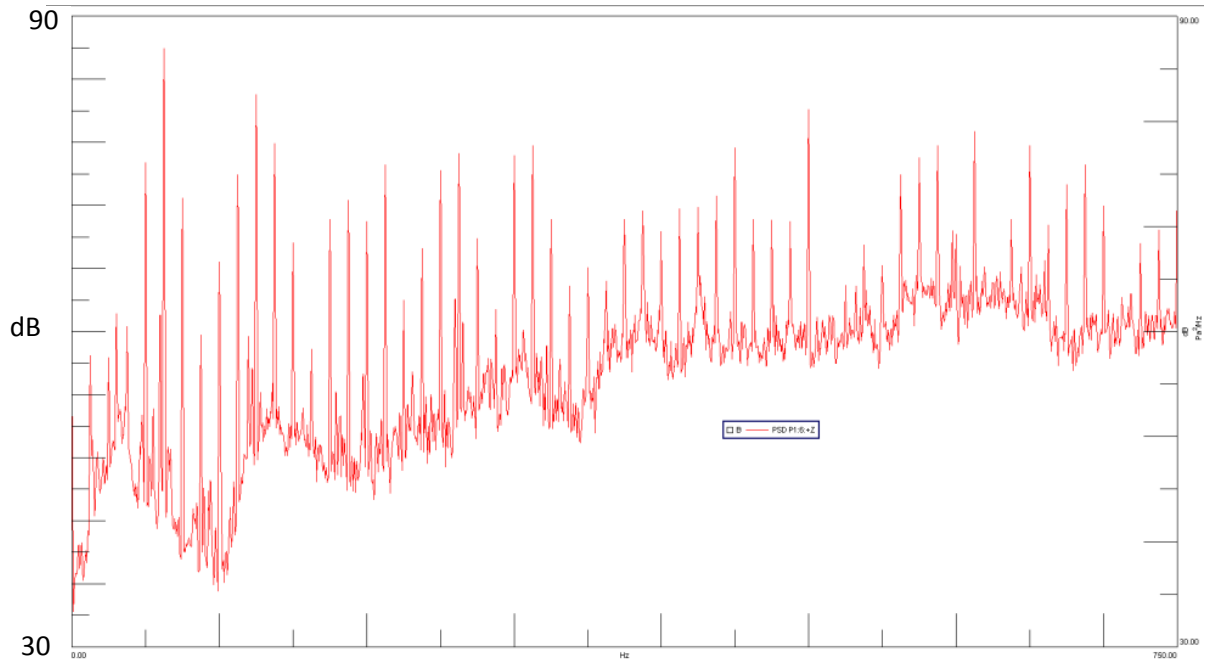


**Figure 4-9 typical PSD of engine noise, (1500 rpm, full load)**

### 4.2.1 Inverse square law

In section 4.1.2 reflection from the loudspeaker was discussed. The question may be asked: what would happen if the source were the engine instead of the loudspeaker? Six different locations underneath the engine have been considered and measurement has been carried out as shown in Figure 4-10. The results are presented and compared with the loudspeaker in Appendix F. In general, there is correlation between the results from the loudspeaker and engine but not in every frequency bands especially not in the regions of 200 and 250 Hz. This could be the effect of reflection or radiation from the test cell floor, since there are some metal sheets there, which can be excited by engine vibrations via mountings. These results indicate that however the sound source is changed there is a good agreement in the

sound trend; still, one has to consider that there is a risk of deviation. In the final arrangement presented, it is recommended to place the minimum number of microphones right underneath the engine where absorption is known to be poor. It should be mentioned also that this is only reflection in vertical incident otherwise, results could be very different.

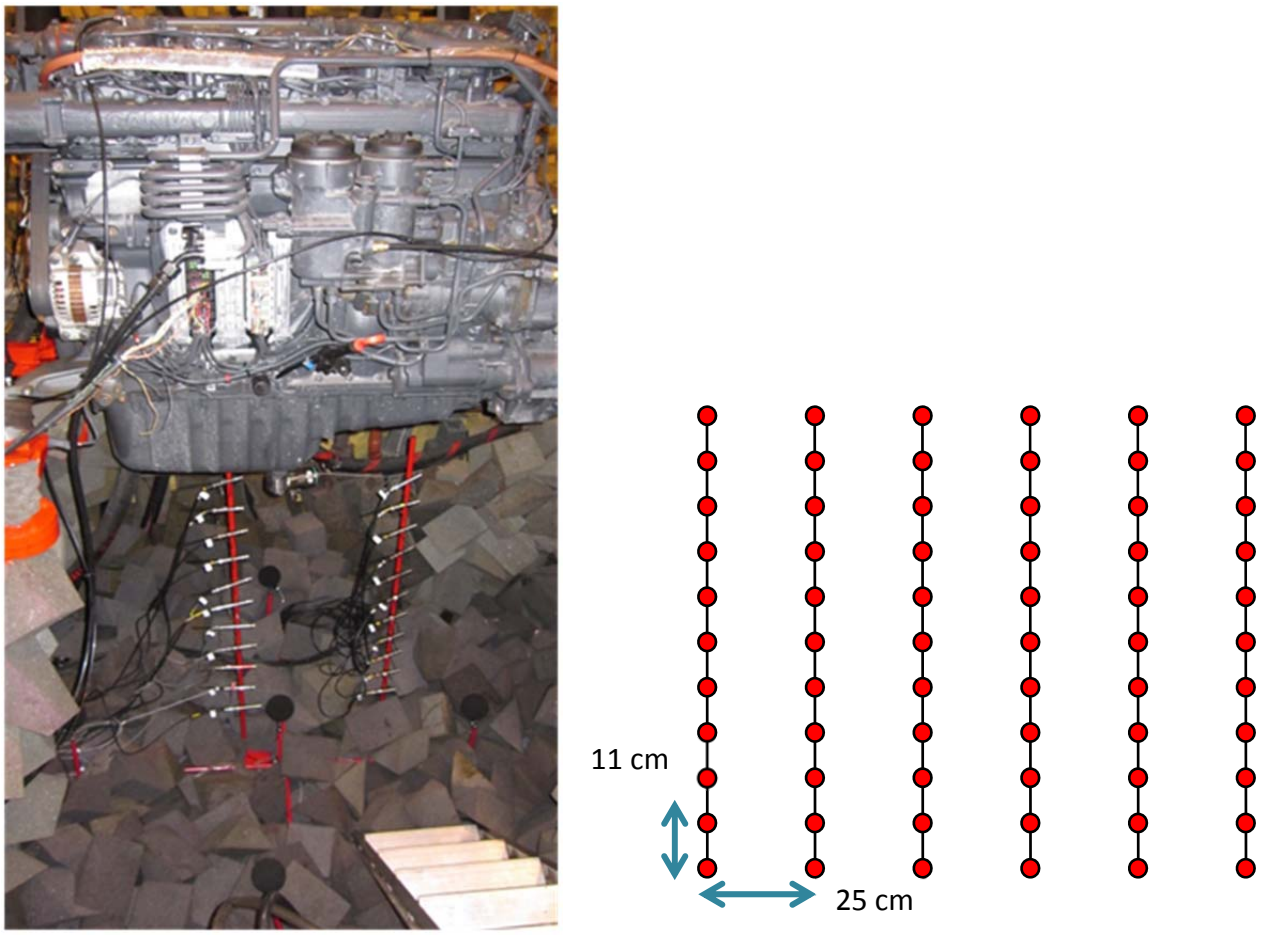


**Figure 4-10 The inverse square law measurement underneath the engine**

### 4.2.2 Microphone array, 4 plane measurement (DC929 15)

**The results from the engine acoustic model show high directivity in the sound field causing from constructive and destructive contributions (Appendix G). The question is does this directivity exist in reality? Another question is if the sound field is incoherent at higher frequencies, which help to average out the effect of high directivity. To examine the directivity, coherence and repeatability of the engine sound field, this test was carried out using the arrays of microphones as shown in**

Figure 4-11. Two arrays of microphones (each eleven) have been used each time and moved around in space to cover four planes (24 sets of measurement in total),Figure 4-12. The results are presented here and discussed.

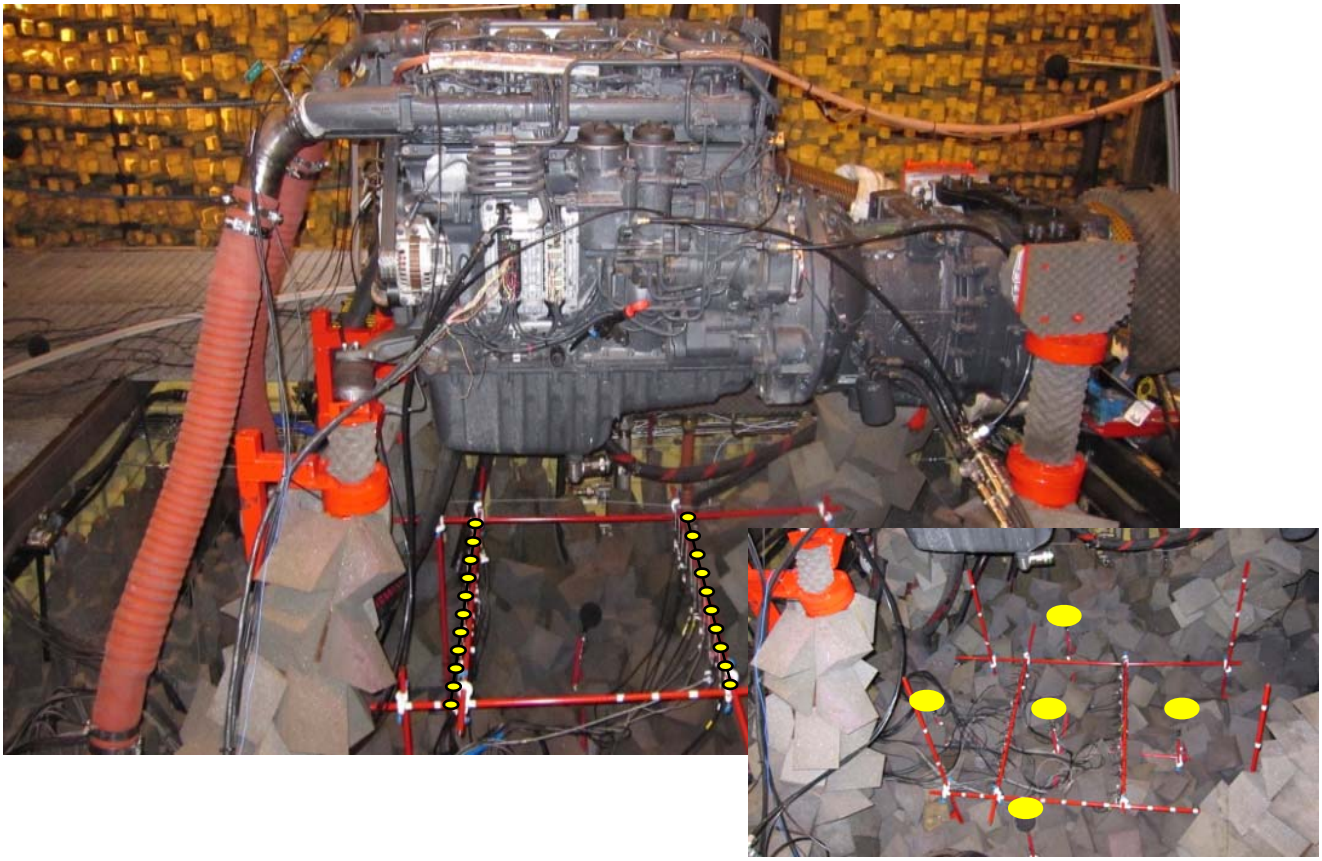

**Figure 4-11 The Microphone arrays and references (big ellipse in small picture) , 4 plane measurement, the big ellipse in the small pictures are five references**

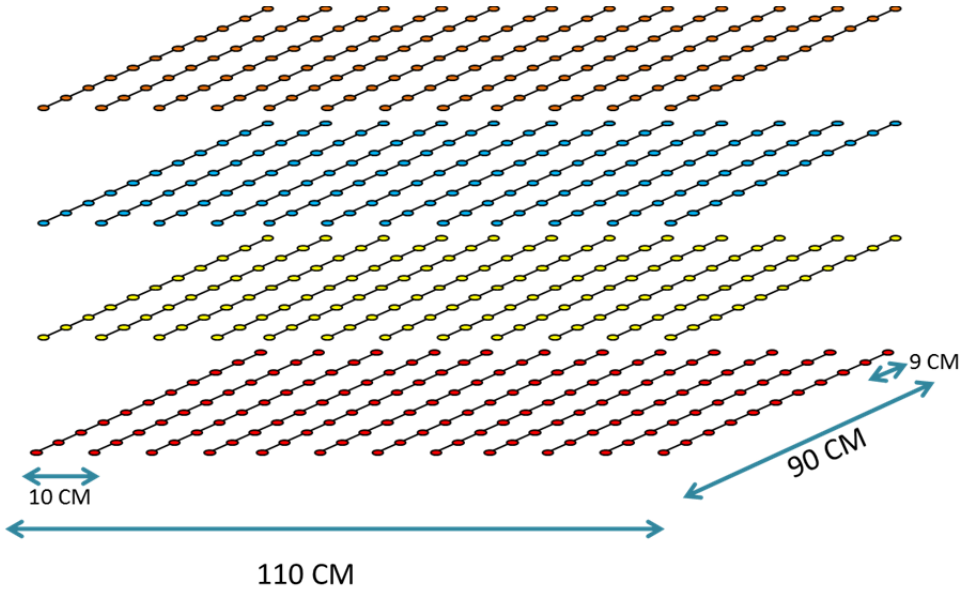


**Figure 4-12 The microphone locations in three-dimensions, Microphone array, 4 plane measurement**

### *4.2.2.1 Coherence*

It has been mentioned that if the sound field from the engine is incoherent, then this can be used as an advantage in averaging the sound field in the case of having stationary microphones. However, results indicate otherwise due to high coherence of the signals on arrays with references. There have been five references and 524 measurement points. For indication, the sound coherence between one of the microphones in the array with center reference microphone is presented in Figure 4-13 (all other microphones the array have similar pattern more or less). The measurements have been performed at different speed and loads, even motoring i.e. rotation of the engine and negative torque, and still the sound fields are coherent in engine orders. On the other hand, at low speeds such as idle where the transmission noise (gear train and gearbox) with its higher random characteristics is dominant, lower coherence has been observed. The high coherence shows that averaging by stationary microphones is not possible. One has to consider that this is sound coherence in only one set of the measurement i.e. one ensemble.

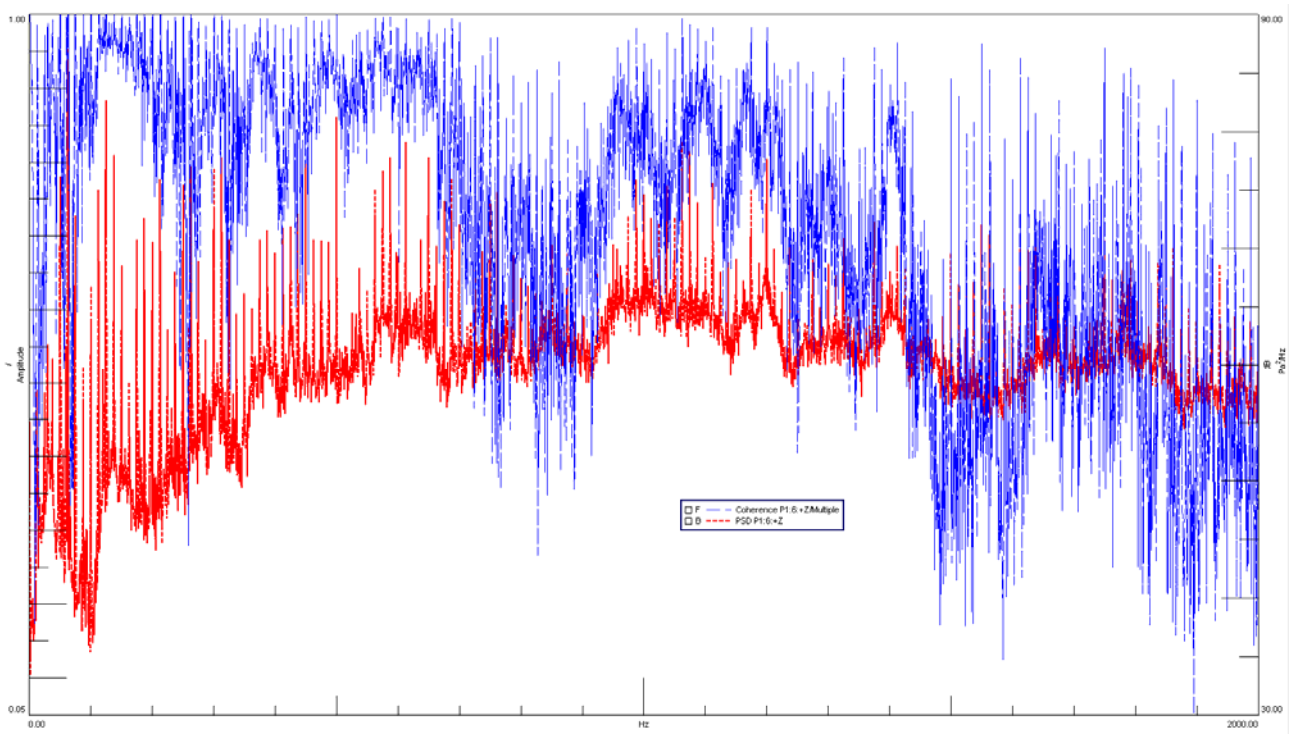


**Figure 4-13 A typical sound coherence underneath the engine 0-2000 Hz, engine at full load and 1500 rpm, (blue dashed line is coherence with level from 0.05 to 1, the red line is the sound pressure of the signal with levels from 30 to dB)**

### *4.2.2.2 Sound repeatability*

**As previously stated there have been 24 different measurement sets (twenty-four ensembles), in which all of the reference microphones underneath the engine are kept in the same place. These microphones locations are shown in**

Figure 4-11 on the right small picture with yellow ellipse. The question is does engine sounds same in similar working condition in different set of measurements in these references in similar working condition. For the case of 1500 rpm and full load (without the compressor as which causes the engine speed to fluctuate) and in a near-steady state situation and same torque, the repeatability in three out of five references has been presented. Everything in all the measurement was similar, only the engine has been turned off the arrays have been replaced, and ran again in steady state situation (10 min at 1500 rpm and full load and then repeats this cycle).

The "*repeatability*[4]", here the differences between the maximum and minimum sound pressures in these 24 ensembles, in left, front and right reference microphones are shown in Figure 4-14. As it is clear, there is a considerable difference despite that the results are in ⅓ octave bands. The measurement shows that in many ensembles, sounds could differ considerably specifically for low frequencies.

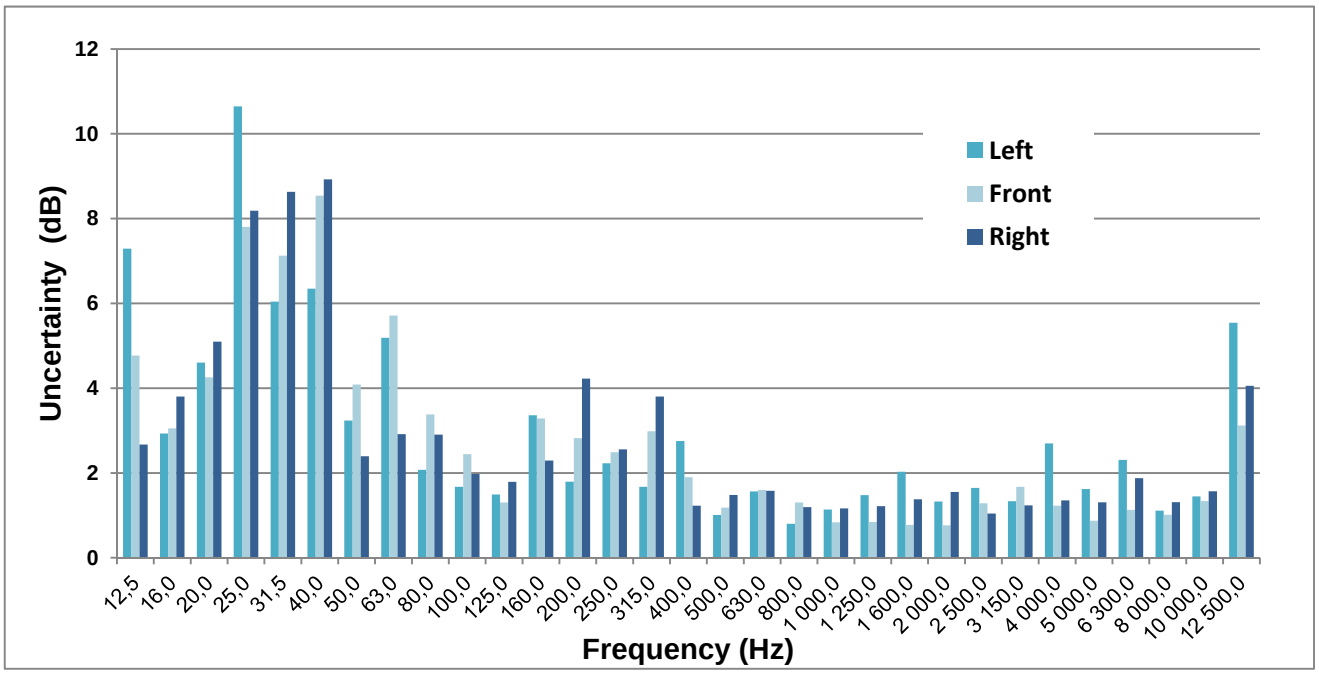


**Figure 4-14 repeatability of sound in the references in 24 different measurement**

[4] Here the word repeatability instead of reproducibility has been used since the laboratory, operator, apparatus are the same and there is short time between tests. (Reference: "What Are Repeatability and Reproducibility? Part 1: A D02 Viewpoint for Laboratories", from DataPoints magazine, ASTM March/April 2009)

#### *4.2.2.3 Sound directivity, (bottom plane)*

In these measurements, the relative locations of these planes to the engine are shown in Figure 4-15. The directivity in the bottom plane has been studied. This does not show the directivity (D) of the whole engine; however, it will show how the sound pressure level is distributed in this plane. The directivity ($Max(L_P)$-$Min(L_P)$) of the sound is presented in Figure 4-16 alongside the uncertainty in the middle microphone to show how much of this directivity may be caused due to the difference between ensembles.

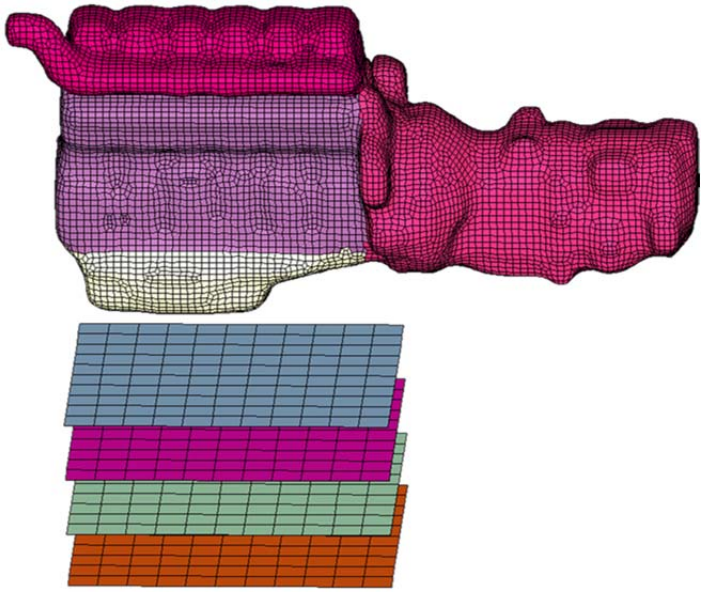

**Figure 4-15 relative locations of measurement planes to engine**

### 4.2.3 Top Hemisphere and Directivity

The third engine measurement was done on another engine type, DC1307. The measurement has been carried out for different speed and loads. Here, only the results for full load and motoring are presented. In previous section, the level of directivity(D) only in a small plane underneath the engine has been discussed. In this section the results for a hypothetical hemisphere over the engine are presented (the array is shown in Figure 2-9). The resulting directivities are shown in Figure 4-17 and Figure 4-18 for full load and motoring respectively in different ⅓ octave bands for different speeds. The sphere radius is 2.7 m. There is higher directivity in lower frequency bands as will be explained in next section. Here the high directivity of the source (higher than 10 dB) demands an increase in the number of microphones based on the standard. The number of microphones has to be increased (or the array should be rotated).

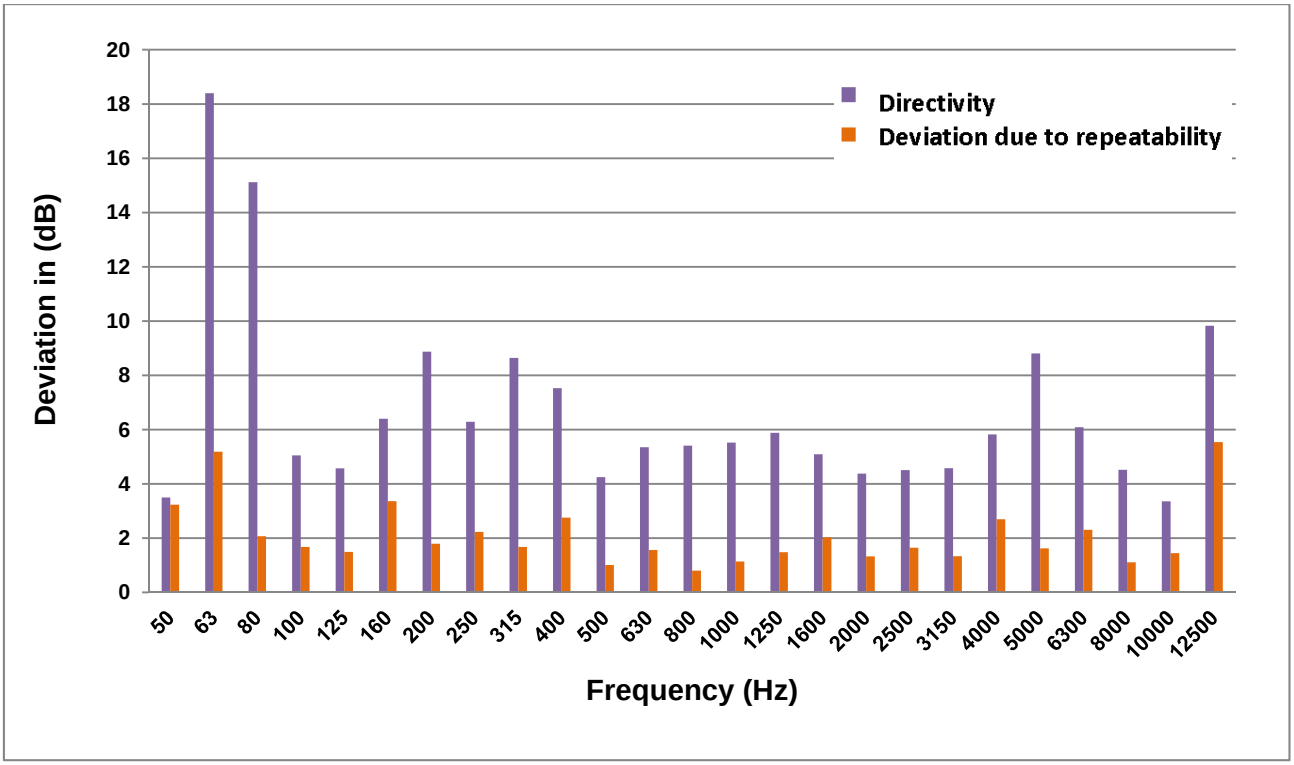


**Figure 4-16 The directivity ($D$) in this bottom plane of the measurement.**

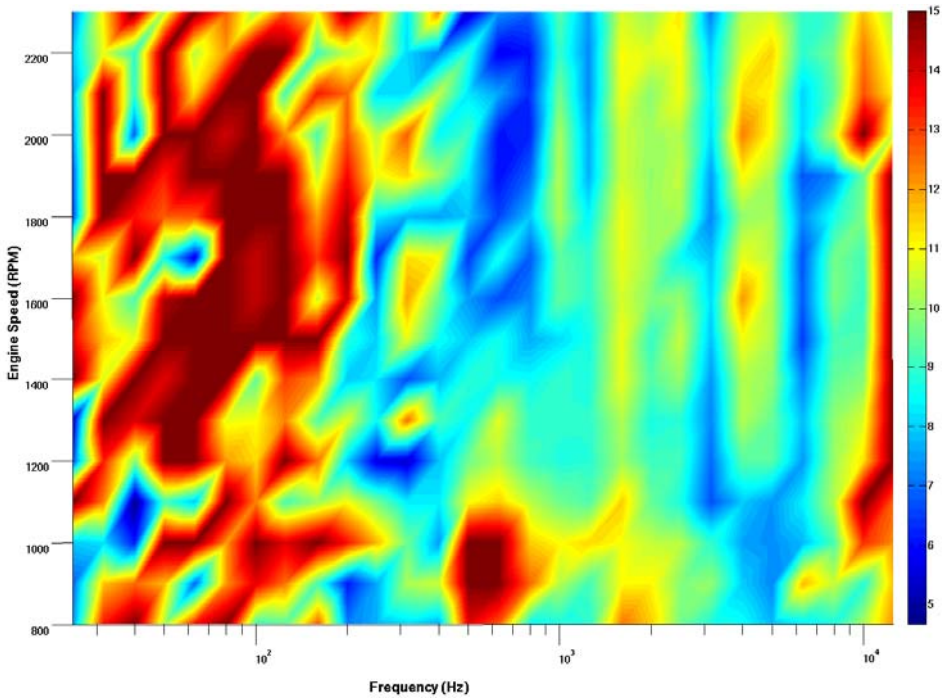


**Figure 4-17 Engine sound field directivity in top hemisphere for different speeds, full load condition**

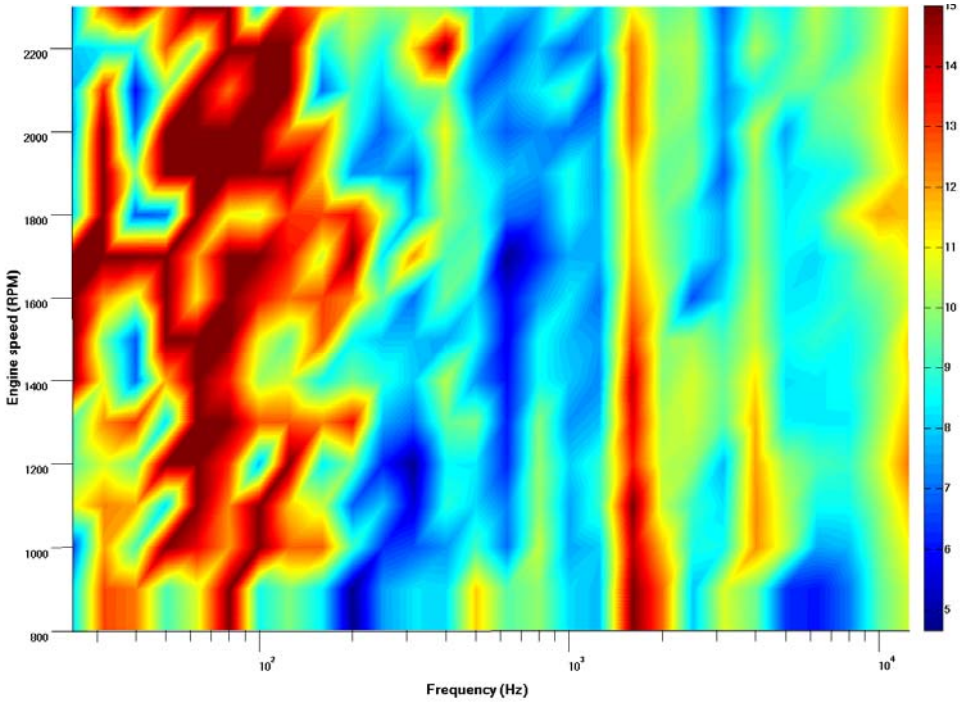


**Figure 4-18 Engine sound field directivity in the top hemisphere for different speeds, motoring condition**

### 4.2.4 Comment on averaging in ⅓ octave bands

The sound power or pressures of the engine are typically reported in ⅓ octave bands. A typical sound power measurement is shown in Figure 4-19.

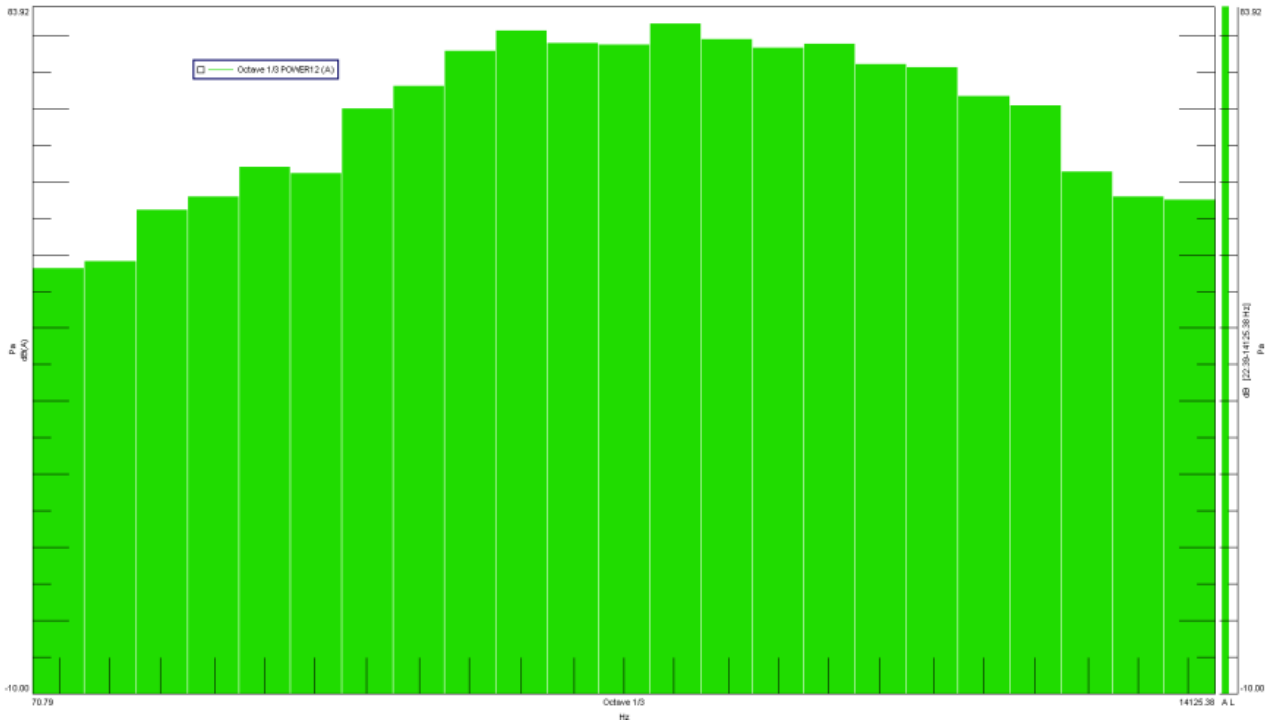


**Figure 4-19 typical ⅓ octave band results of engine noise.**

The ⅓ octave band and narrow band results shown in Figure 4-20 clearly indicate how many engine orders lie in each band; few at lower frequencies and many at higher frequencies. The low number of engine half orders in lower ⅓ octave frequency bands can explain the higher directivity at lower frequencies.

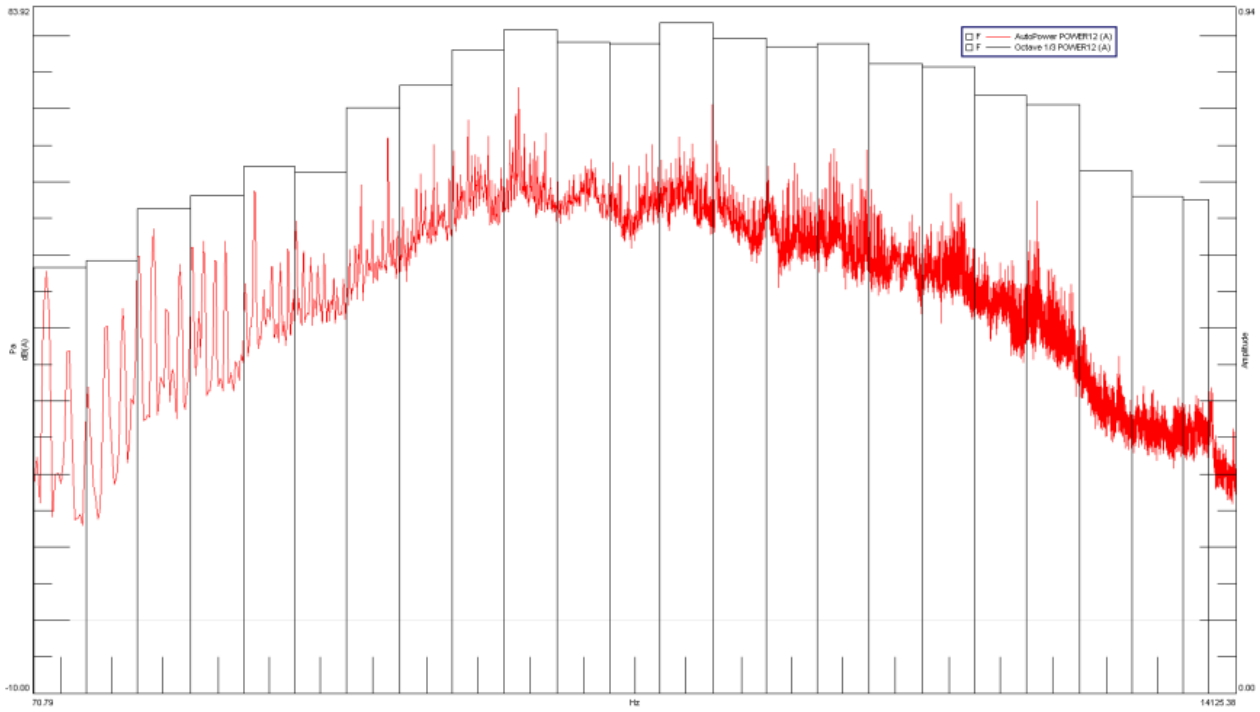


**Figure 4-20 ⅓ octave and narrow band results, lower number of orders in lower bands**

# 5 Result and discussion

There are different restriction and requirements in the standard (ISO 3745), which have been discussed. The results from the simulations have been used to evaluate these criteria, to suggest methods, to apply special considerations, and to discuss uncertainties. Depending on the model mesh size, the maximum frequency limitation is around 1.2 kHz, but the result is still presented up to 2 kHz, however, engine noise contains frequencies up to 14-15 kHz. It is impossible to go this far up in FE simulations, however the basic engine noise consists mostly of harmonics above 2kHz, which often will be reduced when the level is reduced below 2kHz. Many of the forces are impacts / impulses , which in frequency domain will give high level in low frequency and successively lowers level higher up. There are several exceptions to this, like flow induced noise, which need to be treated in another way than FEM.

## *5.1 Number of Microphones and their coverage of measurement surface*

The power calculation is based on equation 2-8 in ISO 3745 and the using a hypothetical sphere, this equation can be rewritten as equation 5-1 (for typical value of air temperature and pressure).

$$L_w = 10 \times \log_{10} \frac{\langle \tilde{p}^2 \rangle}{p_{ref}^2} + 10 \times \log_{10} 4\pi r^2 \qquad \text{Eq. 5-1}$$

Where $r$ is the radius of the hypothetical sphere of microphones, centered at the acoustic center of the source. Based on ISO 3745 the microphones can be in different imaginary surfaces. This means different $r$ values for each microphone. So the equation reads:

$$L_w = 10 \times \log_{10} \frac{\frac{\sum_{n=1}^{N} [\tilde{p}^2 \times 4\pi r_n^2]}{N}}{p_{ref}^2} \qquad \text{Eq. 5-2}$$

Where $r_n$ stands for the distance of the n's microphone to the acoustic center and $L_{pf_n}$ the corresponding sound pressure of same microphone individually. However, this is only valid if the microphones are distributed uniformly all around the sphere. In this case however there are 20 microphones in top and fewer (originally 5 and final recommendation 9 or 10) in bottom. The microphones in top and bottom half should have same weight because they cover same surface areas. So one can write

$$W = W_{upper} + W_{lower}$$

Considering

$$W = \oint I.ds \text{ and } \mathrm{I} = \tilde{p}^2/\rho c$$

$$W_{upper} = \sum_{n=1}^{M} \frac{\tilde{p}_n^2 S_n|_{upper}}{\rho c}$$

In the formula $S_n|_{upper} = 2\pi r^2/M$ if the $M$ microphones are located according to the standard at radius $r$. Using instead $2\pi r^2$ of $4\pi r^2$ since this is only a hemisphere.

$$W_{lower} = \sum_{i=1}^{N} \frac{\tilde{p}_i^2 S_i|_{lower}}{\rho c}$$

The area $S_n|_{lower}$ in the lower half space is somewhat difficult to determine, since microphones may not be located in the same sphere (Figure 5-25). A good estimation can be $S_n|_{lower} = 2\pi r_n^2/N$, where $r_n$ is the distance from that specific microphone to the acoustic center.

The total sound power is then can be calculated by equation 5-3.

$$L_W = 10\log\frac{W}{W_0} = 10\log\left(\frac{\sum_{n=1}^{M} p_n^2 S_n|_{upper} + \sum_{n=1}^{N} p_n^2 S_n|_{lower}}{\rho c W_0}\right) \qquad \text{Eq. 5-3}$$

### 5.1.1 Choice of Acoustic Center

It has been discussed that microphones can be in different radii from acoustic center. The question here is how important is it to choose to the acoustic center, or where is located? How much this would change the total power?

The effect of choosing the acoustic center here has been studied in the acoustic model. As has been discussed, the power can be calculated in two different ways in acoustic model, "*wetted power*" and power from pressure in "*field points*"[5]. The power from field points is calculated in the same way using the equation 5-2, while the wetted power can be used for reference[6], as mentioned before. Here, six different imaginary surfaces are considered, comprising many (890) field points. The first hemisphere with radius 2.7 m is centered around the approximate geometrical center of the engine (and gearbox). The other hemispheres, identical to the first, but shifted 20 cm to left, right, above, below and the finally, a sphere with a radius of 5.4 m with the same center as the first hemisphere. The differences between calculated powers based on the pressures on these surfaces are shown in Figure 5-1 to Figure 5-3 for different speeds. It is clear that it is not that important where to place the

[5] The sound power from wetted power is $\mathbf{W_{wetted\ power}}$ and from field point is $\mathbf{W_{Field\ point}}$

[6] In the next part, which we look at the problem in the top and bottom separately, instead of "wetted power", "many points" are used as reference.

acoustic center. The total calculated power is not very different even with 0.4 m displacement of a hemisphere with a 2.7 m radius.

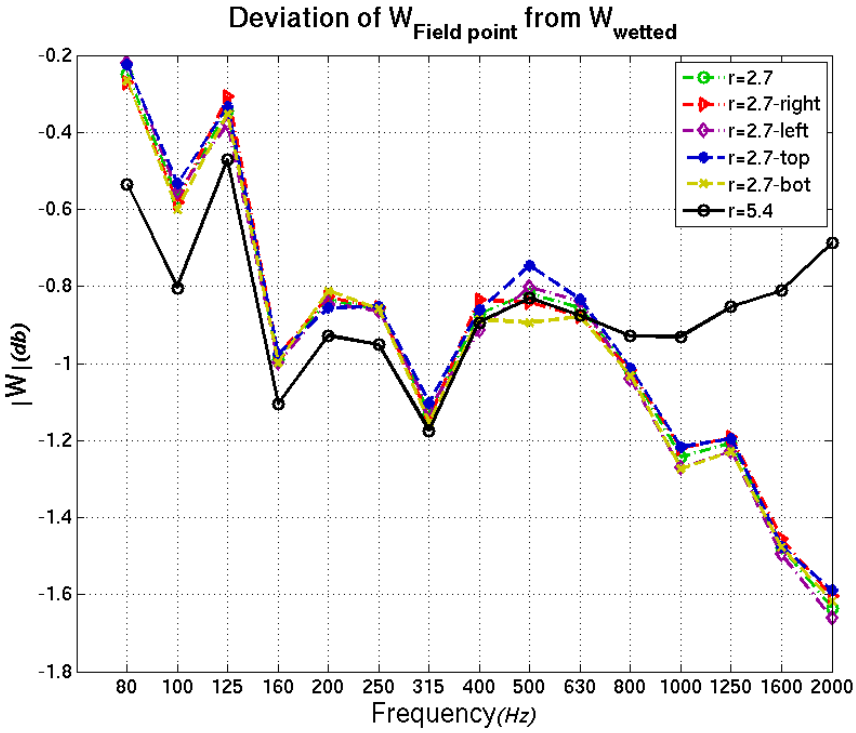


**Figure 5-1 Acoustic center 1100 rpm**

### 5.1.2 Distance from acoustic center

The conclusion to the previous section was that power calculated from the imaginary sphere is not very sensitive to the choice of acoustic center. What is important though, looking at the equation 5-2, is to use the right radius, $r_n$. In other words is not that sensitive where to place the acoustic center, but where it is chosen, all microphones should lie considered with their distances from acoustic center [**13**]. This is very important especially in bottom since the microphones are located in different distances from acoustic center.

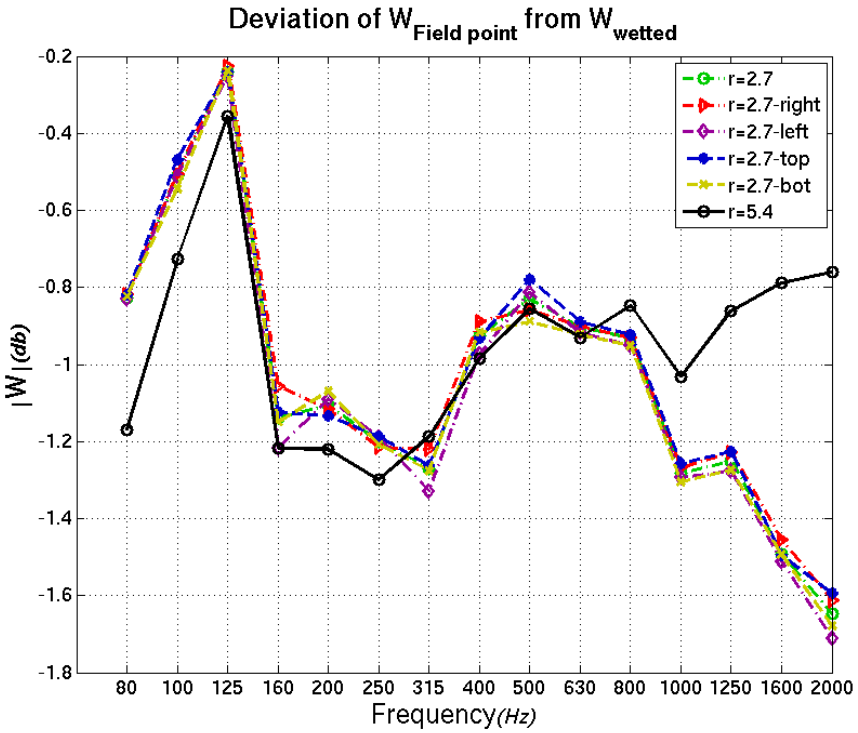


**Figure 5-2 Acoustic center 1500 rpm**

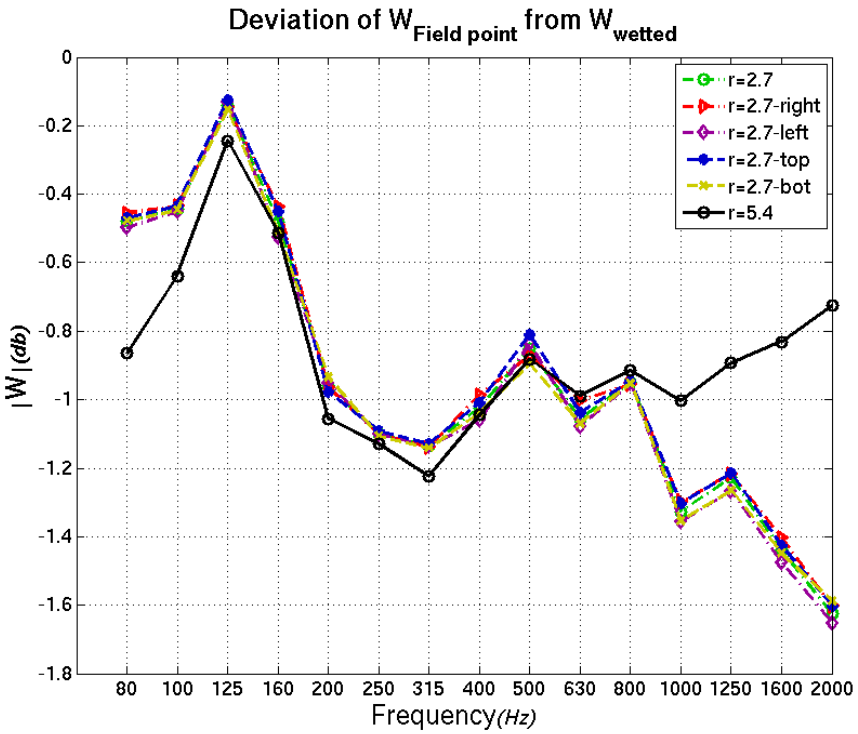


**Figure 5-3 Acoustic center 1800 rpm**

## *5.2 Reflection correction factor*

As said before engine underneath the engine does not have good absorption. The sound field in this area deviates from free field conditions. This deviation, discussed in 4.1.2, is almost consistent for different sources. The corrections for deviation for microphones installed at 20 and 30 cm from absorbent surface are shown in Figure 5-4, extracted from appendix E. Connecting the peaks with lines, one can see the trend of these factors in Figure 5-5 . This factor is only valid for almost normal incidence, i.e. just underneath the engine, not for the whole area.

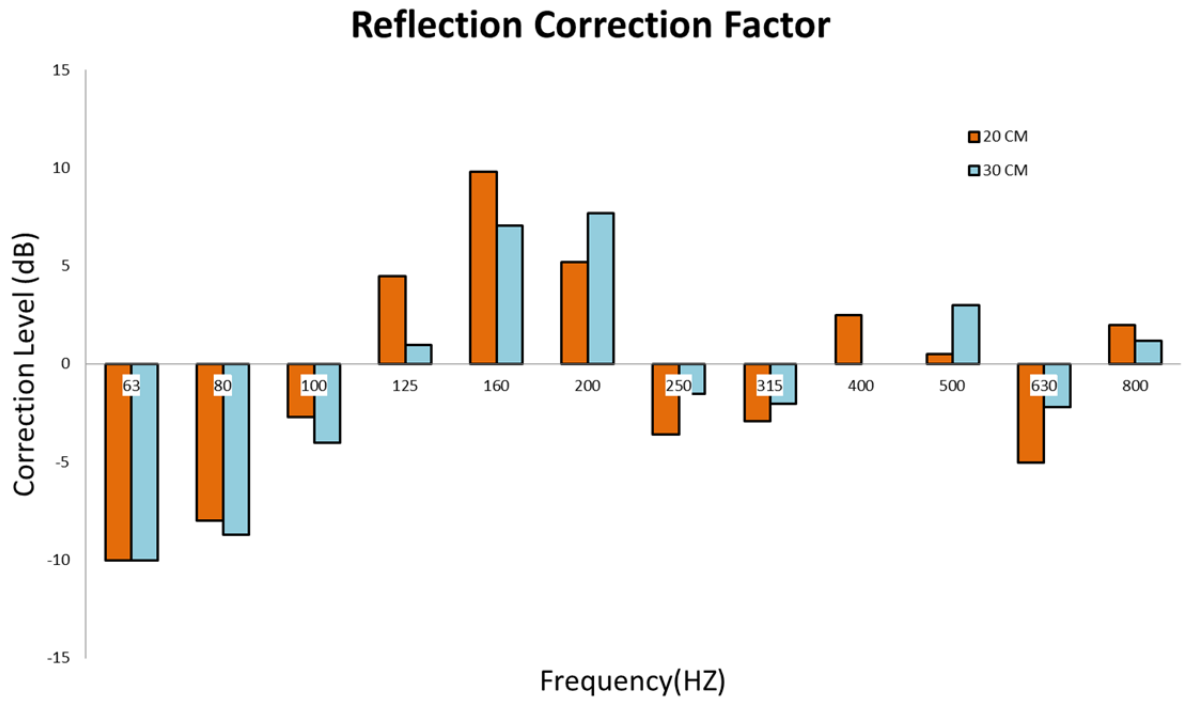


**Figure 5-4 reflection correction factor, Normal incident, for michrophones located at 20 and 30 cm from the surface**

**Figure 5-5 Trend of reflection correction factor (note: the axis and scale are simliar to figure 5-4, and here only the plot is repeated by lines)**

## *5.3 Directivity*

The requirement for the number of microphones in ISO 3745 and the limitation of difference between maximum and minimum SPL is an indication of its importance.

Here the problem is separated into two different regions, top hemisphere and bottom hemisphere, which have been treated separately, because of the structure of the room. On the top there is an arrangement of 20 microphones which (shown in Figure 2-9). The question is how much uncertainty this will introduce to the sound power since the number of microphones doesn't fulfill the requirements of the standard because of the high directivity.

The ISO arrangement locations are generated in software with different sphere radii as shown in Figure 5-6 and the results are compared with many points[7] (the outer layer). The result in narrow bands is presented in Figure 5-7. The twenty microphones and the uncertainty in ⅓ octave bands are presented in Figure 5-8 to Figure 5-10 for different engine speeds and different sphere radii. This shows that microphone distance higher than 1.9 m doesn't have a significant effect on the power; we will see similar results for bottom half, have the same conclusion. Results for different speeds for a 2.7 m hemisphere are shown in Figure 5-11, these results show an uncertainty of 2 dB in ⅓ octave bands can be expected.

Increasing the number of microphones will decrease this uncertainty. Rotating the array of microphones is another solution to obtain better averages; however in this case is rather difficult because of limited access of operator to test cell when the engine is running, beside the problem of piping, etc. which limits the possibility for the array to rotate.

[7] Many points here are the outer layer in figure 5-6 since it has 445 points compare to ISO points which are only 20 point, and this is a much better average. So many points are as reference here and the deviation of ISO points are studied here. We can't use the wetted power since it is for whole engine not top or bottom.

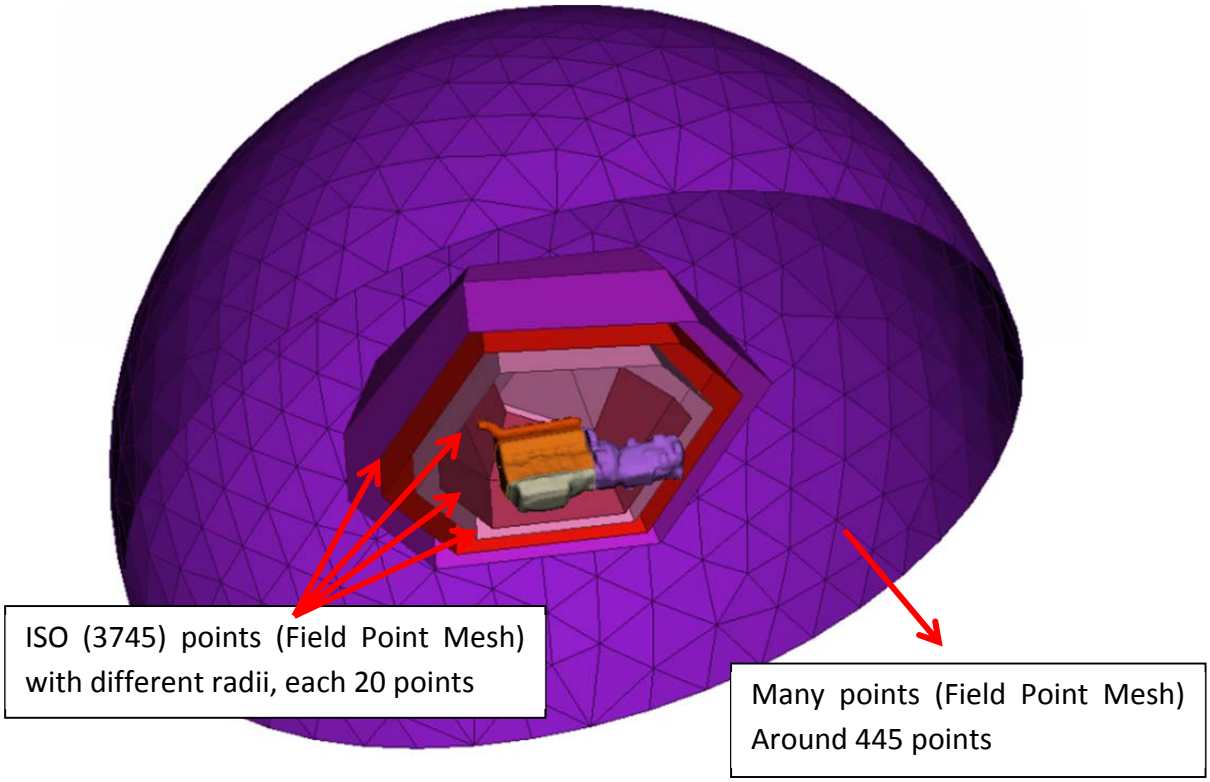


**Figure 5-6 Field point mesh , ISO points[8] vs. Many points in NASTRAN**

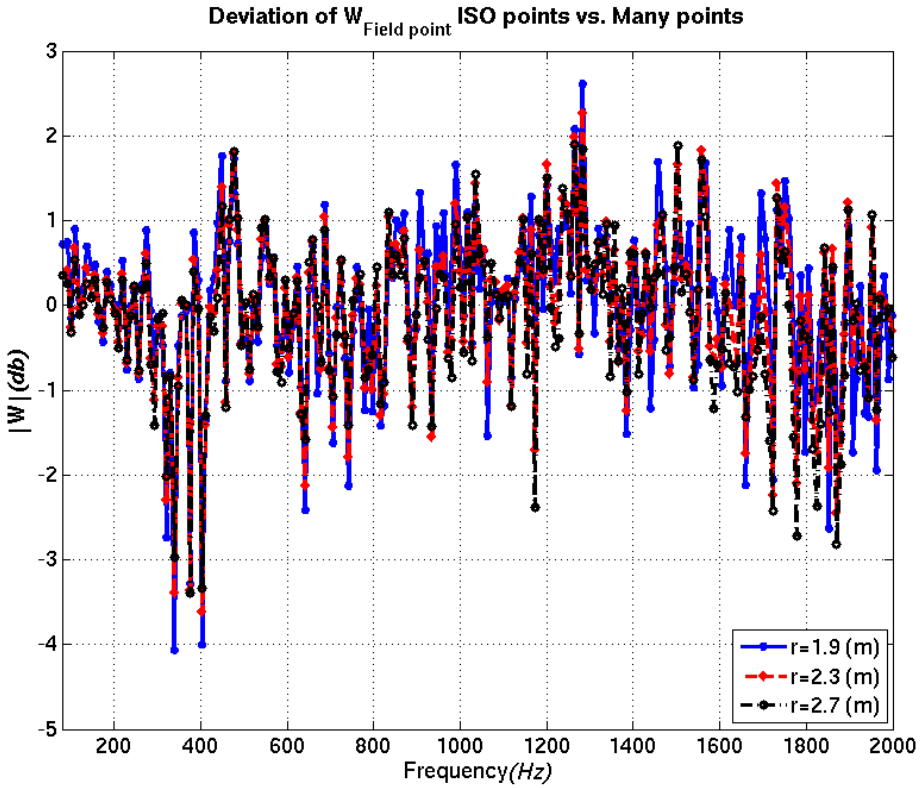


**Figure 5-7 Top hemisphere 1100 rpm, narrow band**

[8] ISO points here the ones in the Figure 2-9, they are 20 points but with different radius

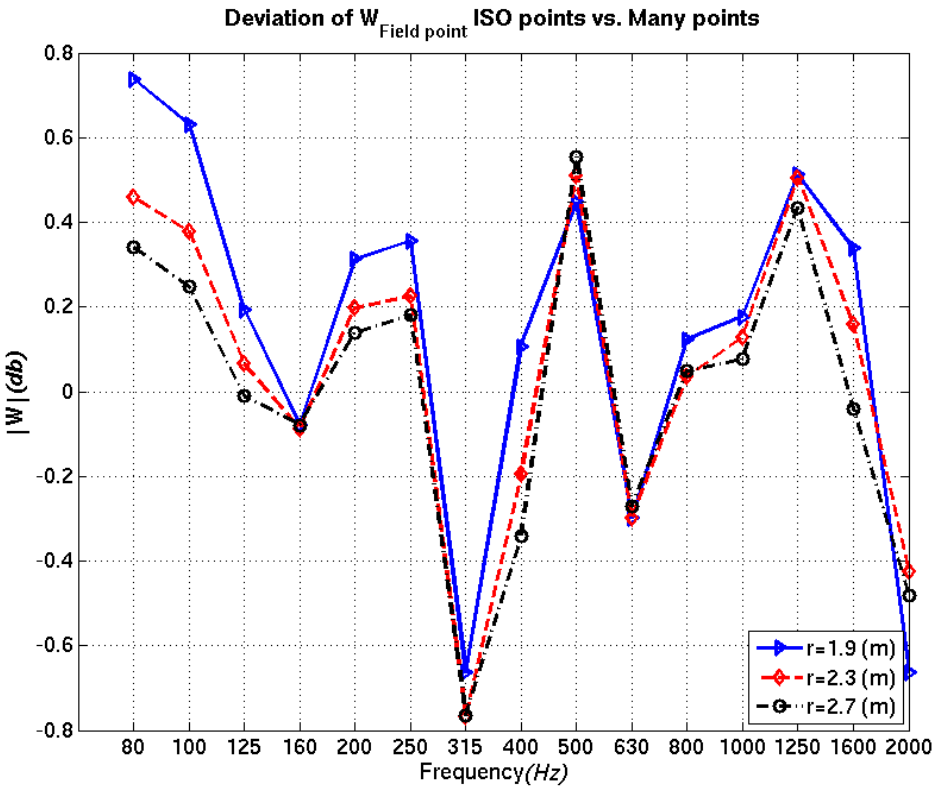


**Figure 5-8 Top hemisphere 1100 rpm**

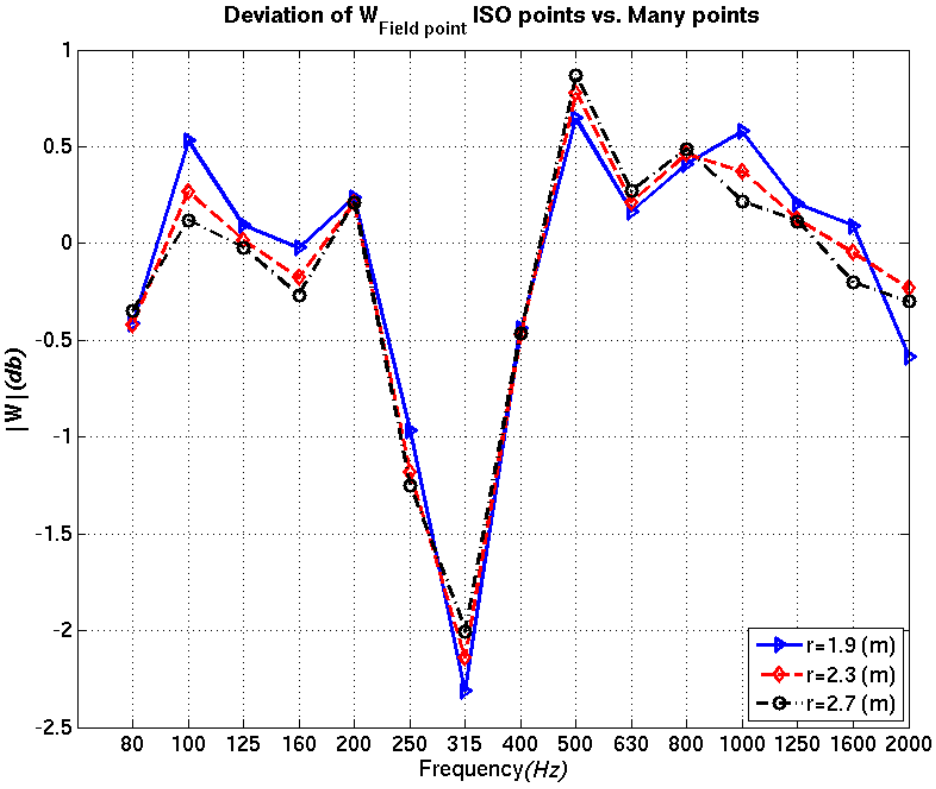


**Figure 5-9 Top hemisphere 1500**

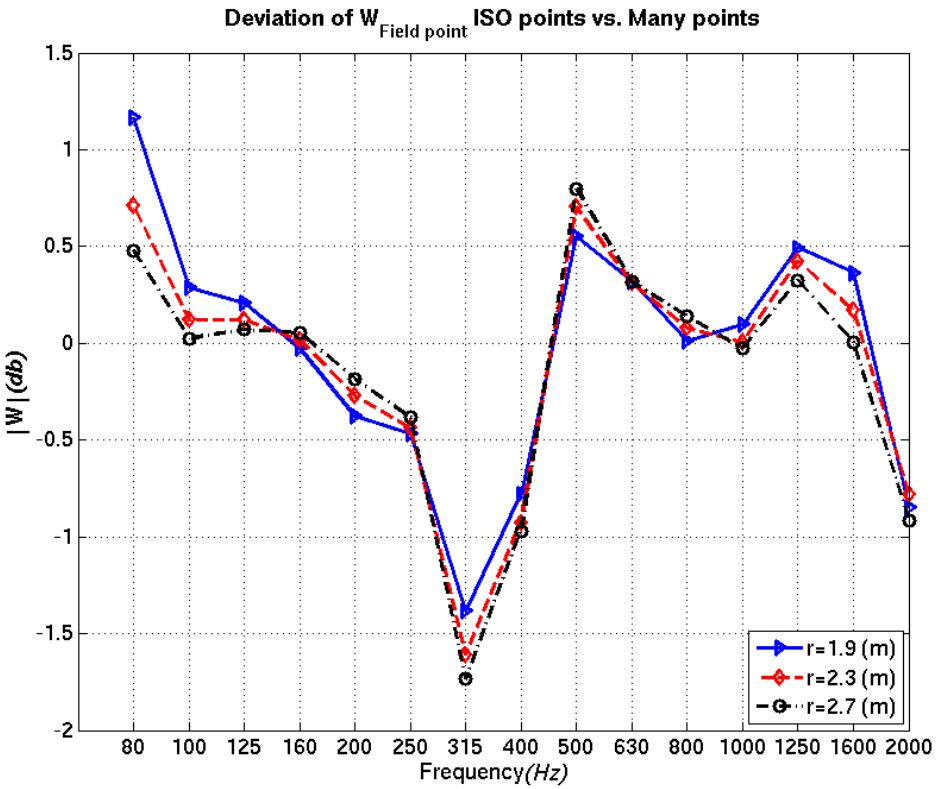


**Figure 5-10 Top hemisphere 1800 rpm**

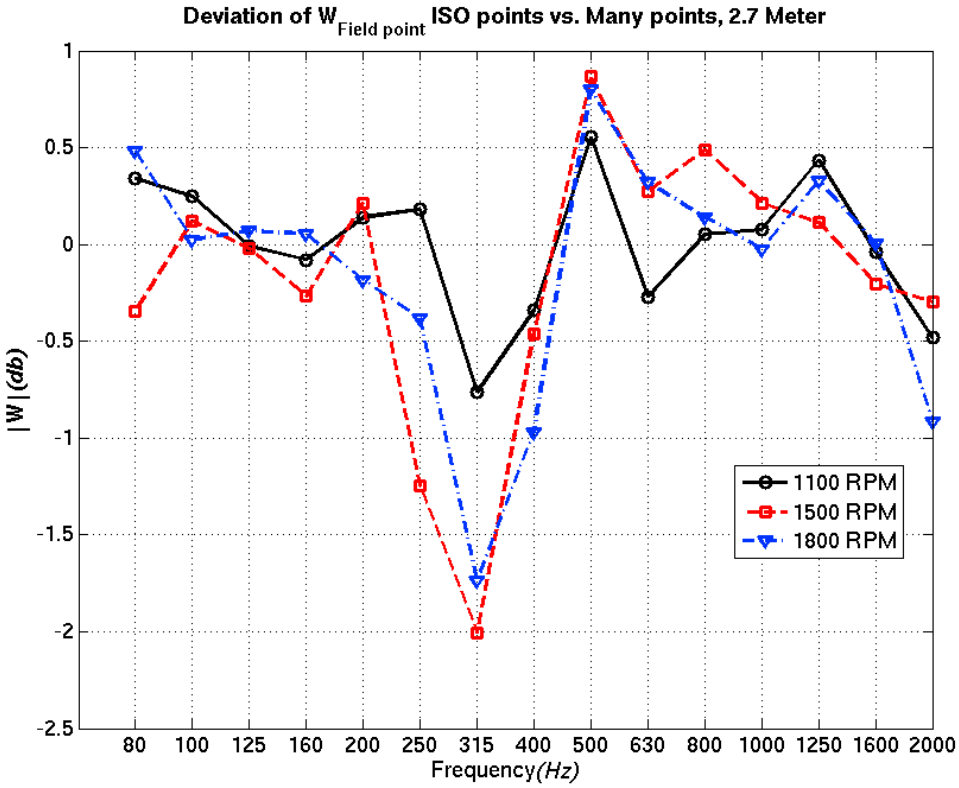


**Figure 5-11 Top hemispheres different speeds**

The directivity as it has been discussed before can only be averaged by increasing the number of microphones (or by rotating microphones). The directivity of the engine in the top half sphere has been discussed for engine DC1307 in section 4.2.3.

The engine in the acoustic model is the same engine type but lacks some details. The sound directivity for simulation and measurement are compared in Figure 5-12 to Figure 5-14. Expecting the exact same sound fields is not realistic, however directivities in general are similar and there is fair agreement between the results from measurement and simulation.

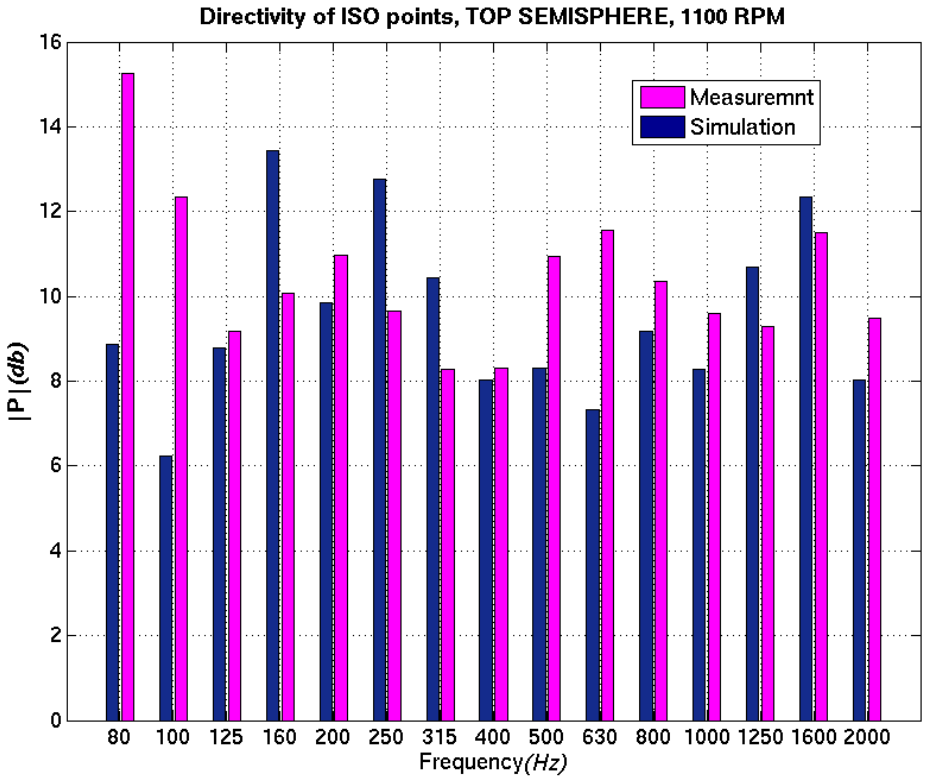


**Figure 5-12 Directivity in ISO 20 points, top hemisphere, measurement vs. simulation, 1100 rpm**

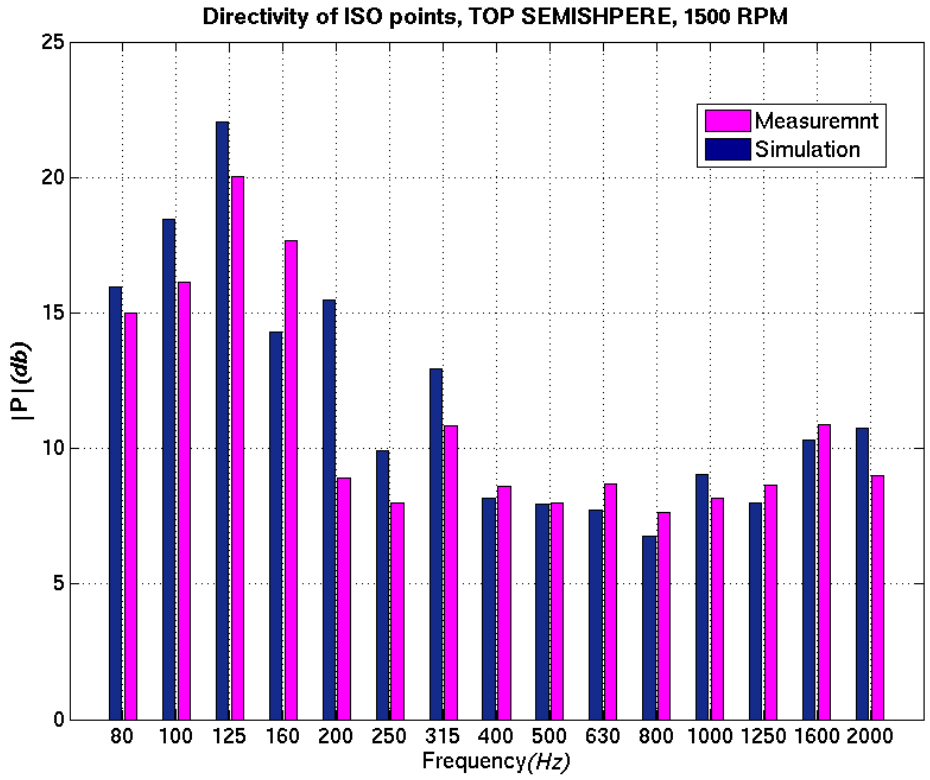


**Figure 5-13 Directivity in ISO 20 points, top hemisphere, measurement vs. simulation, 1500 rpm**

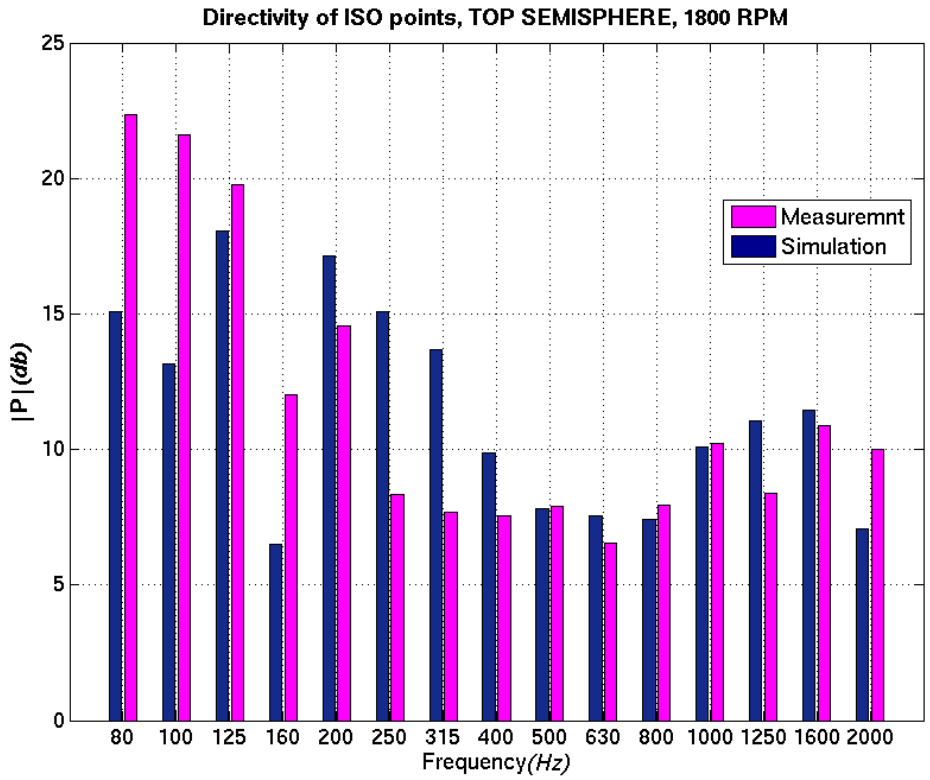


**Figure 5-14 Directivity in ISO 20 points, top hemisphere, measurement vs. simulation, 1800 rpm**

The bottom hemisphere has been treated differently, since there is not enough space to place the microphones in the ISO arrangement. The power from the ISO arrangements with different radiuses is presented in Figure 5-16 to Figure 5-18 to compare with semi-sphere results for the top-half. With a larger radius than 1.9 m the total power is rather similar.

New arrangements other than ISO points have to be found due to space limitations underneath the engine. In standards there are different arrangements of microphones such as rotating microphones. Here different microphones arrangement are considered underneath the engine as shown in Figure 5-15 (rotating microphone with different radii). The results are presented in Figure 5-19 to Figure 5-21 for different radiuses. The *r* value is the distance from acoustic center and the number in parentheses the radius of the circle in the bottom. There are large deviations for smaller radii but there is simply not enough space in the bottom to accommodate large radius, and even in such a case, reflections would cause problems.

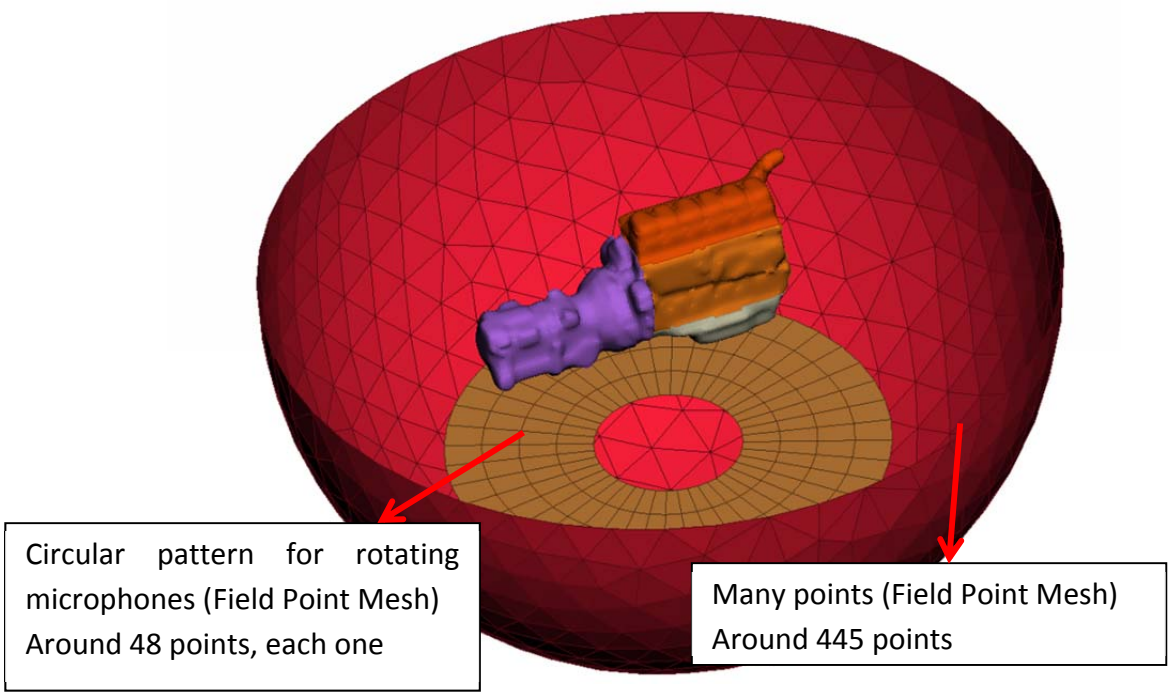


**Figure 5-15 The bottom hemishpere and rotating microphone path**

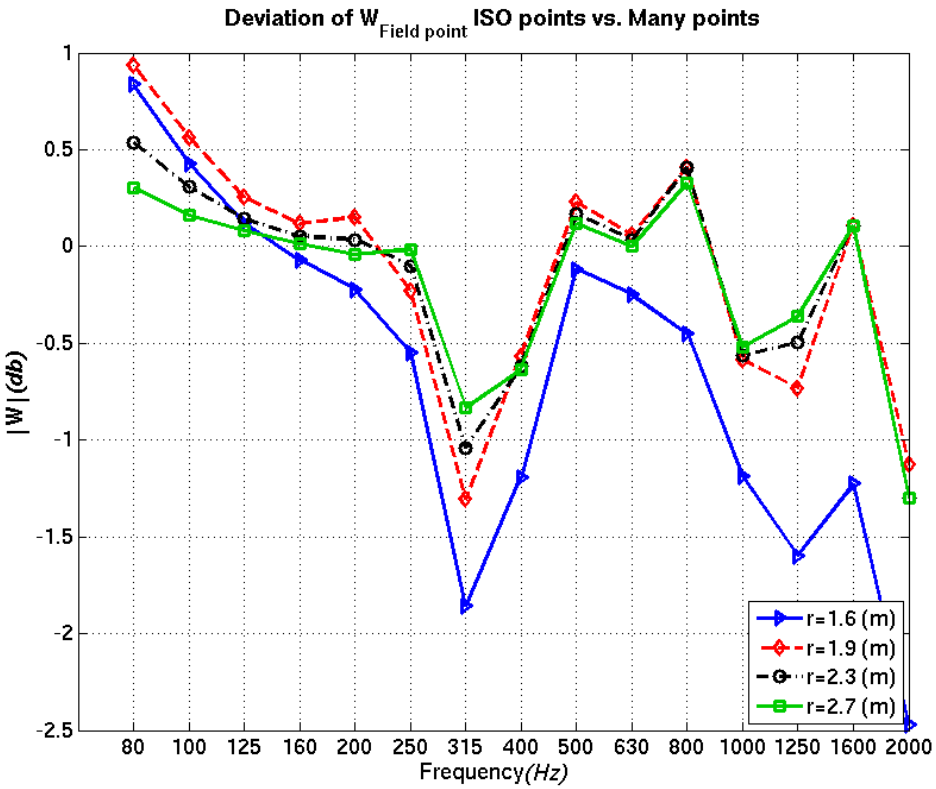


**Figure 5-16 bottom, ISO point 1100 rpm**

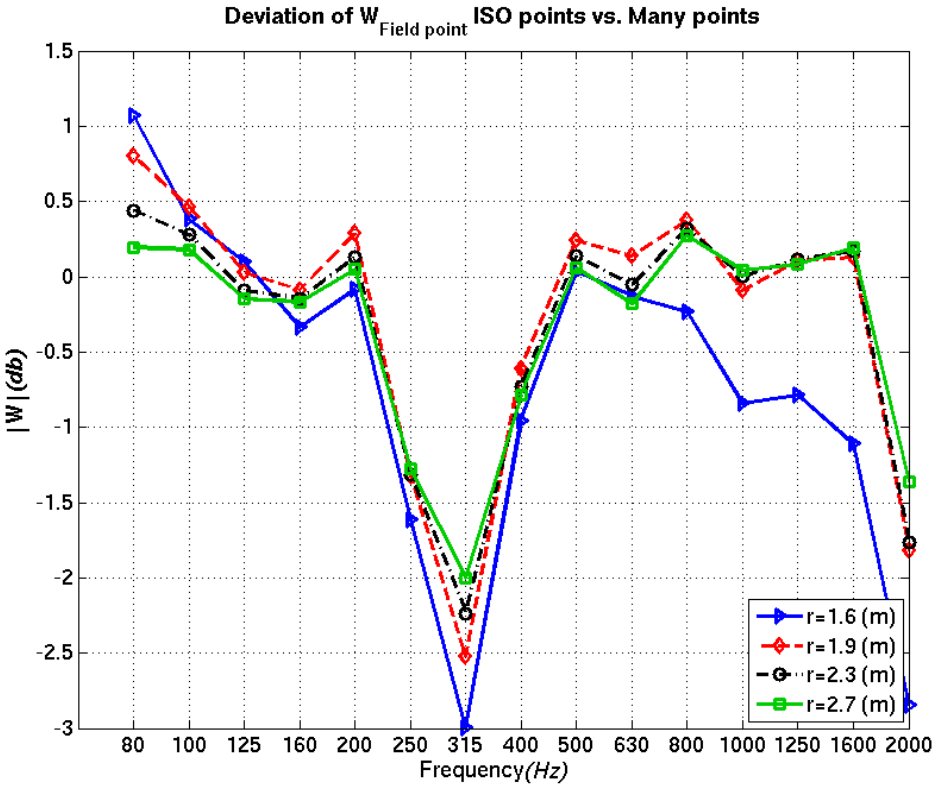


**Figure 5-17 bottom, ISO point 1500 rpm**

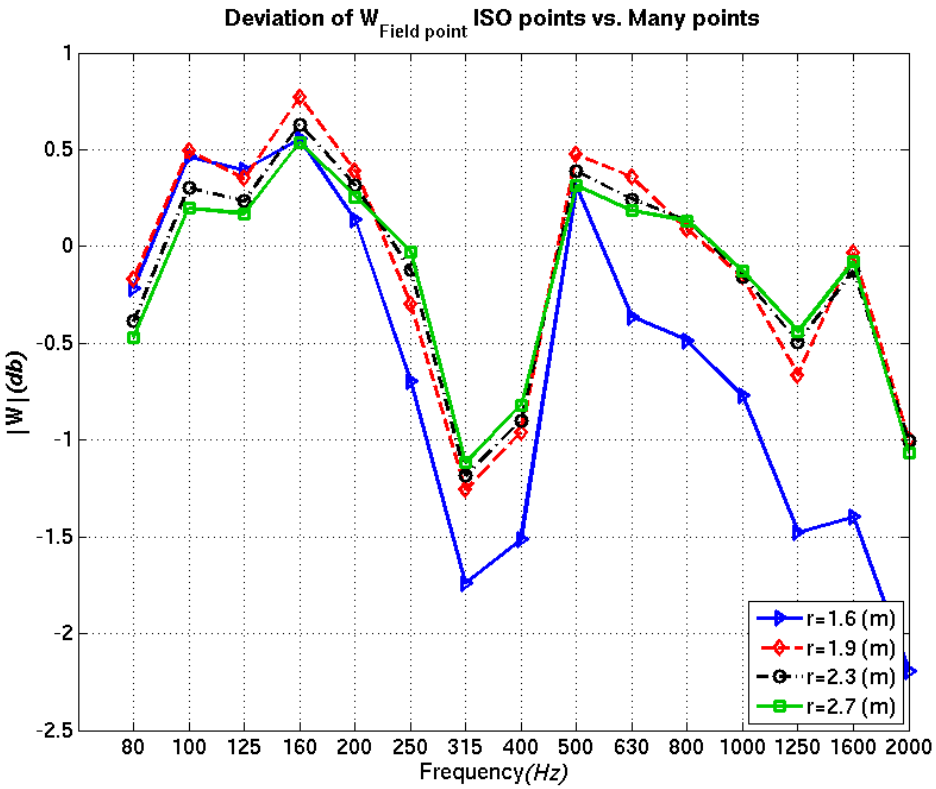


**Figure 5-18 bottom, ISO point 1800 rpm**

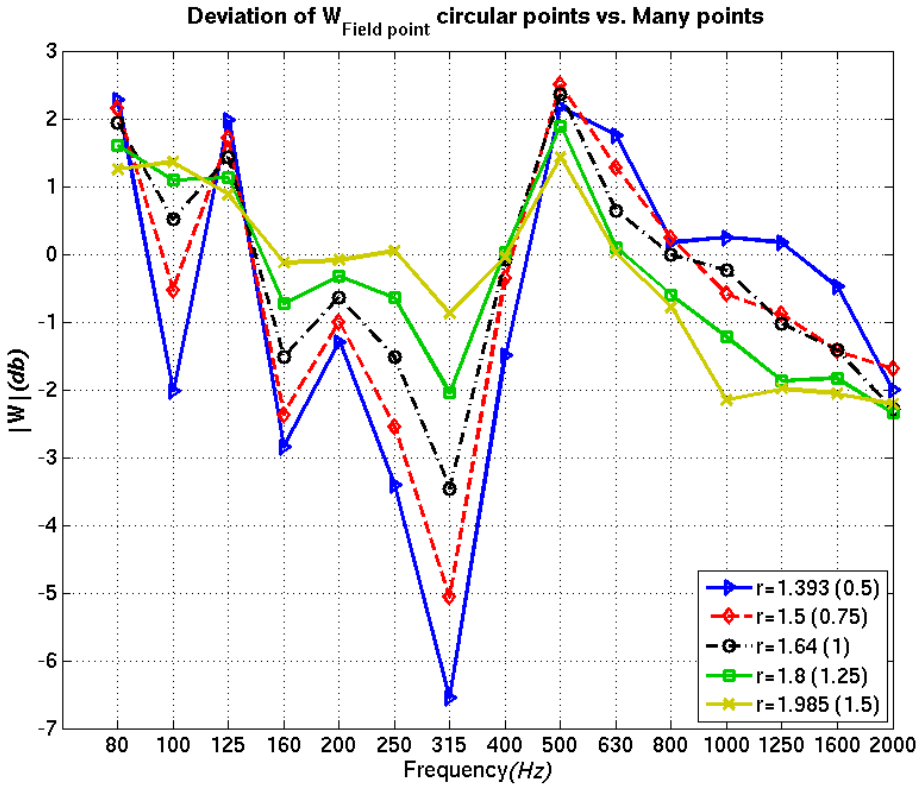


**Figure 5-19 Bottom, different circles 1100 rpm**

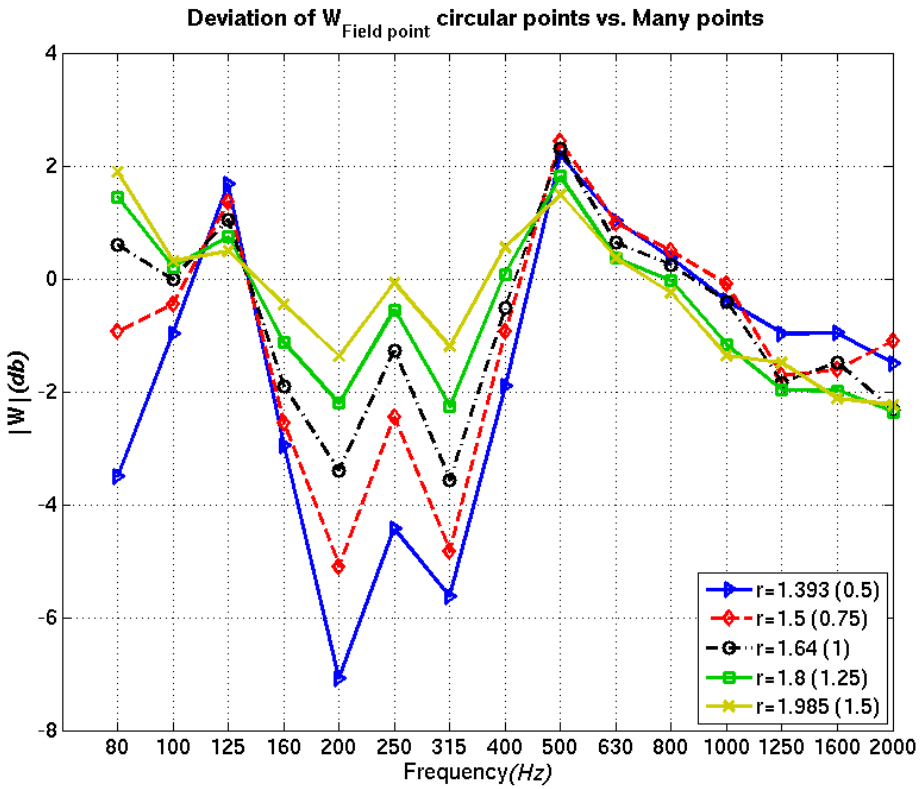


**Figure 5-20 Bottom, different circles 1500 rpm**

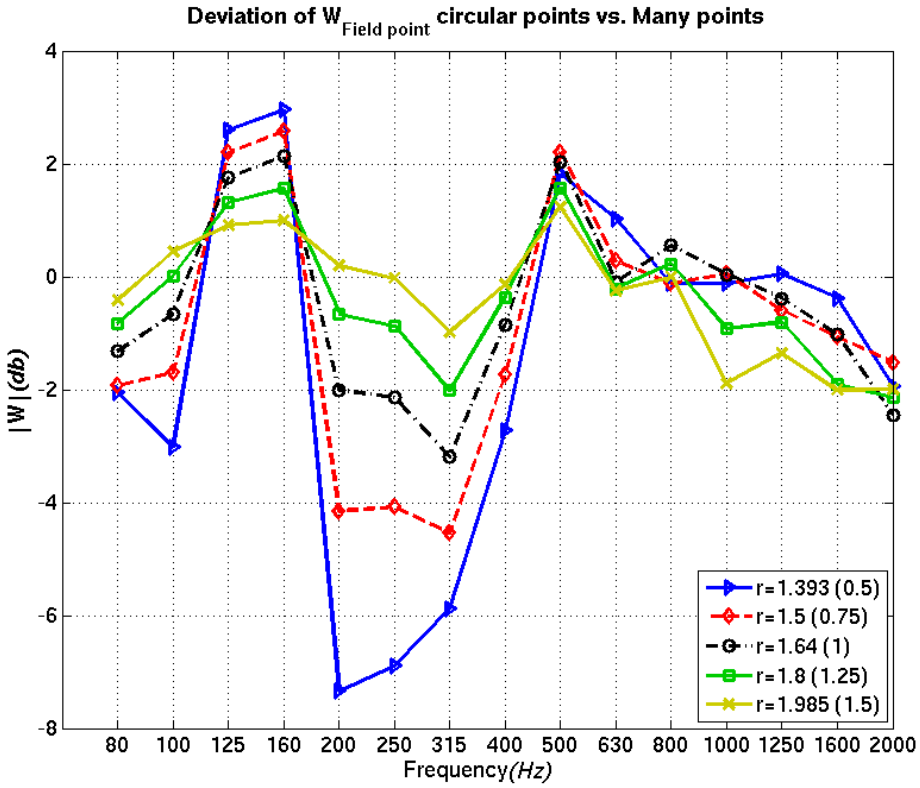


**Figure 5-21 Bottom, different circles 1800 rpm**

Results for one microphone, four microphones (similar to current arrangement at Scania), rotating microphone, ISO-points and half of the ISO-points are shown Figure 5-22 to Figure 5-24. The conclusion is that half of the total number of ISO points is a good choice, especially because of the limitation of the number of channels. Additionally, the use of stationary microphones makes it possible to run rpm sweep (run-up) tests.

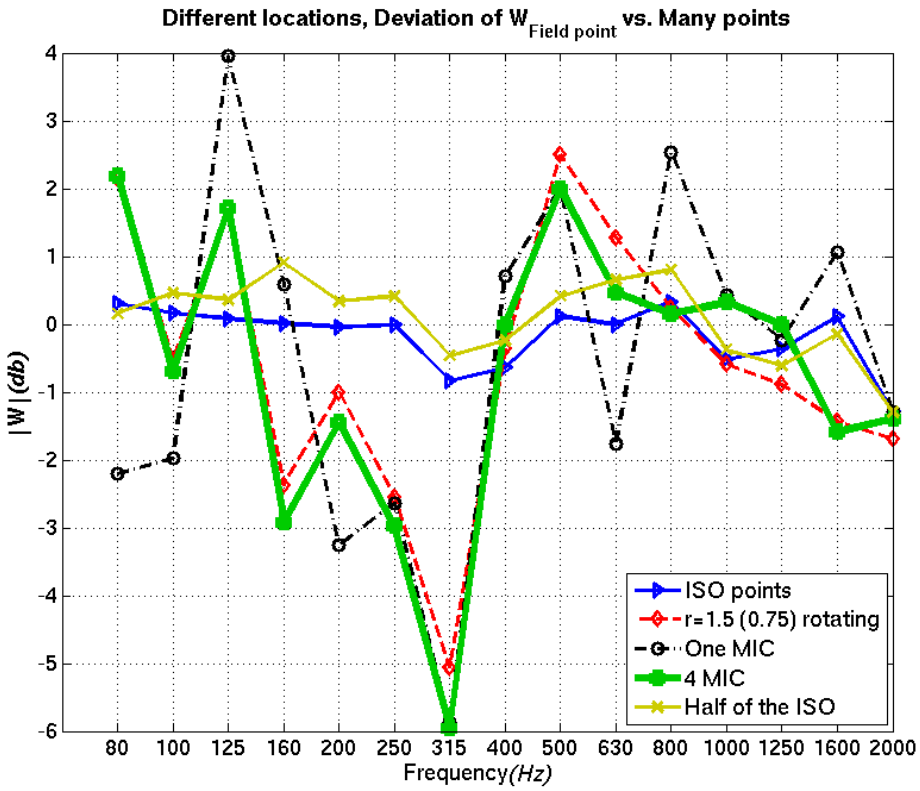


**Figure 5-22 Bottom, different cases, 1100 rpm**

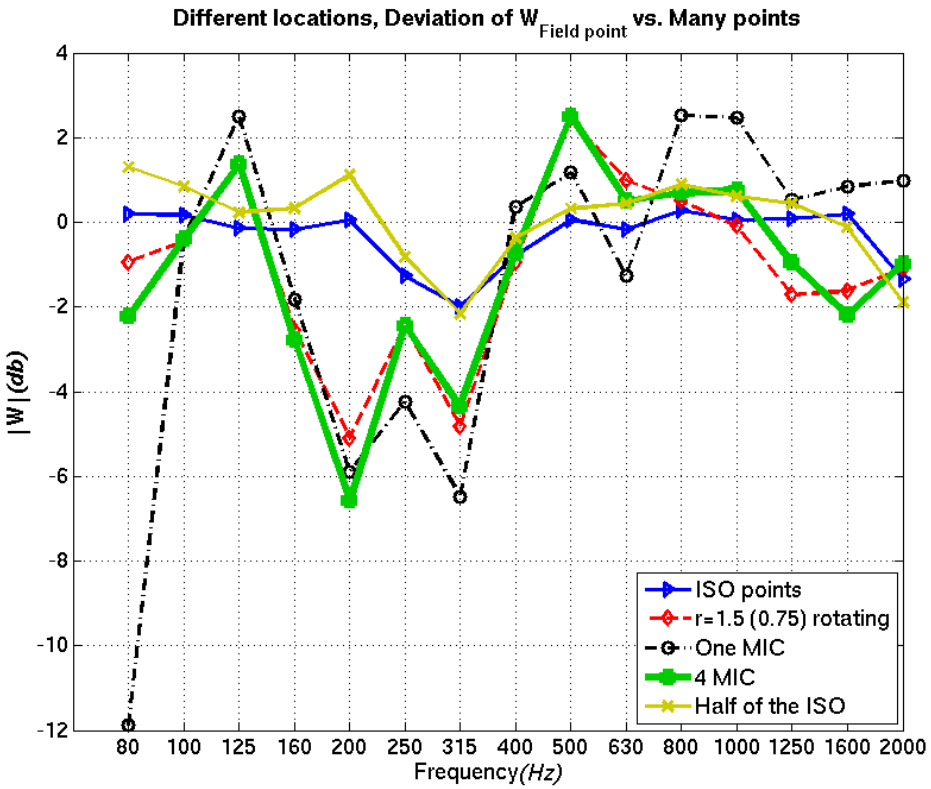


**Figure 5-23 Bottom, different case, 1500 rpm**

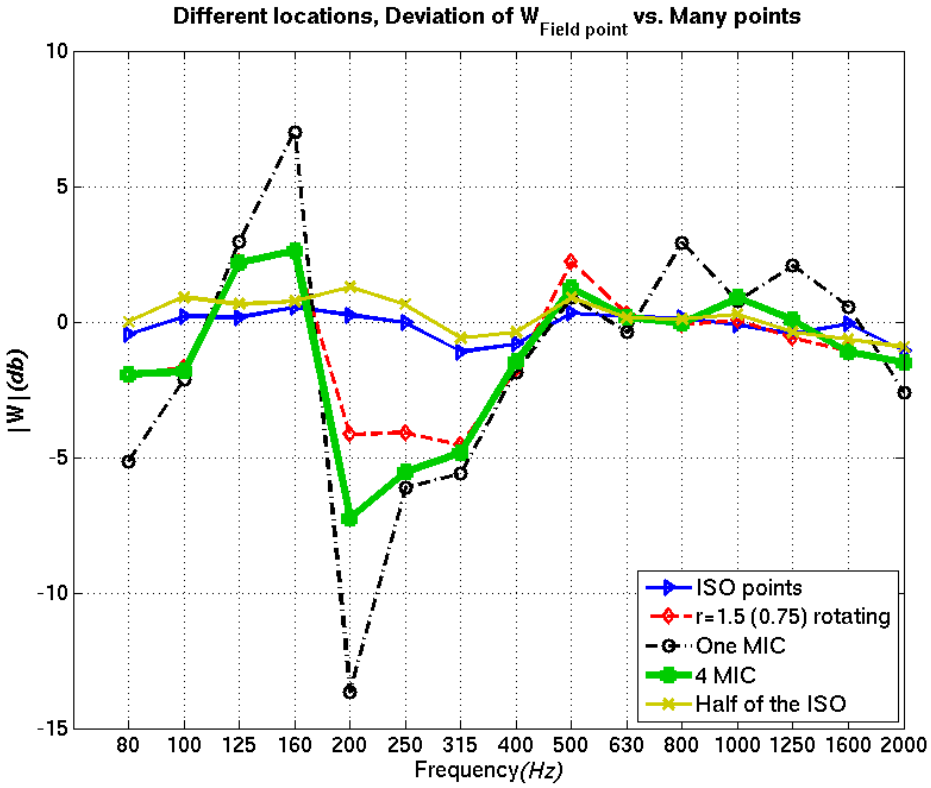


**Figure 5-24 Bottom, different case, 1800 rpm**

The final arrangement is shown in Figure 5-25, 20 microphones in the top hemisphere and nine or ten microphones in the bottom. It is very important to consider that the power from bottom and top has the same weight in the total power. Therefore, it is recommend calculating them as $W_{top}$ and $W_{bot}$ and using equation 6-2.

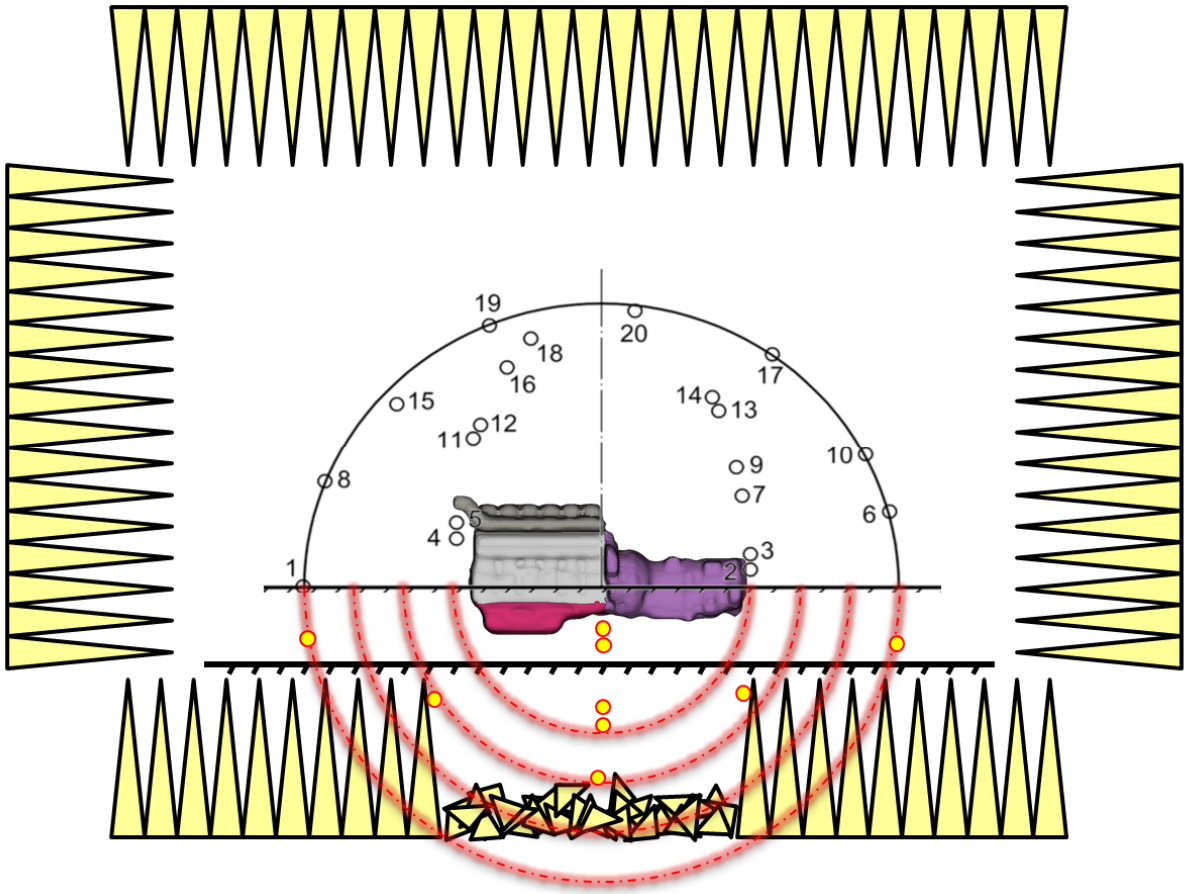


**Figure 5-25 The final arrangement of the microphones.**

## *5.4 Near field requirement*

Sound power calculation using the equations 2-2 or 5-2 or 6-2, has to be carried out outside the hydrodynamic near field. On the other hand, the proper directivity can only be measured outside the geometric near field where the field has developed completely

### 5.4.1 Hydrodynamic near field

The limitation on the location of microphones by hydrodynamic near field is very important in sound power calculation using sound pressure only. The restriction from

the standard, as discussed before, is that the distance between the noise source and the microphone array need to be at least a quarter of a wavelength for ⅓ octave bands away from the object; However for pure tones this can be two wavelengths [**3**]. This means that this is a frequency dependent limitation and there are more problems at lower frequencies (larger wavelengths). Here the lowest frequency for measurement is 80 Hz, because of the limitation in room absorption below this frequency; this would make the limitation almost one meter at typical air speed. This is fulfilled since the microphones are further away.

### 5.4.2 Geometrical near field

Previously discussed in 2.2.3 another requirement for a free field condition for an extended source is the geometric near field. This depends on object size, and will again limit how close microphones can be to the object. In the standard, sphere radius should be at least two times the object's largest dimension. Here the total power for different ISO surfaces with different distances from source center are presented in Figure 5-8 to Figure 5-10 for the top hemisphere and Figure 5-16 to Figure 5-18 for the bottom. There is not a big difference where the sphere radius is greater than $1.9\ \mathrm{m}$. This result is consistent for different speeds. For all Scania engines the largest dimension is the engine length and varies between 1.8 to 2.3 meters (coupled with a gearbox). This is approximately the value for the minimum distance (1.9 m) for near field limitation, so for having a non-dimensional value, it can be said microphones should be at least in distance equal to the engine largest dimension. However the total power is almost unchanged but it should be noted that directivity information is not valid until 4 to 5 meters from source as discussed in 0.

# 6 Summary and Guidelines

Different aspects of the standard, requirements and different microphone arrangements have been discussed so far. What is interesting for Scania though is to have a brief and straightforward recommendation on where to put the microphones and what corrections can be applied with an error estimation, preferably with a maximum number of 30 microphones (the maximum number of input channels on the present frontend).

The final recommendation for distance is to place microphones no closer than 1.9 m (largest dimension of the engine). Putting all microphones at 1.6 m from acoustic center will increase the uncertainty up to two dB in ⅓ octave bands.

The reflection correction factor for microphones positioned under the engine is provided given that microphones are directly under the engine. Still it is not recommended to put microphone there and in the final arrangement only one microphone is positioned there; the other ones are moved further out.

Due to the limited number of channels, the final arrangement is as follow:

- Top: twenty microphones result in a 2-3 dB uncertainty in ⅓ octave frequency bands.
- Bottom: half the number of microphones as in the top hemisphere at almost the same locations of ISO microphone arrangement [**13**], will give 3 to 4 dB uncertainty(note: these can be in different radii but same arrangement).

It is very important to note that the each microphone in bottom may have its own distance $r_n$. Putting a general r for all microphones will add considerable error to the power. Another point is that since this is integration over a surface, the top and bottom half should be treated with the same weight as is explained in section 5.1. Therefore, for M microphones in top and N microphones in bottom one should separately calculate the powers and then add them as in equation 6-1.

$$L_w = 10\log\left[\frac{\overbrace{\frac{\sum_{n=1}^{M}[\tilde{p}_n^2 \times 2\pi r_n^2]}{M}}^{Power\ in\ top\ half} + \overbrace{\frac{\sum_{n=1}^{N}[\tilde{p}_n^2 \times 2\pi r_n^2 + 10^{R_n/10}]}{N}}^{Power\ in\ bottom\ half}}{p_{ref}^2}\right] + C_1 + C_2 \qquad \text{Eq. 6-1}$$

In these equations $R_n$ is the reflection correction factor $C_1$ and $C_2$ are decripbed in equations 2-9 and 2-10. The estimated uncertainty is about 2-3 dB in ⅓ Octave band results in total power.

# 7 Future work

Standard ISO 3745:2004 assumes that the room does not have any reflections and from the investigations, we found that the absorption underneath the engine does not fulfill this criteria. One recommendation would be to improve the absorption in this direction.

It is recommended to verify the level of uncertainties using a known power source which has the same directivity property such as a loudspeaker engine. Also, the effect of increasing the number of microphones on the level of uncertainty can be studied by rotating the top hemisphere array.

It has also been observed that there are some vibrations in the room which have to be investigated. Probably these come from the shaft system. Running tests with involve attaching a shaker to the mounting legs and shaft could illustrate the case.

In the case of Scania planning to build a new anechoic test room, the data here can be used for achieving a proper outline and dimensions of the room and microphones.

# 8 Bibliography

[1] ISO 362:2009, Acoustic: Measurement of noise emitted by accelerating road vehicles -- Engineering method.

[2] Bruno M. Spessert and Hans A. Kochanowski, "Diesel Engine Noise," in *Handbook of Diesel Engines*. Berlin, Heidelberg: Springer-Verlag, 2010.

[3] David A Bias and Calin H Hansen, *Engineering noise control; Theory and Practice*.: Spon press, 2003.

[4] Frank Fahy, *Foundations of Engineering Acoustics*.: Elsevier Ltd, 2001.

[5] Leping Feng, *Acoustical Measurment*. Stockholm: KTH, 2010.

[6] F J Fahy, *Sound Intesity*.: Champan and Hall, 1995.

[7] H.P Waliin, Carlsson U, M Åbom, H Boden, and R Glav, Sound and Vibration, course book, 2010.

[8] David Alan Bias, "Uses of Anechoic and reverberent rooms for the investigation of noise sources ," *Noise control Engineering* , vol. November- December, pp. 154-163, 1976.

[9] Tomas D Rossing, *Handbook of Acoustics*.: Springer, 2007.

[10] Hans Jonasson and Lennert Eslon, "Determination of the sound power levels of external noise sources (Part I- Measurment Method)," Båras, 1981.

[11] Oskar Lundberg, Kalibreringsmätning av halv-ekofrittrum, 2010.

[12] f. P. de Rezende correa, "Acoustic Center Determination on Anechoic Half-Space," *Applied Acoustics*, vol. 48, no. 4, pp. 357-361, 1996.

[13] ISO 3745:2003, Acoustics: determination of sound power levels of noise sources. Precision methods for anechoic and semi-anechoic rooms.

[14] Kihong Shin and Joseph K. Hammond, *Fundamentals of Signal Processing for Sound and Vibration Engineers*.: John Wiley & Sons, Ltd, 2008.

[15] D.A Bies and G.E. and Bridges, "Sound power determination in the geometric near field of a source by pressure measurements alone," in *In Proceedings of the Australian Acoustical Society Annual Conference*, Glenelg, South Australia, 1993.

[16] (2012) MD NASTRAN documentation.

[17] Johannes Wandinger. (2007) Exterior Acoustics.

[18] M S HOWE, *Acoustics of Fluid-Structure Interactions*.: Cambridge University Press, 1998.

[19] L., Heckl, M., Petersson, Björn A.T. Cremer, *Structure-Borne Sound*, 3rd ed.: Springer, 2005.

[20] T. Otsuru, R. Tomiku, and Y. Takahashi, "In situ measurements of surface impedance and absorption coefficients of porous materials using two microphones and ambient noise," *Applied Acoustic*, vol. 66, pp. 845–865, 2005.

[21] J F Allard, C Depollier, and P Guignouard, "Free Field Surface Impedance Measurements of Sound-absorbing Materials with Surface Coatings," *Applied Acoustics*, vol. 26, pp. 199-207, 1989.

[22] J. NICOLAS and Y. CHAMPOUX, "Measurement of Acoustic Impedance In a Free Field at Low Frequencies," *Journal of sound and vibration* , vol. 125, pp. 313-323, 1988.

[23] J F ALLARD, R BOURDIER, and A M BRUNEAU, "The Measurement of Acoustic Impedance at Oblique Incidence With Two Microphones," *Journal of Sound and Vibration*, vol. 101(1), pp. 130-132, 1985.

[24] (2006) OmniPower Sound Source Type 4292.

# 9 Nomenclature

| | |
|---|---|
| $m$ | meters |
| $dB$ | Decibel |
| $dB(A)$ | Decibel, A-weighted |
| $Hz$ | Hertz |
| $kHz$ | kiloHertz ($10^3$) |
| $sec$ | seconds |
| $^0C$ | degrees Celcius |
| $K$ | Kelvin |
| $deg$ | degree |
| $\rho_0$ | Air Density |
| $c_0$ | Sound speed in air |
| $f$ | Frequency (Hz) |
| $\omega$ | Angular Frequency |
| $\tilde{p}^2$ | RMS value of sound pressure square |
| $\langle\ \rangle$ | Spatial average |
| $D_\theta$ | Directivity factor |
| $DI$ | Directivity index |
| $D$ | Directivity or $Max(L_P)$-$Min(L_P)$ |
| $W$ | Sound power |
| $I$ | Sound intensity vector |
| $I_\theta$ | Sound intensity vector at angle of θ |
| $L_P$ | Sound pressure in dB with reference $p_{ref}$ |
| $W_{ref} = 10^{-12}$ | Reference valve for sound power (W) |
| $p_{ref} = 2 \times 10^{-5}$ | Reference valve for sound power (pa) |
| $S_{ref} = 1$ | Reference valve for surface measurement ($m^2$) |
| $S$ | Surface area of hypothetical sphere encompassing the source |
| $\lambda$ | wavelength *in m* |
| $l$ | characteristic dimension of the source in *m* |
| $r$ | distance from effective source center to the observation point, in *m* |

| | |
|---|---|
| $\alpha$ | Absorption coefficient |
| $C_{ref}$ | reflection coefficient |
| $H_{12}$ | FRF between two microphones sound pressures |
| $\gamma_{xy}$ | coherence between two signals |

# 10 Abbreviations

| | |
|---|---|
| RPM | Revolutions per Minute |
| RMS | Root mean square value |
| SPL | Sound pressure level in dB |
| FRF | Frequency Response Function |
| I.C. Engines | Internal combustion engines |

# 11 Appendix

## *11.1 Appendix A: effect of focus point outside of source acoustic center*

Here the resultant sound pressure field for a monopole model is shown in Figure 11-1 for two different frequencies. All around of the monopole are infinite elements. The focal point is considered in the bottom plane (highlighted with a black dot) however, for a monopole it is simply the middle of the sphere. It is clear from that the sound field is erroneous since it is not a uniform pressure around the sphere like in Figure 11-3. One reason why reflections cannot be modeled is that we can only have one focal point especially for very large sources, which is the case here. This is because that the reflection means a mirrored source and this make two different acoustic centers for each source. It also worse to mention that adding a curvature in bottom does not change (not presented here).

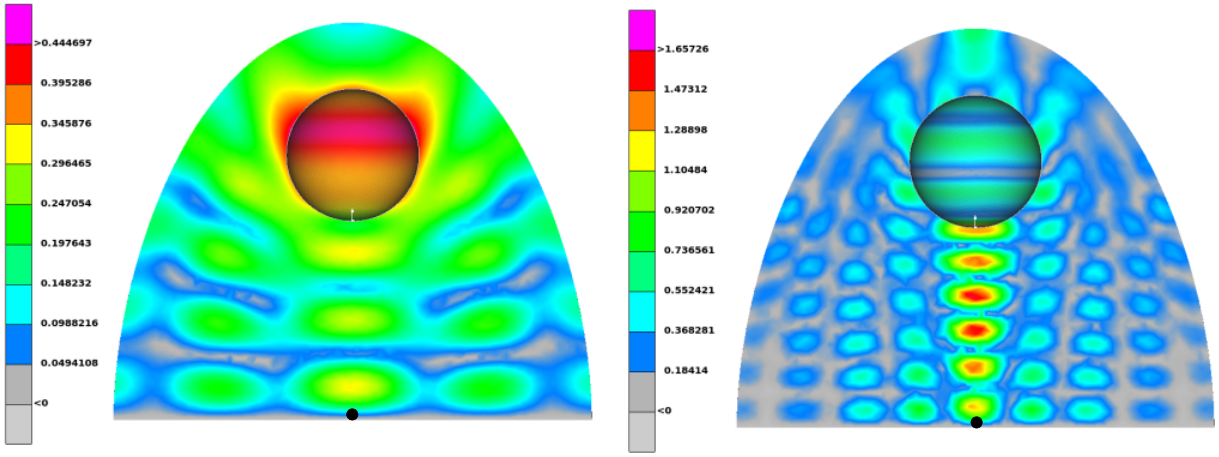


**Figure 11-1 Sound pressure, Monopole model, 800 Hz (Left) and 1600 Hz (Right), effect of offset of focal point.**

## *11.2 Appendix B: Effect of infinite element surface shape on results*

Two different and similar monopole problems have been studied but with different reflection-free shapes, Figure 11-3. The inner radius of the sphere is from 0.4 m and the outer radius is 0.8 m. The element size varies starting from 20 mm in sphere to 40 mm on reflection free surface. Iso-pressure[9] surfaces in 2 kHz are shown in Figure 11-3. As it, clear in cases of half spheres and half cylinders the sound field is distorted. The deviation may be small but the point is that velocity results would be

[9] Iso –pressure: The Surfaces (in 3D or lines in 2D) in the fluid mesh (air) that have same pressures value, the word is borrowed from µETA a multi-purpose post-processor.

largely incorrect since they are derivate of pressure. This again means reflection cannot be studied in model since there are boundary condition are impedance and accurate velocities are needed. Many more shapes (flat bottom, curved bottom, cone shape in top with curve in bottom) have been studied, and yet this distortion exists. For brevity all results are not presented here.

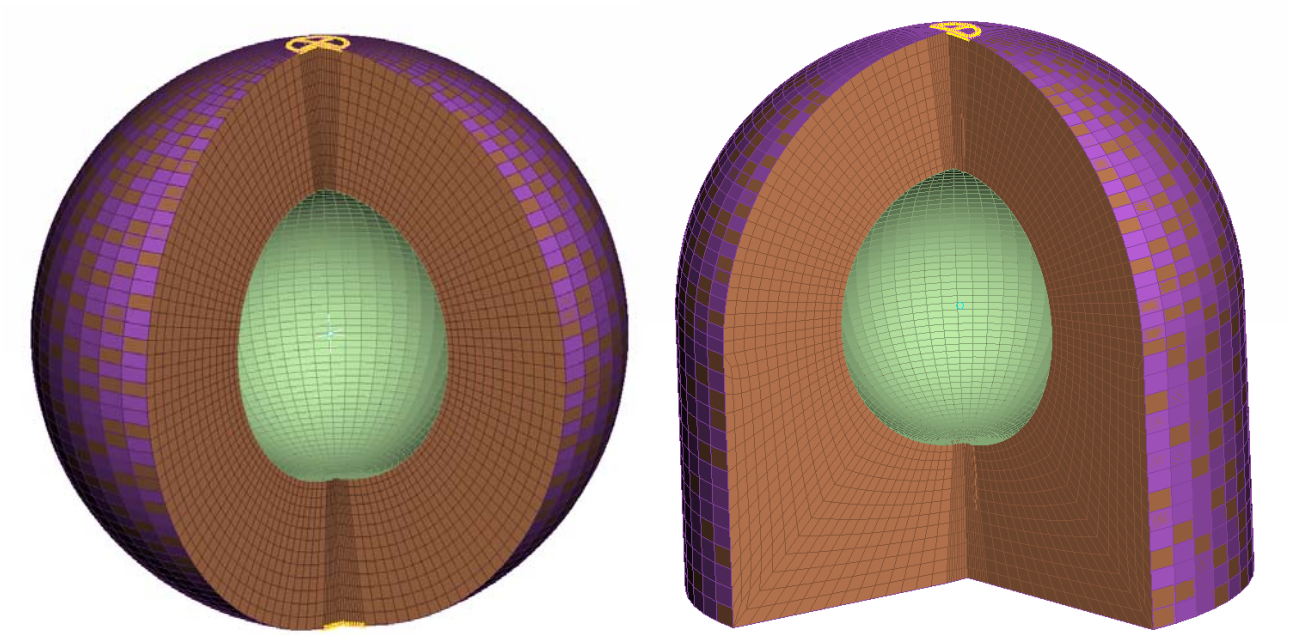

**Figure 11-2 Hex mesh of the monopole, different cuts of surrounding fluids.**

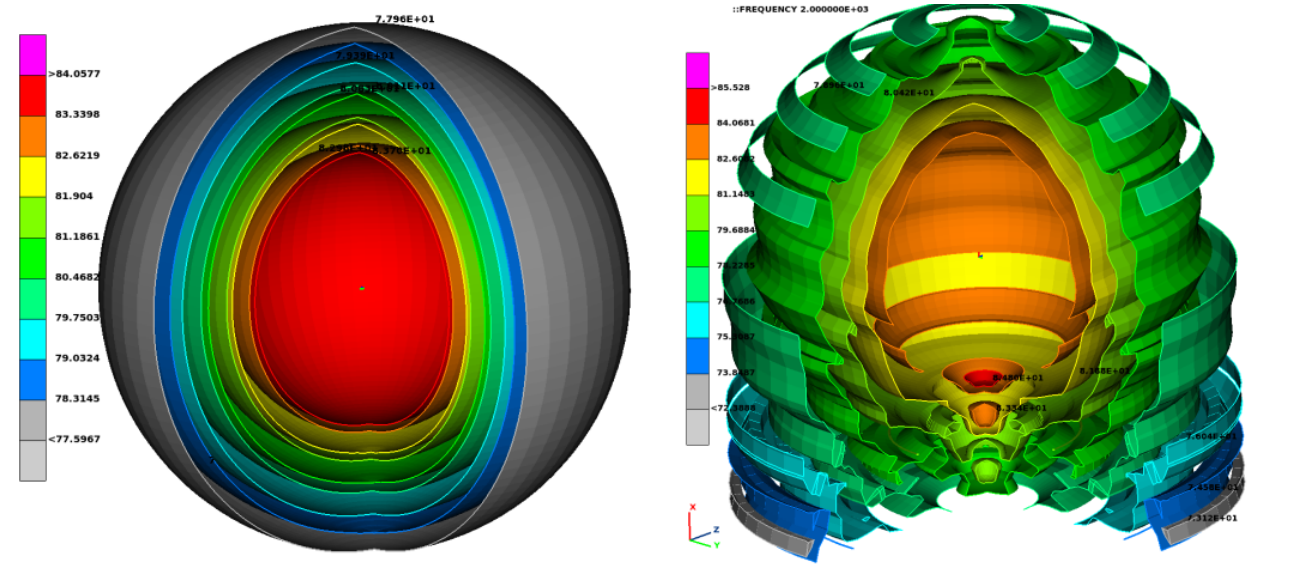


**Figure 11-3 ISO pressure surfaces in monopole models; Left: monopole with spherical infinite boundary, Right: deviation in results compared to sphere (left), levels 72.4 to 85.5 dB**

## *11.3 Appendix C: Sphere vs. egg shaped monopole*

To study the sensitivity of the software to surface shape of the reflection-free boundary condition two cases have been studied: egg-shaped and spherical (Figure 11-4). The inner radius of the sphere is 0.8 meter. The mesh size is 25-50 mm. There are 14000 elements and around 40e5 tetra fluid elements.

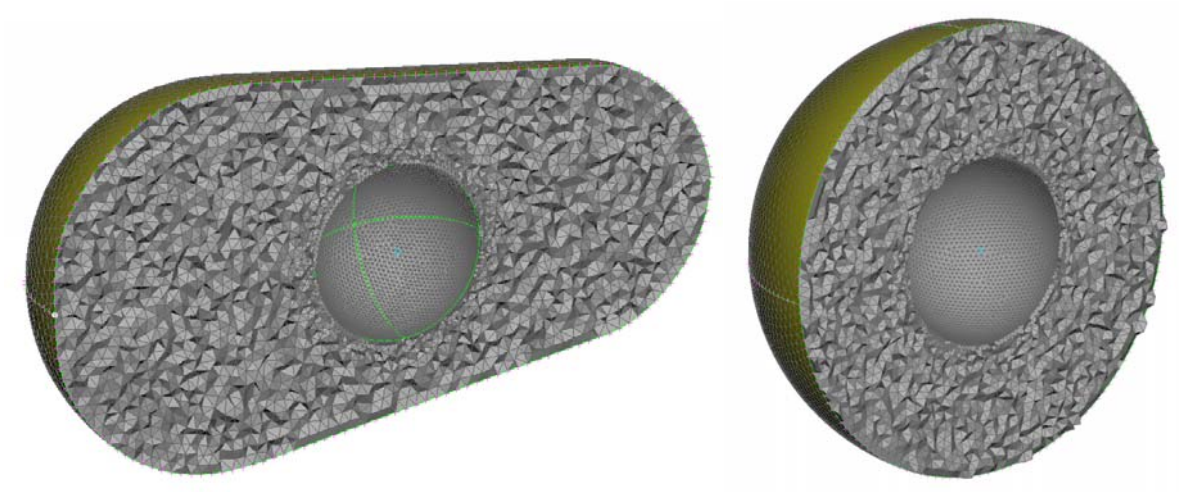

**Figure 11-4 The monopole model Left: egg shaped Right: Sphere**

Sound pressure results are presented for 400 and 2000 Hz in Figure 11-5 and Figure 11-6 respectively. As it clear, the sound field in 2 kHz is distorted and there are errors in the numerical model.

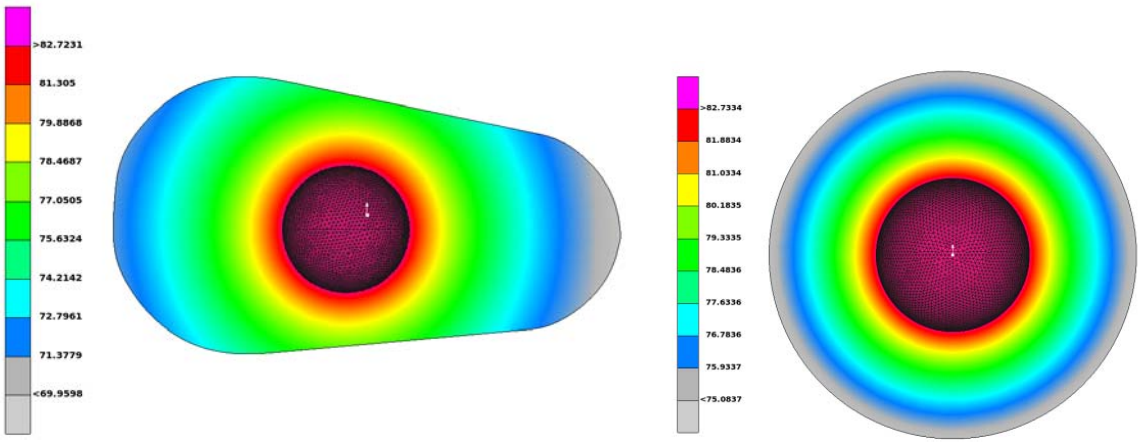


**Figure 11-5 The monopole model results, Sound pressure dB, 400 Hz Left: egg shaped Right: Sphere**

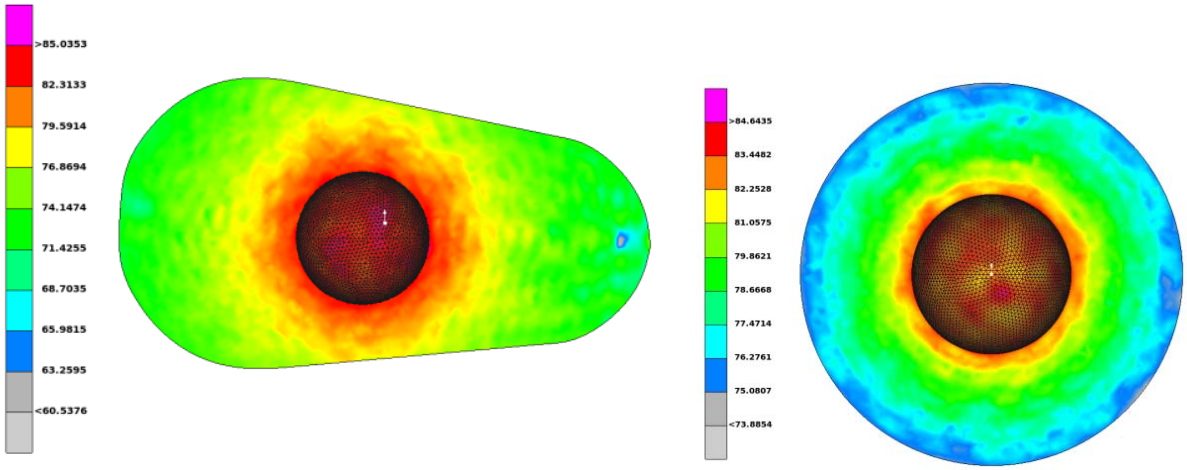


**Figure 11-6 The monopole model results 2 kHz, Sound pressure dB, Left: egg shaped Right: Sphere**

The error in the prediction of the sound field could be observed as directionality in monopole results (there shouldn't be any directivity for a monopole problem). The levels of this directionality for two different cases for 1.8 and 2 kHz are presented in the following diagram, as it is clear the egg shaped has a slightly worse situation but in this case, because of the rather rough element size there effect of the outer shape is masked.

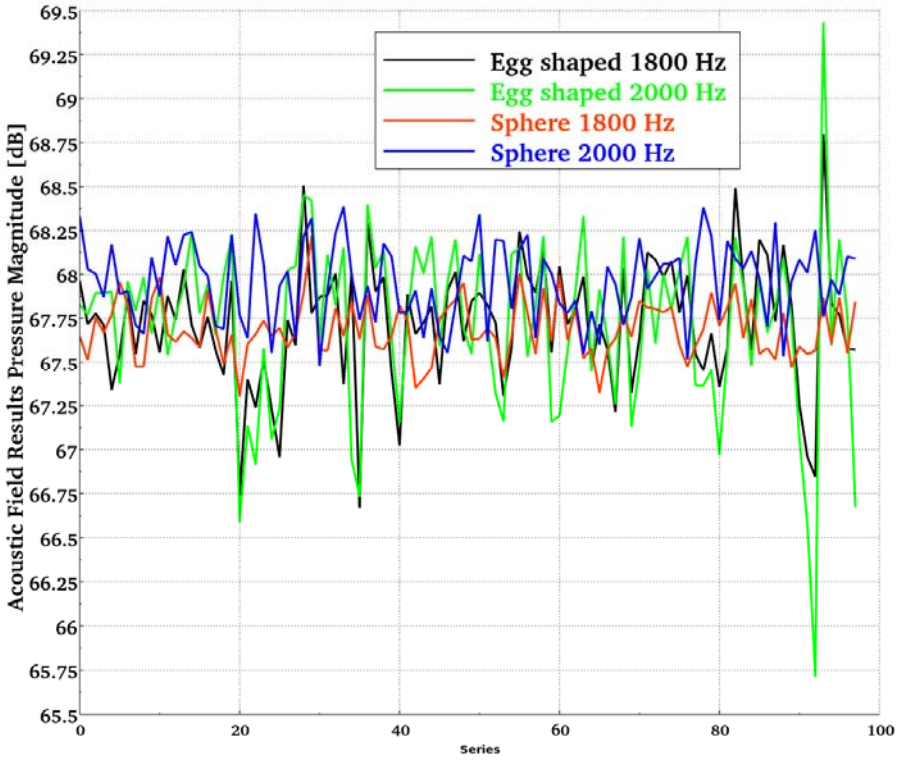


**Figure 11-7 directionality in a monopole problem in Nastran with a rather large elements size**

The sound power calculated from a monopole model for two different cases is presented here. The deviation from the analytical solution for wetted power and field points in spheres at different radiuses are presented in Figure 11-8 and Figure 11-9. Below 2 kHz, the upper limit, the results deviate very little from the analytical solution; especially the wetted power is very exact below 1.5 kHz. Both shapes have good prediction - even better results for the egg-shape which was not expected since there is a higher error in pressure results.

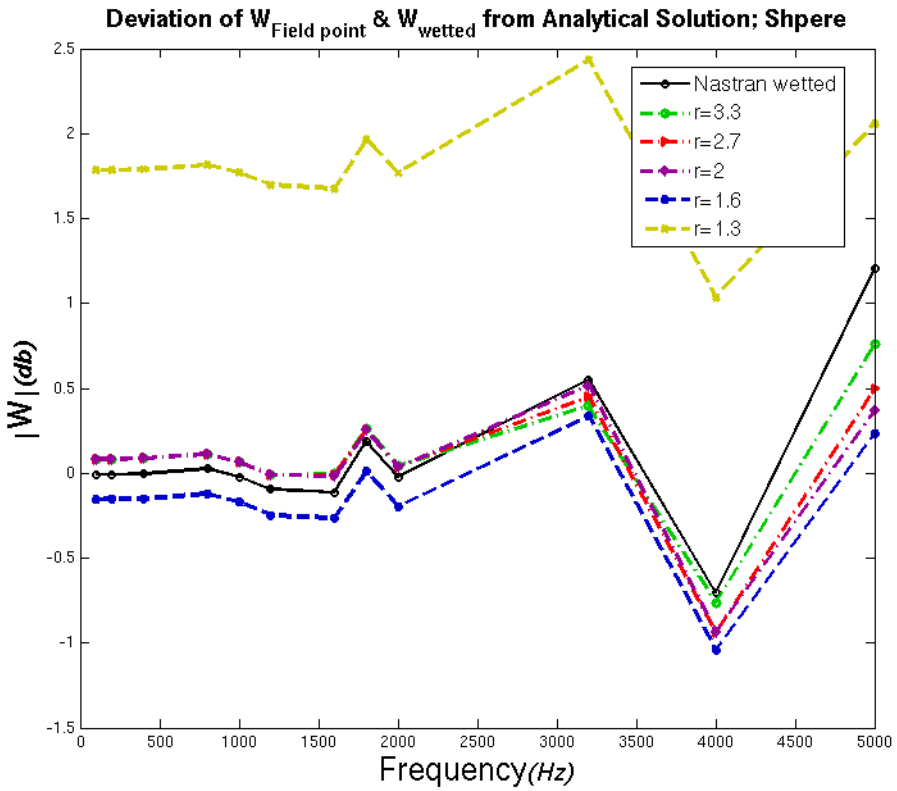


**Figure 11-8 Sound power calculated based on the monopole model, deviation from analytical solution, sphere**

## *11.4 Appendix D: Absorption measurement results & filtrations*

The measured data has been filtered using Low-pass filter data in MATLAB. Original and filtered data has been presented in Figure 11-10 and Figure 11-11.

The low pass filter in Matlab is defind as follow:

```
hs=fdesign.lowpass('n,fc',100,10,10240)
d=design(hs); %Lowpass FIR filter
y=filtfilt(d.Numerator,1,x); %zero-phase filtering
```

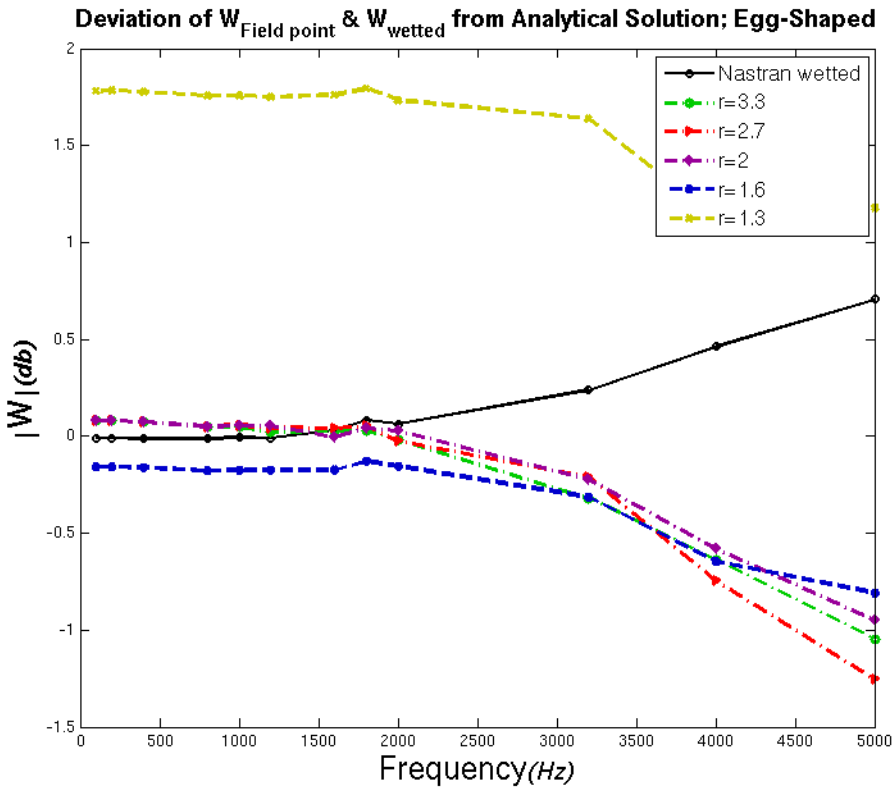


**Figure 11-9 Sound power calculated based on the monopole model, deviation from analytical solution, egg shape**

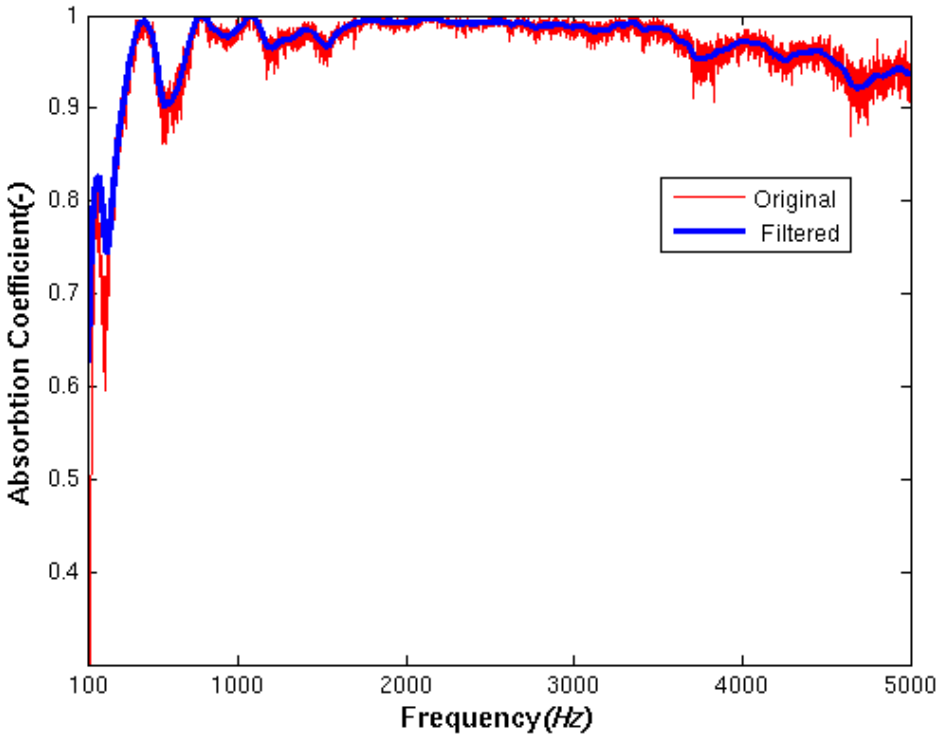


**Figure 11-10 Absorption coefficient before(Red) and after (Blue) filteration**

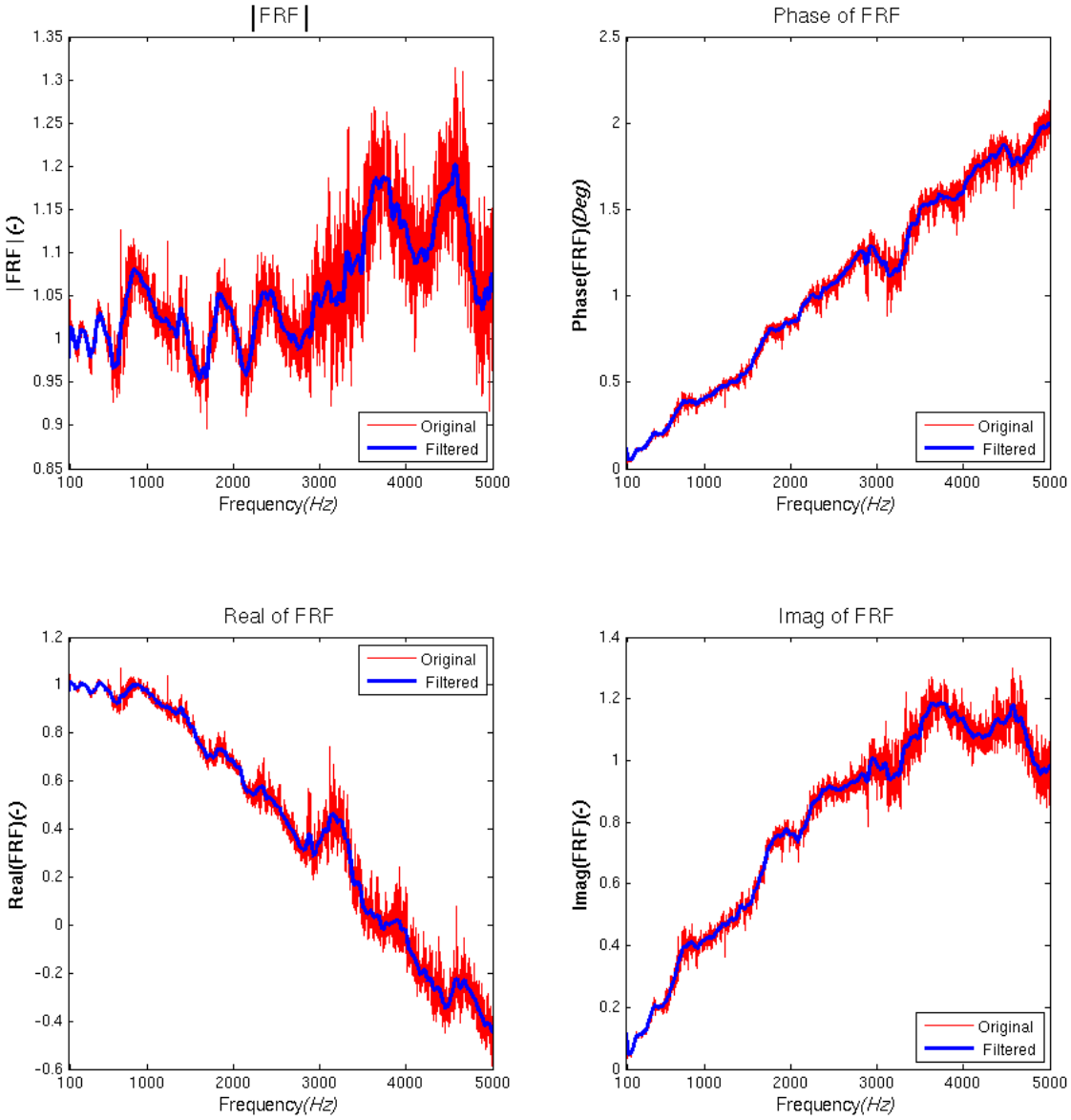


**Figure 11-11 The Frequency response function(FRF), original and filtered data**

## *11.5 Appendix E: Inverse square law, room*

The comparison between pressure based on the distance from the wall, three cases, Vertical wall, Middle close source (floor) and far close source (floor) are presented here. The blue line is the reflection-free case deviation from this line it is considered as a correction factor. The results for very low frequencies are not very stable for engine measurement. Practically they are not included. It has to be mentioned that the curves are shifted (only in levels, y axis) to adjust the same sound pressure level since they have different distances.

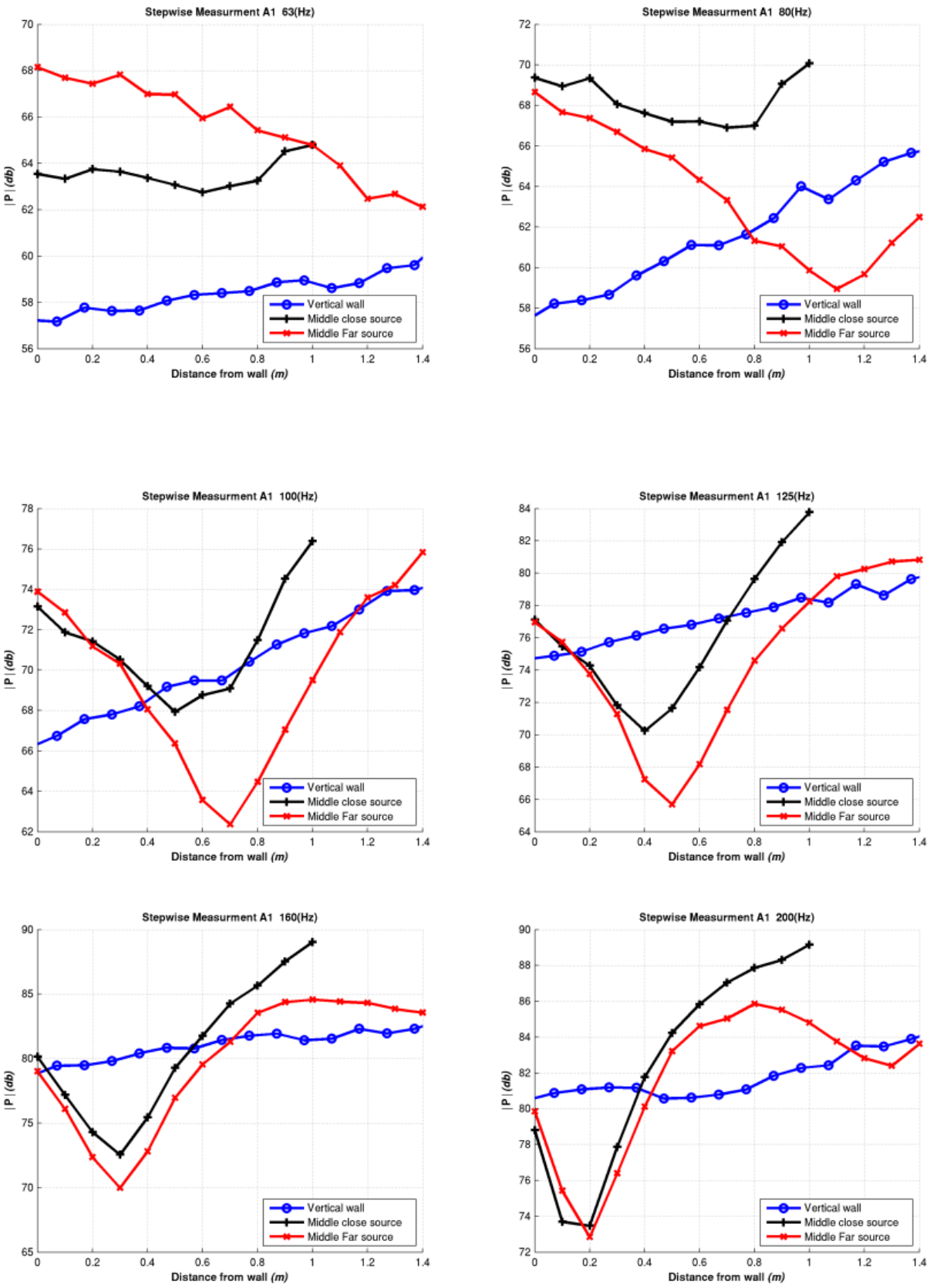


**Figure 11-12 inverse square law measuremnt, different cases, loudspeaker**

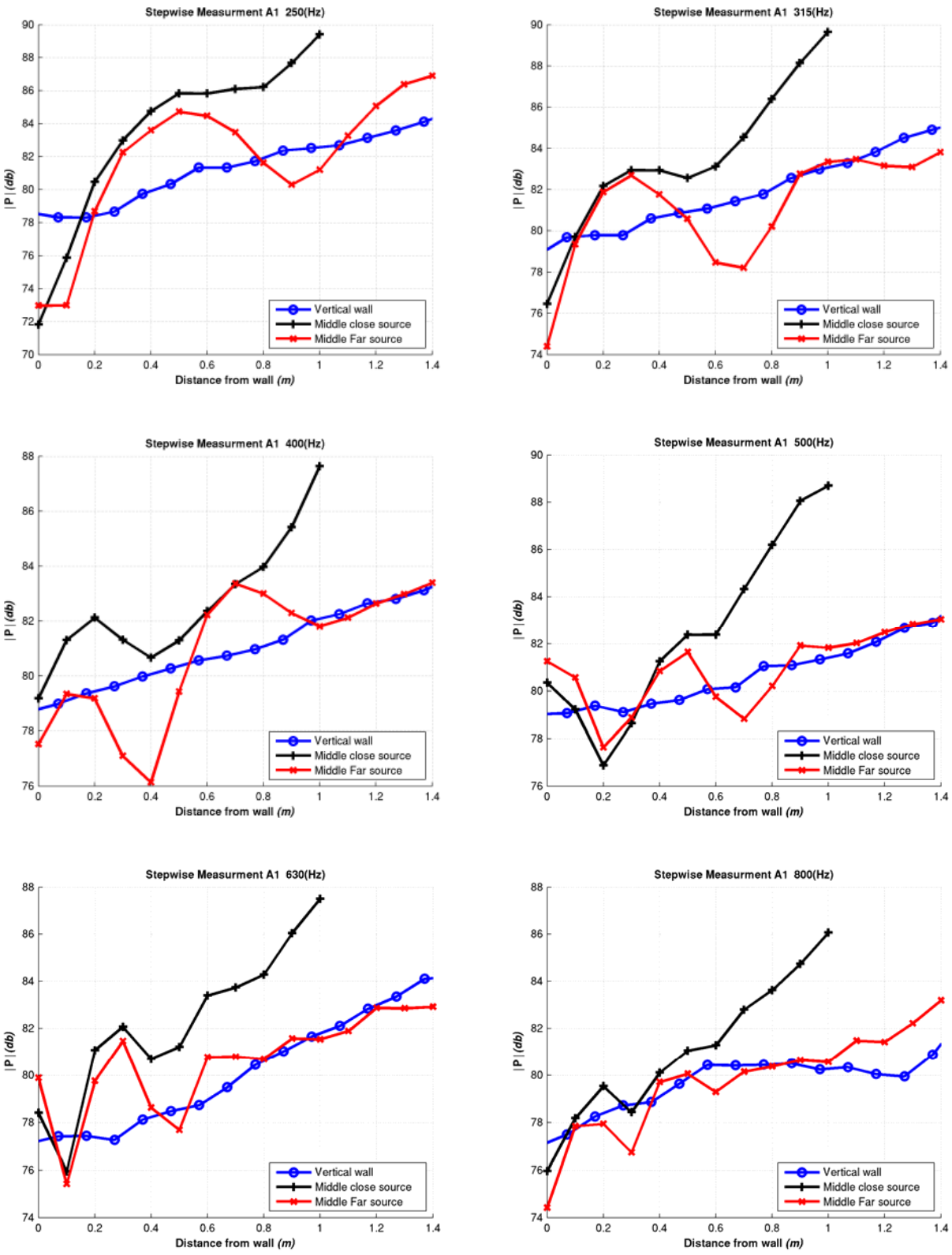


**Figure 11-12 inverse square law measuremnt, different cases loudspeaker (continue)**

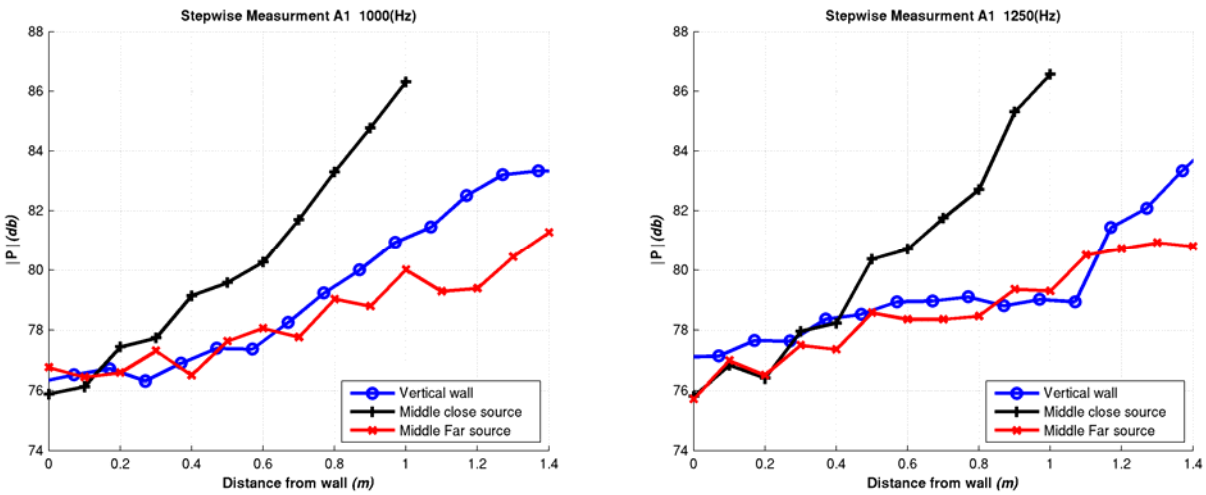


**Figure 11-12 inverse square law measuremnt, different cases loudspeaker (continue)**

## *11.6 Appendix F: Inverse square law, engine vs. room*

In this section the result from inverse square law of the different sources i.e. engine and loudspeaker has been compared. This will show how much the deviations due to the reflection from floor are different. In most the frequencies the result are acceptable and the sources are not extremely different.

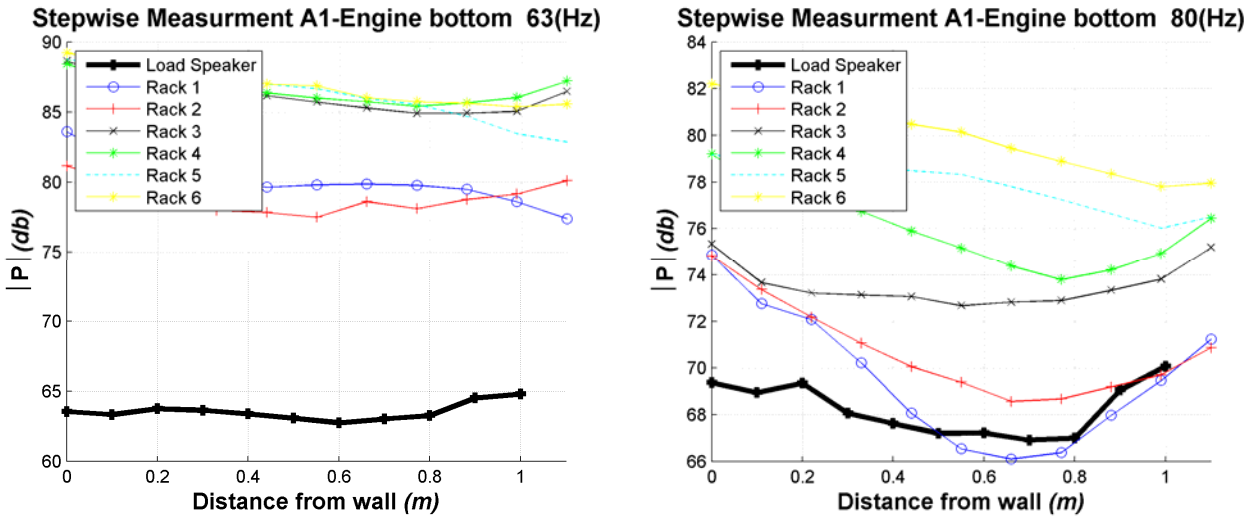


**Figure 11-13 inverse square law measuremnt, different cases, loudspeaker vs. Engine**

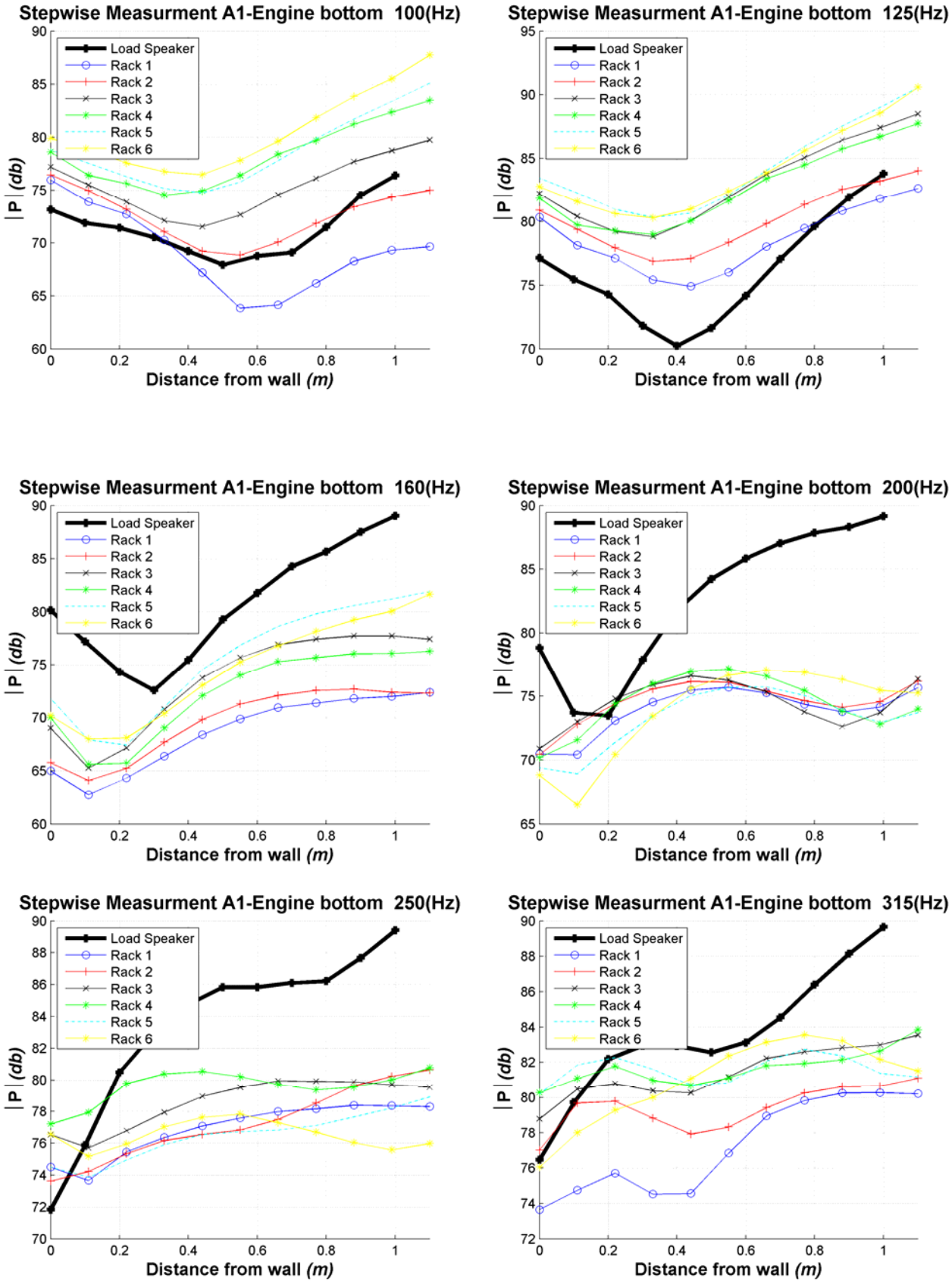


**Figure 11-13 inverse square law measuremnt, different cases, loudspeaker vs. Engine, (continue)**

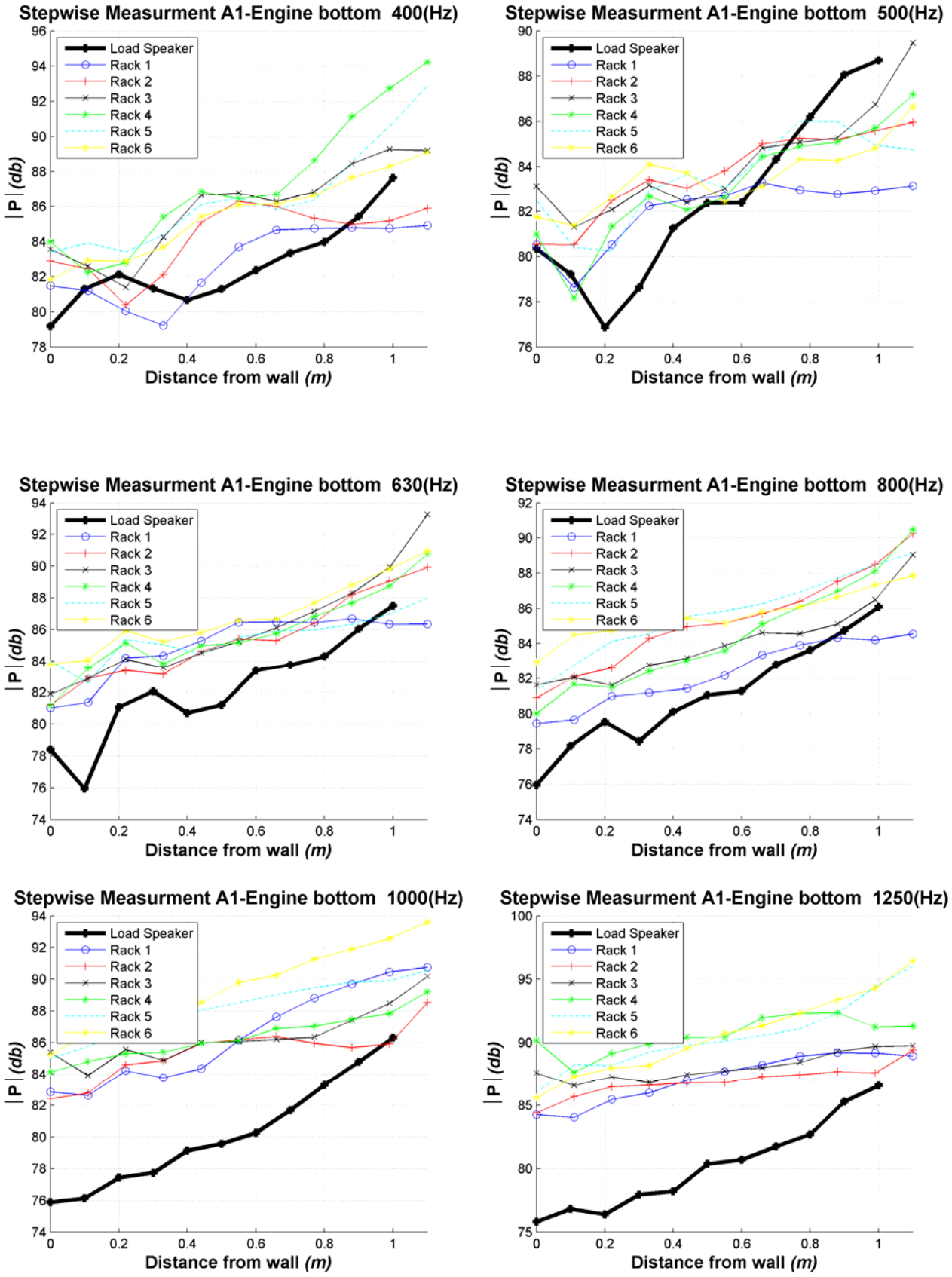


**Figure 11-13 inverse square law measuremnt, different cases, loudspeaker vs. Engine, (continue)**

## *11.7 Appendix G: some sample engine sound fields*

Some sample cases of the engine sound directivity in different frequencies are shown in figure 11-14. (note: The results here are for sphere case to have a wider view)

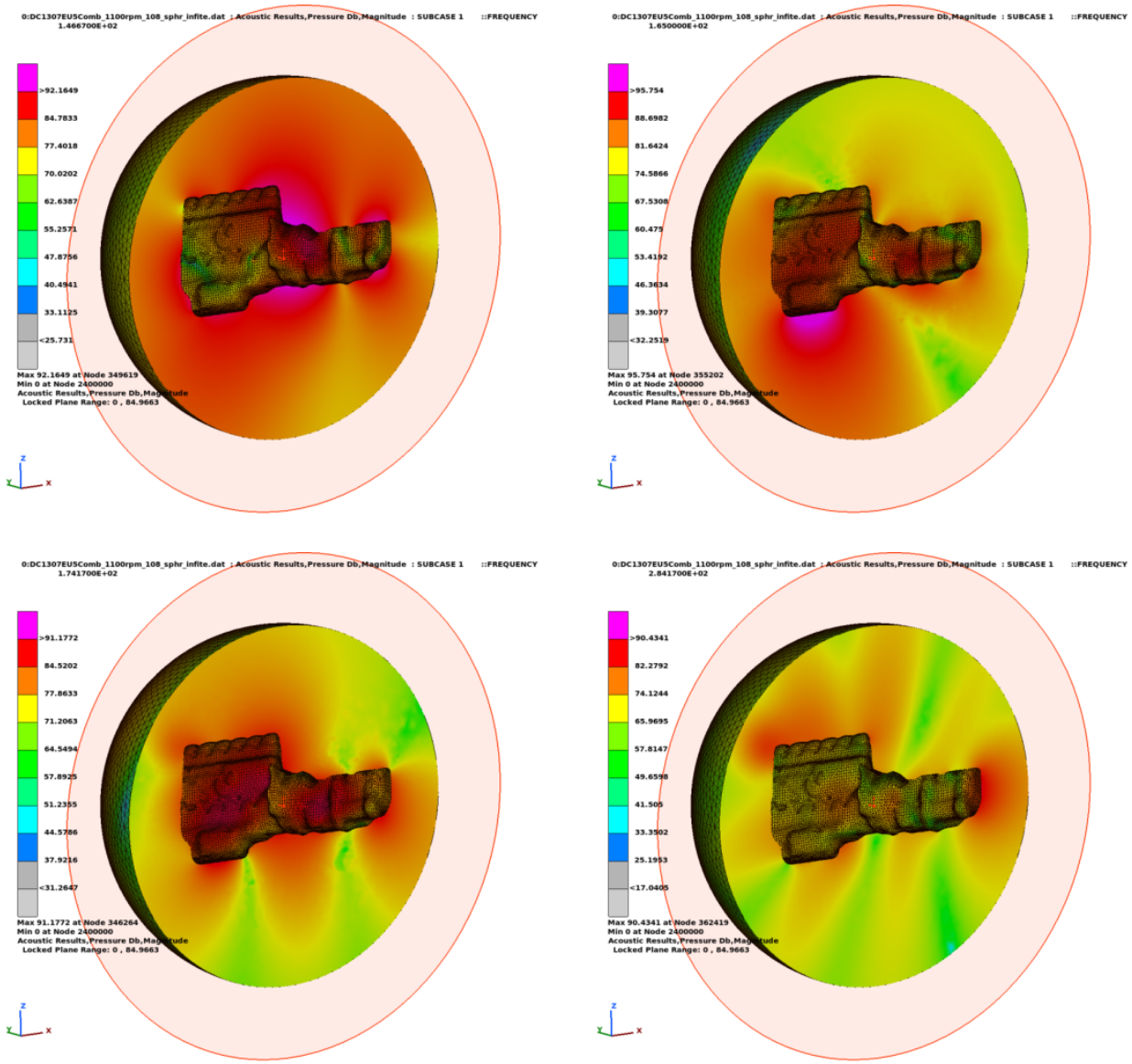


**Figure 11-14 Typical sound filed in engine acoustic model for frequencies 144.6, 165, 174, 284 Hz**

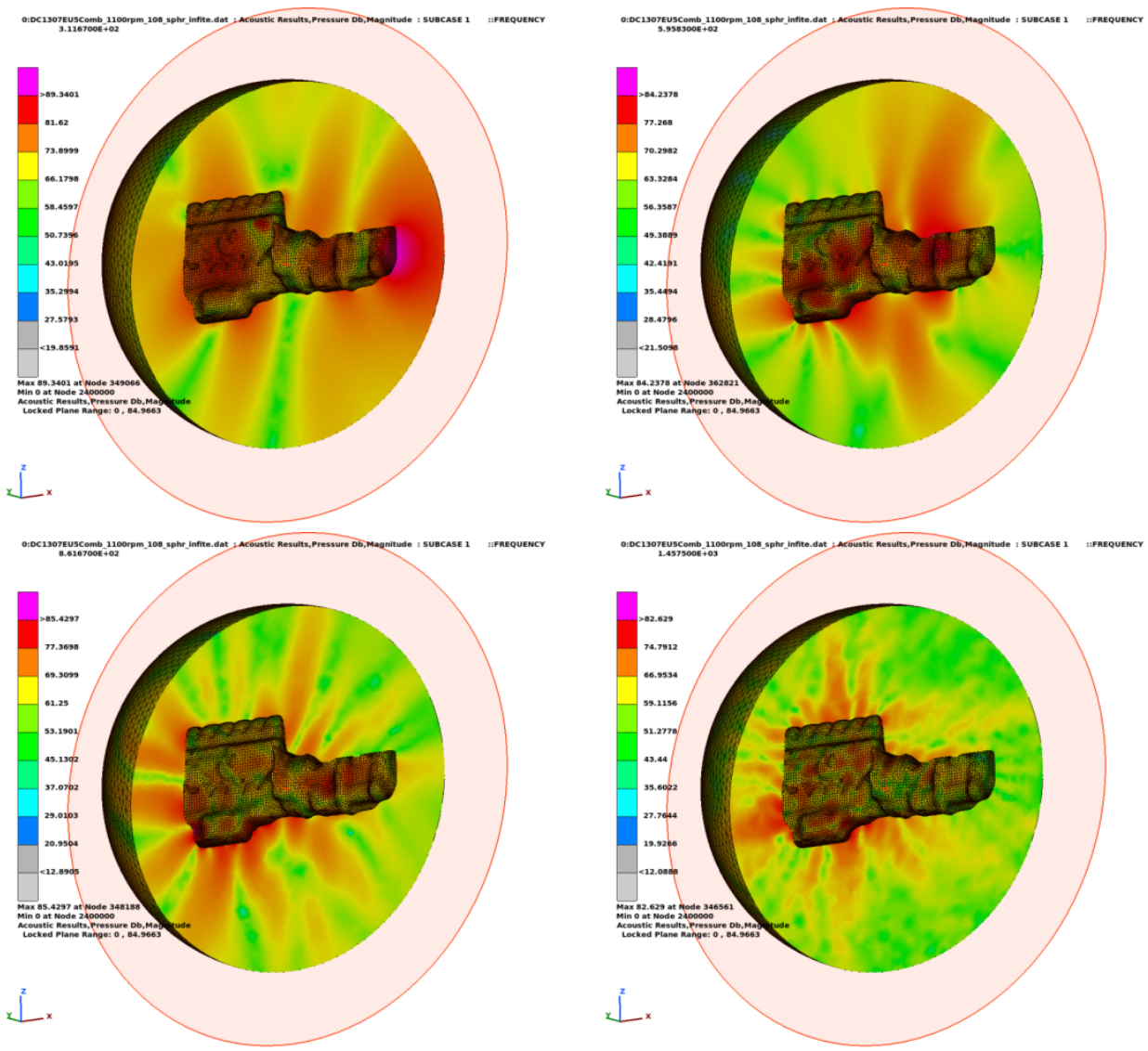


**Figure 11-14 Typical sound filed in engine acoustic model for frequencies 311, 595, 861, 1457 Hz (continue)**